CHANGES IN SUSCEPTIBILITY TO VESICULAR STOMATITIS VIRUS DURING PROGRESSION OF PROSTATE CANCER

BY

NANMENG YU

A Dissertation Submitted to the Graduate Faculty of

WAKE FOREST UNIVERSITY GRADUATE SCHOOL OF ARTS AND SCIENCES

In Partial Fulfillment of the Requirements

for the Degree of

DOCTOR OF PHILOSOPHY

in Biochemistry and Molecular Biology

December 2013

Winston-Salem, North Carolina

Approved by:

Douglas S. Lyles, Ph.D., Advisor

Examining Committee:

Steven Kridel, Ph.D., Chairman

Roy Hantgan, Ph.D.

John Wilkinson, Ph.D.

Mercedes Porosnicu, M.D.

Acknowledgements

I would like to thank my advisor Doug Lyles, for teaching me and shaping me scientifically. I have learned so much from you. I also appreciate your patience as we interpreted my data and experiments together.

I would like to thank my committee members, for valuable suggestions and guidance in my project. You redirected the focus of my research whenever necessary.

I would like to thank my current and former lab members: Shelby Puckett, for teaching me everything I know about animal care and experiments with animals and Dr. Karishma Rajani, for guiding me in cellular and molecular biology techniques. I would like to thank the other members of my lab, whose support was very important in this process.

I would also like to thank my friends and family, whose constant encouragement has been very supportive. To my father, who always believed in me. To Dee Ann, who always listened whenever I needed someone to talk. To Gary, whose support was central to my research process.

Table of Contents

List of Figures iv

List of Abbreviations vii

Abstract x

Introduction 1

Materials and Methods 21

Results

- Chapter 1. Susceptibility of prostate cancer to VSV oncolysis during progression of prostate cancer 28
- Chapter 2. Effects of *Rb* deletion or Tak1-downregulation on susceptibility to VSV oncolysis 52
- Chapter 3. Activation of IL-6/STAT3 pathway in murine prostate cancer cells 70

Discussion 107

References 120

Scholastic Vitae 131

List of Figures

1. Primary cultures of mouse prostate epithelial cells express cytokeratin. 30
2. Prostate tumors contain a mixture of resistant and susceptible cells. 32
3. Castration resistant tumor cells are susceptible to VSV infection. 35
4. Tumor derived *Pten* $^{-/-}$ cells support very little viral gene expression even at high MOI. 38
5. Control *Pten* $^{L/L}$ cells and acutely deleted *Pten* $^{-/-}$ cells support viral gene expression. Tumor derived *Pten* $^{-/-}$ cells support very little if any viral gene expression. 41
6. Control *Pten* $^{L/L}$ and acutely derived *Pten* $^{-/-}$ cells are susceptible to virus-induced cell death. Tumor-derived *Pten* $^{-/-}$ cells are resistant to virus induced cell death. 43
7. In a multiple cycle infection, control *Pten* $^{L/L}$ cells and acutely deleted *Pten* $^{-/-}$ cells are susceptible to rwt induced cell death. Tumor derived *Pten* $^{-/-}$ cells are resistant to rwt and rM51R induced cell death. 45
8. Tumor derived *Pten* $^{-/-}$ cells constitutively express higher levels of antiviral genes. Control *Pten* $^{L/L}$ cells activate and upregulate higher levels of antiviral genes than acutely deleted *Pten* $^{-/-}$ cells with rM51R infection. 48
9. Control *Pten* $^{L/L}$ cells responds to IFN stimulation. Acutely deleted *Pten* $^{-/-}$ cells poorly respond to IFN stimulation. 50
10. Model for changes in susceptibility to VSV during progression of prostate cancer 51
11. *Rb* $^{-/-}$ mouse prostate epithelial cells show increased susceptibility to VSV-induced cell death. 54

12. In a multiple cycle infection, *Rb* $^{-/-}$ mouse prostate epithelial cells show increased susceptibility to VSV-induced cell death. 56

13. Control and *Rb* $^{-/-}$ cells are responsive to IFN. 59

14. Control and *Tak1*-downregulated cells support viral gene expression. 62

15. Control and *Tak1*-downregulated cells are susceptible to VSV-induced cell death. 64

16. In a multiple cycle infection, control and *Tak1*-downregulated cells are susceptible to VSV-induced cell death. 66

17. Control and *Tak1*-downregulated cells are responsive to IFN. 69

18. Model for crosstalk between the IL-6-STAT3 axis and the STAT1 pathway 71

19. Tumor-derived *Pten* $^{-/-}$ cells constitutively express high levels of IL-6. 73

20. rwt infection does not shut down IL-6 production in tumor derived *Pten* $^{-/-}$ cells. Tumor derived *Pten* $^{-/-}$ cells dramatically upregulate IL-6 production in response to rM51R infection. 75

21. Tumor derived *Pten* $^{-/-}$ cells dramatically upregulate IL-6 production in response to rM51R infection. 78

22. Tumor derived *Pten* $^{-/-}$ cells have constitutively activated STAT3. 82

23. IL-6 mediates activation of STAT3 in tumor derived *Pten* $^{-/-}$ cells. 86

24. Anti-IL-6 antibody has very little effect on activation and expression of STAT1 in tumor derived *Pten* $^{-/-}$ cells. 90

25. Inhibiting STAT3 activation has very little effect on viral gene expression in tumor derived *Pten* $^{-/-}$ cells. 93

26. IL-6 induces activation of STAT3 in control *Pten* $^{L/L}$ cells 96

27. IL-6 induces very little activation or upregulation of STAT1 in control *Pten* $^{L/L}$ cells. 99

28. Treating control *Pten* $^{L/L}$ cells with IL-6 has a modest effect on decreasing viral gene expression.....102

29. IL-6 provides a small amount of protection to control *Pten* $^{L/L}$ cells from rwt-induced cell death at low MOI. 105

List of Abbreviations

AKT	Protein kinase B
AR	Androgen receptor
BSA	Bovine serum albumin
CD	cytosine deaminase
cdk2	cyclin dependent kinase 2
DAPI	4',6-Diamidino-2-Phenylindole
DMEM	Dulbecco's modified Eagle's medium
ELISA	Enzyme-Linked Immunosorbent Assay
G protein	Viral glycoprotein, VSV
GFP	Green fluorescence protein
GSK-3β	Glycogen synthase kinase-3β
HPI	Hours postinfection
HBS	HEPES-buffered saline
HSV-TK	herpes simplex virus thymidine kinase
IFN	interferon
IL-1R	IL-1 receptor
IL-6	interleukin 6
IRF	IFN stimulatory factor
ISGF3	Interferon stimulated gene factor 3
ISREs	IFN-sensitive response element
JAK	Janus activated kinase
JNK	cJun N-terminal kinase
L protein	Large polymerase protein, VSV
LDL	Low density lipoprotein

LOH	Loss of heterozygosity
M protein	Matrix protein, VSV
MEF	Mouse embryonic fibroblast
MKK	MAP kinase kinse
MOI	Multiplicity of infection
mTOR	Mammalian target of rapamycin
N protein	Nucleocapsid protein, VSV
P protein	Phosphoprotein, VSV
PBS	Phosphate-buffered saline
PBST	PBS containing 0.25% Triton X-100
PE	Phycoerythrin
PI3K	Phosphatidylinositol-3-kinase
PIAS	Protein inhibitor of activated STAT
PIP_2	Phosphatidylinositol 4,5-bisphosphonate
PIP_3	Phosphatidylinositol 3,4,5-triphosphate
PKC- δ	Protein kinase C- δ
PKR	Protein kinase R
pRb	Retinoblastoma
PRRs	athogen pattern recognition receptors
PTEN	Phosphatase and tensin homology deleted on chromosome 10
PVDF	Polyvinyl difluoride
RIG-I	Retinoic-acid inducible gene I
ROI	Region of interest
shRNA	Short hairpin RNA

STAT3	signal transducer and activator of transcription 3
TAK1	TGF-β-activated kinase-1
TLRs	Toll-like receptors
TNFR	Tumor necrosis factor receptor
Tyk	tyrosine activated kinase
VSV	Vesicular stomatitis virus

Abstract

Yu, Nanmeng

CHANGES IN SUSCEPTIBILITY TO VESICULAR STOMATITIS VIRUS DURING PROGRESSION OF PROSTATE CANCER

Dissertation under the direction of

Douglas S. Lyles, Ph.D., Professor and Chair of Biochemistry

Vesicular stomatitis virus (VSV) is an attractive oncolytic virus. Differing sensitivity to VSV oncolysis of human prostate cancer cell lines has been observed in previous experiments. The goal of my experiments was to determine the mechanisms of sensitivity and resistance to VSV.

In Chapter 1, the changes in sensitivity to VSV during progression of prostate cancer were determined to test the hypothesis that sensitivity to VSV changes during prostate cancer evolution, from the stage of initiating mutation, to invasive adenocarcinoma and castration-resistant adenocarcinoma. In primary cultures of prostate *Pten* $^{-/-}$ tumor cells, the response of prostate cancer cells within the same tumor to VSV infection was heterogeneous. Some cells were susceptible to VSV, whereas other cells were resistant. The resistance of tumor-derived *Pten* $^{-/-}$ cells was not simply dependent on Pten loss, as acute deletion of the *Pten* gene resulted in sensitivity to VSV infection and poor interferon responsiveness. The resistant tumor-derived *Pten* $^{-/-}$ cells overexpressed antiviral signaling protein STAT1, and rapidly activated antiviral signaling in response to

VSV infection. Upon castration, castration-resistant prostate cancer cells gained sensitivity to VSV treatment.

In Chapter 2, the effect of mutating a single cancer-initiating gene on susceptibility to VSV infection was determined. Deletion of the *Rb* gene increased susceptibility to VSV infection and reduced interferon responsiveness of prostate epithelial cells. Downregulation of TAK1 had very little effect on sensitivity to virus.

In Chapter 3, the effect of activated IL-6/STAT3 pathway on sensitivity to VSV was evaluated. The resistant tumor-derived *Pten* $^{-/-}$ cells have activated IL-6/STAT3 signaling, overexpressing IL-6 that constitutively activates STAT3. Upon inhibition of STAT3 activation, signaling through type I interferon system was unaffected, and had very little effect on viral gene expression. However, inducing the activation of this pathway in normal *Pten* $^{L/L}$ cells had a small effect on protection from VSV infection. Together, these data suggest that activation of IL-6/STAT3 pathway does play a small role in antiviral defense against VSV in murine prostate epithelial cells.

Introduction

Prostate cancer poses a significant health problem worldwide. It is the most common visceral malignancy among men in the United States, and is the second leading cause of male cancer-related deaths (58, 62). Prostate carcinogenesis occurs through a series of genetic mutations and epigenetic alterations, such that normal prostate epithelium develops into invasive adenocarcinoma. For patients with localized prostate cancer, radiation therapy and/or radical prostatectomy typically achieve > 90% disease-free survival within five years (23, 142). However, treatment for metastatic disease is less effective. Since androgenic effects are important for growth of normal and malignant prostatic cells, androgen deprivation therapy was developed to control prostate cancer growth. Nonetheless, nearly all men with metastatic prostate cancer eventually develop castration-resistant disease after treatment with androgen deprivation, such that the cancer cells continue to proliferate under conditions of very low serum androgen. Patients who present with castration-resistant disease typically have poor prognosis, with median survival of 14 months following diagnosis (7, 65, 82). These patients have limited options with conventional anti-cancer therapy and would be candidates for oncolytic virus therapy.

Vesicular stomatitis virus (VSV) is an attractive oncolytic virus agent. It infects a wide range of cell types and readily induces apoptosis in the cells that it infects (85). VSV has been shown to infect and induce apoptosis in cancer cell lines from various tissue types, such as breast adenocarcinomas, pancreatic ductal adenocarcinomas and glioblastomas (2, 5, 25, 28, 90, 94). Although VSV demonstrates permissiveness in cancer cell lines of each tissue type, the common trend observed is that some cancer cell lines are susceptible to VSV infection and VSV-induced cell death, whereas other

cell lines are not. In prostate cancer, previous studies from our lab demonstrated that LNCaP cells are sensitive to infection and killing by VSV, while PC-3 cells are resistant to killing *in vitro* (2, 25). Similar results were obtained upon VSV treatment of the LNCaP and PC-3 tumors grafted into nude mice, where tumor regression was achieved in LNCaP tumors but not in PC-3 tumors (2). This differential response to VSV infection may result from the intrinsic heterogeneity of prostate cancer, such that various genetic aberrations within each tumor cause this variability in sensitivity to VSV treatment. The differential susceptibility to prostate cancer may also result from progression to tumor, such that sensitivity of to VSV treatment changes at different stages of tumor development. The goal of the experiments presented here is to determine susceptibility of prostate cancer to VSV during development of prostate cancer, from the stage of initiating mutation, to invasive adenocarcinoma to castration-resistant tumor. The experiments presented here also examine the mechanisms of susceptibility or resistance to VSV in prostate cancer.

Genetic Alterations in Prostate Cancer

Human prostate cancer develops as normal prostate epithelium acquires an initiating mutation that leads to formation of prostatic intraepithelial neoplasia or PIN, a proliferation of benign epithelial cells. Additional mutations and epigenetic changes lead to invasive adenocarcinoma of the prostate, in which there is an overwhelming proliferation of malignant cells that breaches the basal layer of epithelial cells, resulting in severe disruption of prostatic glandular architecture. Further mutations lead to development of metastatic prostate cancer that spreads to other organs. Patients with localized disease are treated with radiation therapy and radical prostatectomy.

Treatment for metastatic prostate cancer involves androgen deprivation therapy, which typically leads to formation of castration-resistant metastatic cancer by a number of mechanisms, including additional mutations and epigenetic changes.

There are several known risk factors for prostate cancer. The most important of which are age, ethnicity and genetic factors. The incidence of prostate cancer has a strong correlation with age due to accumulation of genetic mutations. Some of these genetic alterations include loss of heterozygosity (LOH) in the tumor suppressor *PTEN* (129, 131). Other tumor suppressors commonly lost in prostate cancer include pRb and TAK1 (81, 130). The role of these tumor suppressors in prostate carcinogenesis are discussed below.

PTEN (phosphatase and tensin homology deleted on chromosome 10) is one of the most frequently mutated tumor suppressor genes in human cancer. Its role as a major tumor suppressor gene was suggested when LOH was found in chromosome 10q23 in 31% of glioblastoma cell lines, 100% of prostate cancer cell lines and 6% of breast cancer cell lines (75, 116). These findings have been further confirmed in primary breast, endometrial, lung, colorectal, glioblastoma and prostate tumors. The role of *PTEN* as a tumor suppressor is further suggested by syndromes associated with germline mutations of the *PTEN* gene. This group of syndromes, known as *PTEN* hamartoma tumor syndromes, is characterized by aberrant growth of benign tumors, reviewed in (22). Patients with this syndrome have significantly higher risk of developing aggressive tumors (22).

In prostate cancer, *PTEN* undergoes copy number loss early in prostate carcinogenesis, in 20-30% of primary prostate cancer samples (129, 131). Overwhelmingly, deletion and/or mutations in the *PTEN* gene has been detected in advanced and metastatic prostate cancers (114, 123). The loss of *PTEN* in murine prostate cancer models demonstrates the functional role of *PTEN* as a tumor suppressor in the prostate. Mice with conditional deletion of the *Pten* gene in the prostate develop invasive adenocarcinoma as early as 9 weeks of age, whereas *Pten* heterozygotes develop invasive adenocarcinoma much later in life (129). Conditional prostate *Pten* knockout mice are also one of the few murine models that readily develop metastatic prostate cancer. Following castration, these mice develop castration resistant disease (129). Together, these studies demonstrate a major role for Pten as a tumor suppressor and indicate that Pten loss is involved in progression of prostate cancer.

The tumor suppressive properties of Pten are exerted by antagonizing the phosphatidylinositol-3-kinase (PI3K) signaling pathway (as reviewed in (44)). Upon stimulation of cells with growth stimuli, PI3K catalyzes the conversion of phosphatidylinositol 4,5-bisphosphonate (PIP_2) to phosphatidylinositol 3,4,5-triphosphate (PIP_3), a second messenger that promotes survival, growth and proliferation. PTEN is a plasma-membrane lipid phosphatase that negatively regulates PIP_3-mediated downstream signaling by hydrolyzing 3-phosphate on PIP_3 to generate PIP_2. With PTEN loss, PIP_3 accumulates and promotes the recruitment of the serine threonine kinases AKT1, AKT2, AKT3 and PDK1. Once recruited to the cellular membranes, AKT isoforms are activated by phosphorylation at two different residues. Activation of AKT signaling promotes cell survival through phosphorylation of proapoptotic factors such as BAD and procaspase-9, and cell progression and growth through glycogen synthase kinase-3

(GSK-3) and p21. Activation of AKT signaling also leads to indirect activation of mTORC1, which plays a role in mediating translation of proteins, and is a regulator that links nutrient sensing and to cell growth and cancer, (reviewed in (102)). In an analysis of mTOR signaling by Hsieh et al in prostate cancer, ribosomal profiling showed that mTOR regulates translation of mRNAs that are involved in cellular invasion and metastasis (59). Together, activation of this PI3K/AKT pathway plays a major role in mediating progression to tumor upon PTEN loss.

More recently, there has been an interest in AKT-independent roles of PTEN. Pten-null prostates eventually develop invasive adenocarcinoma. But transgenic models with prostate-specific overexpression of a constitutively active AKT develop only localized and mostly preneoplastic lesions (88). Discrepancies between other mouse models of *Pten* loss and *Akt* suggest that an AKT-independent mechanism contributes to PTEN tumorigenesis. A more recent cDNA analysis of isogenic cell line pairs silenced for PTEN showed a strong association of PTEN loss with activation of JNK pathway (127). The authors determined that that activation of JNK pathway upon PTEN loss is independent of AKT activation. They also demonstrated that JNK activation cooperates with AKT activation in tumorigenesis. As a member of the MAPK pathway, the role of JNK in carcinogenesis needs to be further investigated. However, these data suggest that the role of PTEN in regulating carcinogenesis is more than only regulating the AKT pathway.

Analyses of *Pten* deletion in genetically engineered mouse models have uncovered its cooperativity with other key genes that are deregulated in prostate carcinogenesis.

Inactivation of *Pten* has been shown to cooperate with loss of function of the Nkx3.1 homebox gene, a putative tumor suppressor specific to the prostate, to promote neoplastic formation (64). The loss of *Pten* also cooperates with the loss of tumor suppressor retinoblastoma (pRb) to promote earlier adenocarcinoma formation (64). Together, these studies demonstrate a role for PTEN to cooperate with other tumor suppressors in regulating prostate cancer progression.

The role of another tumor suppressor, the retinoblastoma (Rb) protein has been debated among prostate cancer biologists. Rb can prevent tumor progression by binding to transcription factors such as E2F and blocking their ability to activate transcription. E2F is a transcription factor that controls activities involved in transitioning from G_1 to S phase in the cell cycle. The genes that E2F control include DNA replication proteins, nucleotide biosynthetic proteins, cyclin E and cyclin dependent kinase 2 (cdk2), all of which are involved in mediating DNA replication. Thus, many of the genes involved in activation of DNA replication and the regulation of the G_1/S transition are under the control of the Rb/E2F pathway (24).

In prostate cancer, loss of chromosome 13q, including a region containing the *Rb* gene, occurs in at least 20% of the prostate tumors. Wang et al. demonstrated that with embryonic prostatic rescue and tissue recombination approaches, homozygous loss of Rb results in dysplasia and invasive adenocarcinoma (130). In a conditional Cre-dependent *Rb*-null model, only development of focal hyperplasia was observed within the mouse prostate (87). In another transgenic mouse model, SV40 large T antigen was dominantly expressed in prostate epithelia to inactivate Rb (56). These mice developed

aberrant proliferation and abundant apoptosis in prostatic luminal epithelial cells, which caused murine PIN development and confirmed the previous experiment. However, it was only with introduction of heterozygous *Pten* that the invasive adenocarcinoma phenotype was observed. Together, these studies demonstrate that loss of Rb early leads to development of low grade prostate cancer. More recently, Sharma et al. finds that Rb deficiency in prostate cancer cells offers very little proliferative advantage in the presence of androgen *in vitro* (107). But in androgen-deprived media, Rb deficient prostate cancer cells had significant proliferative advantage. A follow-up analysis determined that RB loss is overrepresented in prostate cancer metastases and castration-resistant disease (110). As a consequence of RB downregulation, E2F1 mediates overexpression of AR. RB downregulation also promotes more rapid tumor growth following castration (110). Together, these studies suggest a role for Rb in restricting tumor development in prostate cancer.

TGF-β-activated kinase-1 (TAK1) is a member of the MAP3K family, and a recently discovered tumor suppressor in the prostate. It is also a key intermediary in the signaling of Toll-like receptors (TLRs), IL-1 receptor (IL-1R), TNF receptor (TNFR) and TGF-β receptor (101). On activation by corresponding ligands, TLR/IL-1R and TNFR recruit and phosphorylate TAK1. Phosphorylated TAK1 subsequently activates IKB (IKK) and MAP kinase kinse (MKK) 4/7, leading to the activation of NF-KB and JNK respectively. NF-KB and JNK are important pathways for regulating immune response and inflammation (101).

Although TAK1 plays a major role in immune response, its role in cancer development is less apparent. Hepatocyte-specific deletion of *Tak1* leads to development of spontaneous hepatocyte death, but compensatory proliferation develops eventually causing carcinoma nodules to form (61). In this analysis, TAK1 appears to act as a tumor suppressor in hepatocytes. However, activation of TAK1 appears to promote metastasis of colorectal carcinoma to the lung (31). This analysis suggests a role for TAK1 as a proto-oncogene. It appears that TAK1 may have different effects on carcinogenesis depending on the tissue type.

In the prostate, deletion of DNA sequences from chromosome 6q14-21 is one of the most common deletion events in the genome of prostate cancers. High resolution SNP arrays and allele-specific analyses performed by Liu et. al detected deletion at 6q14-21 region in 38% of the prostate cancer specimens examined (81). Contained in this region is the *TAK1* gene. Deletion of the *TAK1* gene was considerably more frequent in high grade tumors, found in 75% of the Gleason grade 9 (high tumor grade) tumor specimens. *TAK1* deletion is also associated with poor PSA recurrence-free survival (66). Recently, Wu et. al demonstrated that deficiency of Tak1 in mouse prostate stem cells promotes cell growth *in vitro* and tumor development in tissue recombination studies *in vivo* (136). Together, these studies validate the role of TAK1 as a tumor supressor in the prostate.

The role of inflammation in tumor initiation and malignant progression has become a point of focus in cancer research. Of note, signal transducer and activator of transcription 3 (STAT3) activity has been linked to inflammation-associated tumorigenesis (141). STAT3 is a signaling protein that transduces extracellular signals

to the nucleus and regulates transcription of genes. Upon ligand stimulation, STAT3 is phosphorylated at Y705 tyrosine residue, dimerizes and translocates to the nucleus to bind to its cognate DNA response element. In many tumors, STAT3 directly interacts with the NF-kB family member RELA, trapping it in the nucleus and thereby contributing to constitutive NF-kB activation. Together, activation of these proteins leads to transcription of genes involved in tumor proliferation, survival, angiogenesis and invasion. Many STAT3-regulated genes encode cytokines and growth factors, notably interleukin 6 (IL-6), the receptors of which in turn activate the same STAT3 pathways, thereby propagating a positive feedback loop between tumor cells, promoting inflammatory responses that further support tumor growth and survival (52).

In prostate cancer, activation of STAT3 has been found in 77% of lymph node and 67% of bone metastases of clinical human prostate cancer specimens (1). Transduction of prostate cancer cell lines with STAT3 promoted migration and cell invasion *in vitro*, and significantly increased the number of prostate cancer metastases to the lung (1). Inhibiting expression of STAT3 induced apoptosis in prostate cancer cell lines (16). Together, these studies suggest that overexpression and activation of STAT3 promotes prostate cancer tumorigenesis and inhibiting STAT3 can be used as a strategy for treating prostate cancer.

Oncolytic Viruses in Prostate Cancer

The use of replication-competent viruses that can selectively replicate in and destroy neoplastic cells is a novel strategy in cancer therapy. Current oncolytic viruses under research include DNA viruses such as adenovirus, herpes simplex virus and vaccinia and RNA viruses such as Newcastle disease virus, reovirus and VSV (2, 4, 28, 39, 45,

60, 126, 143). Several of these viruses have been used in phase I clinical trials to determine safety and toxicity in prostate cancer patients. Just like conventional cancer therapy, strategies have been developed to target the oncolytic virus towards tumor cells and spare the normal cells. One of the first oncolytic viruses tested in prostate cancer patients is an adenovirus mutant that contains prostate-specific enhancer in the adenovirus genome in order to drive prostate-specific expression of adenovirus genes (36). Intraprostatic administration of this virus achieved 25-50% PSA reduction in some patients with local recurrence of prostate cancer. Strategies to enhance cancer cell death following virus infection include the incorporation of suicide genes such as the herpes simplex virus thymidine kinase (HSV-TK) into the virus genome, such that HSV-TK converts gancyclovir into a toxic product that specifically kills cancer cells. Incorporation of the cytosine deaminase (CD) gene that converts 5-fluorocytosine into a toxic metabolic also enhances tumor cell death. Adenoviruses that incorporate both of these suicide genes were also able to achieve PSA reduction in some of the patients with prostate cancer (115). Among RNA viruses, reovirus has been tested clinically for treatment of prostate cancer. Reovirus is a double-stranded RNA virus that demonstrates permissiveness in cells with aberrant Ras/RalGEF/p38 signaling (120). When administered to patients with prostate cancer, PSA reduction was observed in very few patients (126). The overall trend observed for oncolytic virus therapy in prostate cancer patients, is that some tumors respond to treatment, but many tumors do not. Better oncolytic viruses are still needed for prostate cancer patients.

Vesicular Stomatitis Virus

Vesicular stomatitis virus (VSV) is a member of the *Rhabdoviridae* family of viruses. It is an enveloped virus with helical nucleocapsid containing single-stranded, negative sense RNA. The 11kb RNA genome of VSV encodes genes for five proteins. The nucleocapsid (N) protein encapsidates the viral RNA genome, and together with the phosphoprotein (P) and the large polymerase protein (L), form the viral ribonucleoprotein complex. The L protein is responsible for transcribing viral RNA genome. The P protein binds L Protein to the nucleocapsid, and its phosphorylation is necessary for transcription activation (14, 15). Cryo-EM analysis showed that two nested, left-handed helices exist within the virion (47). The outer helix consists of the matrix (M) protein and the inner helix consists of the nucleoprotein N and RNA. The M protein also links neighboring M and N subunits, providing rigidity by clamping adjacent turns of the nucleocapsid (47). The M protein also binds to the lipid bilayer of the virus envelope. Contained in the viral envelope is the viral glycoprotein (G), whose role is to mediate virus attachment and penetration during infection.

The VSV lifecycle consists of the early events of attachment, penetration and primary transcription. Later steps in the lifecycle include secondary transcription and virus budding. Although VSV infects a wide range of cell types, the cellular receptor for G protein has been under debate. It has been proposed that nonspecific electrostatic and hydrophobic interactions mediate attachment of VSV G protein to the cell surface. Recently, Finkelshtein et. al demonstrated that LDL receptor and its family members may serve as a means for VSV G protein attachment (43). Following attachment, VSV penetrates into the cells via clathrin-dependent endocytosis and actin is involved at the completion of this process because the virus is too long to fit completely within a clathrin-coated vesicle (34, 89, 121). The process of fusion of viral membrane with endocytic

membrane to release the nucleocapsid is mediated by pH-dependent conformational changes in the G protein (99, 100). Upon membrane fusion, the internal virion components are released into the cytoplasm. The M protein dissociates from the nucleocapsids to allow primary transcription to occur. The viral RNA polymerase transcribes the leader RNA and the five viral transcripts from the viral genome. The viral mRNA transcripts are 5'-capped and polyadenylated in the 3' region by the viral L protein, and are translated into viral proteins using host cell translation machinery. Expression of viral proteins is required for the viral polymerase to begin replication of the viral genome. Also required for this process is encapsidation of nascent RNA, which serves as a signal for the viral polymerase to begin replication of the full length genome versus transcription of viral RNA. The positive sense antigenome is first synthesized, and serves as a template for replication of the negative sense progeny genome.

Once the viral progeny genomes are encapsidated, they can be assembled into progeny virions, or can be used as templates for secondary transcription. Secondary transcription is the major amplification step in the virus replication cycle, in which a majority of the viral proteins are synthesized. Assembly of the virus occurs at the plasma membrane. The G protein is synthesized by ribosomes associated with the rough endoplasmic reticulum and are transported to the plasma membrane via the secretory pathway. The M protein is a soluble protein and is found to associate with the plasma membrane. At the site of virus budding, nucleocapsids form complexes with M protein, and M protein directs the formation of the helical structure of the nucleocapsid. Finally, multivesicular body apparatus is relocalized and used for budding of the assembled virus.

Host Antiviral Responses

Intracellular virus replication creates products that are recognized by sensors known as pathogen pattern recognition receptors (PRRs). In the case of many negative stranded RNA viruses, the viral replication products activate the cytoplasmic PRR known as retinoic-acid inducible gene I (RIG-I) or other members of the RIG-I family. They may also activate membrane-associated receptors known as toll-like receptor (TLR) 4, 7 and 13 (49, 84, 104, 113, 140). Engagement of viral ligands of their cognate PRRs leads to activation of multiple signal transduction pathways that lead to activation of transcription factors, such as IFN stimulatory factor (IRF) 3 and NF-kB. These signaling molecules, upon activation, transduce to the nucleus and serve as transcriptional activators for interferon (IFN) production (reviewed in (96)). Type I IFN, which includes IFN-α and –β, bind to their cognate receptor. The type I IFN receptor is associated with Janus activated kinase (JAK) 1 and tyrosine activated kinase (Tyk2). Upon IFN engagement of their receptors, JAK1 and Tyk2 autophosphorylate which leads to phosphorylation and activation of signal transduction and activators of transcription (STAT) 1 and 2. Phosphorylation and activation of STAT1 leads to formation of homo- or heterodimers of STAT1, which interacts with IRF9 to form interferon stimulated gene factor 3 (ISGF3). This complex translocates to the nucleus and binds promoters that contain IFN-stimulated response elements (ISREs) that are present in the promoters of certain IFN-stimulated genes (ISGs). This leads transcription and expression of hundreds of antiviral genes that together induce an antiviral effect.

The functional importance of the type I IFN system in creating antiviral response to VSV was demonstrated when mice lacking type I IFN receptor subunits (IFN-α/βR $^{0/0}$) were

infected with VSV (93). IFN-α/βR $^{0/0}$ mice exhibit increased susceptibility to VSV, such that these mice died within 3-6 days of intravenous VSV inoculation, whereas the all of the wildtype mice survived. This increased susceptibility to VSV was also observed in mice with targeted disruption in STAT1 (38). Although disruption of key signal transduction molecules in the type I IFN system demonstrate the importance of type I IFN system in providing protection from VSV, no particular single downstream interferon stimulated gene product has demonstrated complete protection to VSV. For example, protein kinase R (PKR) inhibits viral replication by inhibiting protein translation through phosphorylation and inactivation of eukaryotic initiation factor 2α. PKR$^{-/-}$ mice were slightly more susceptible to VSV infection, depending on the route of inoculation (117). Recently, Fensterl et. al demonstrated a role for Ifit2/ISG54 gene product P54 in protection from VSV. P54 binds to the translation initiation factor eIF3 and inhibits protein translation. Ifit2$^{-/-}$ mice were not as susceptible to VSV as IFNAR$^{-/-}$ mice, but were more susceptible than wt mice (41). Another interferon-stimulated gene product, Rnase L, does not appear to enhance anti-VSV activity of IFNs (77). Together, these data suggest that the antiviral activity of the type I IFN system is exerted by cooperativity among multiple interferon-stimulated gene products.

Inhibition of Host Gene Expression by VSV

Many viruses evolve mechanisms to suppress or evade host antiviral responses. A primary mechanism by which VSV suppresses host antiviral responses is through inhibition of host gene expression. This occurs at the levels of transcription of host mRNA, transport of host mRNA from the nucleus to the cytoplasm and translation of host mRNA into proteins. The viral M protein is the major viral gene product that mediates this inhibitory activity. Expression of M protein in transfected cells in the absence of other viral components inhibits expression of cotransfected genes driven by

a wide variety of different promoters (19-21, 42). Transfection of cells with M protein, inhibited transcription of genes from RNA polymerase I, II and III -dependent promoters (3). The host protein Rae1 is involved in this process. Rajani et al found that M protein interacts with Rae1 and silencing of Rae1 restored host RNA synthesis to 40% of uninfected control levels (97). M protein has very little effect on transcription in *Xenopus* oocytes, and the role of M protein in inhibiting nuclear-cytoplasmic transport was investigated in these cells. Radiolabeled RNAs were injected into the nucleus of the *Xenopus* oocytes preinjected with M mRNA, and M protein inhibited the movement of radiolabeled RNAs from the nucleus to the cytoplasm (54). This effect is likely independent of Rae1, as silencing Rae1 had little effect on net accumulation of host mRNA in the nucleus upon VSV infection (97). The translational control of protein synthesis by VSV was shown by polysome profiling. The average size of polysomes translating individual cellular mRNAs were reduced following VSV infection, suggesting that VSV infection altered translation of host mRNA (83). Rae1 does not appear to be involved in host translation, as silencing of Rae1 did not alter the rate of host or viral protein synthesis (97). VSV infection does alter the host translation apparatus, by dephosphorylating the cap-binding translation factor eIF4E (33). Thus, VSV inhibits host gene expression at levels of transcription, nuclear-cytoplasmic transport and translation such that host innate immune responses are inhibited and viral replication can occur.

VSV as an oncolytic agent

Vesicular stomatitis virus is an attractive oncolytic agent. It infects a wide range of cell types. This widespread infectivity is an important aspect when considering VSV as a therapeutic agent for the treatment of malignancies, so that different types of tumors can be treated. Although wildtype VSV produces an acute, febrile disease in cattle, it rarely produces significant disease in humans. Some laboratory adapted strains, whose

pathogenicity have been largely attenuated, cause very little if any morbidity and mortality in immunocompromised and immunocompetent mouse models (2, 85, 119). These attenuated strains of VSV are promising as candidate oncolytic viruses because they exhibit very little pathogenicity but show no reduction in their oncolytic potential (2, 119). Compared to other replication-competent vectors, VSV is particularly appealing for its rapid replication rate of 8-12 hours in susceptible tumor cells, such that significant tumor destruction may have occurred prior to the initiation of host adaptive immune system (2, 5, 12, 118). VSV has not been shown to undergo any genetic recombination or reassortment during infection and replication. More importantly, VSV does not exhibit any evidence of transforming potential and does not integrate any part of its genome into the host (12). Seroprevalence studies also indicate that exposure to VSV is generally uncommon, which suggests that there would be very little preexisting immunity that would mediate clearance of VSV when used as an oncolytic virus (85).

Recombinant strains of VSV have been generated to improve the oncolytic capabilities of VSV and to enhance specificity for tumor cells, providing a safer alternative for human cancer therapies. VSV strains harboring mutations in the M protein, compared to those with wildtype M protein, are defective in their ability to suppress host antiviral responses, including the IFN response (119). Since some tumor cells are defective in their antiviral responses, the selectivity of viruses for tumor cells versus normal cells can be enhanced by strategies that activate antiviral response in normal cells. This can be achieved by either pretreatment with IFNs or by using VSV strains that induce IFN production, such as M protein mutant viruses or recombinant VSV that expresses IFN from the viral genome (118, 119). The wt strains of VSV induce relatively little IFN production in infected cell. This is due to inhibition of host gene expression by the viral matrix (M) protein. The rM51R virus is a virus isogenic to recombinant wild type virus. It contains a

mutation that substitutes an arginine for methionine at position 51 of the 229 amino acid M protein. This mutation renders the virus defective in its ability to inhibit host gene expression, but does not compromise the expression of viral genes or the production of infectious progeny (4, 119). The rM51R virus is just as potent as the recombinant wt virus in inducing tumor cell lysis *in vitro* and tumor regression *in vivo* (2, 119).

VSV induces oncolysis by inducing apoptosis. The wt M protein induces apoptosis directly through inhibition of host gene expression (85). The M protein activates the mitochondrial pathway of apoptosis, which involves the release of cytochrome c and other proapoptotic proteins from the mitochondria. This results in the activation of the initiator caspase, caspase 9 (85). The M protein mutant viruses are defective in shut-off of host gene expression. Consequently, the M protein mutant viruses induce apoptosis by a mechanism other than the shut-off of host gene expression. In fact, the M protein mutant viruses appear to induce apoptosis by inducing activation of the death receptor pathway (85). The initiator caspase 8 is activated as part of this response.

Aberrant Antiviral Signaling in Cancer

The current research on oncolytic virus therapy is based on the principle that as some tumors evolve, they pursue proliferative signaling pathways that are antagonistic to antiviral signaling pathways, rendering these tumor cells more susceptible to virus infection than normal cells. IFNs inhibit cell growth and control cellular apoptosis and are generally antiproliferative (48). Activation of STAT1 signaling pathway by IFNs leads to expression of procaspases and induce apoptosis (30, 35). In addition to these proapoptotic effects, IFNs are often cytostatic. This growth-inhibitory activity is mediated through suppression of the pocket proteins and inhibitors of cyclin-dependent kinases, thereby causing cell cycle arrest (103). Thus, many cancers compromise expression of

antiviral signaling molecules to promote cell survival (11, 37, 134). These cancer cells downregulate key components of the antiviral signaling, including STAT1, Jak1 and Rnase L. Such defects in antiviral signaling render these cancer cells susceptible to oncolytic viruses.

It is interesting to note that upregulation of interferon responses may also promote tumorigenesis. Hix et al demonstrated that overexpression of STAT1 in low metastatic breast cancer cells promoted aggressive tumor growth. This may occur through suppression of antitumor T cell function, thereby driving breast cancer progression (57). Microarray comparison of gene expression changes between invasion sites and primary sites of melanomas revealed significant enrichment of STAT1 signaling pathway in invasion sites (105). Silencing STAT1 impaired the migratory and invasive capabilities of metastic melanoma cells (105). These data suggest that upregulation or activation of STAT1 may be necessary for progression to tumor in some cancer cells. In these cases, cells may acquire resistance to oncolytic viruses during progression to tumor.

Human Prostate Cancer Cell Lines are Differentially Susceptible to VSV

Different tumor cell lines, although derived from the same tissue type, show differential sensitivity to VSV infection. In malignant glioblastoma cell lines treated with VSV, some cell lines such as U87 cells are highly sensitive to VSV infection and are not protected by pretreatment with IFN, whereas other cell lines such as A172 retain some IFN-response and are protected from infection by VSV (132). In the case of prostate cancer, PC-3 cells are resistant to VSV infection whereas LNCaP cells are sensitive. These two cell lines derived from metastatic prostate cancers are differentially responsive to VSV treatment, and illustrate the heterogeneous response of prostate cancer cell lines to VSV

infection (2). A subsequent analysis by Carey et. al found that there were major delays in the early events of virus replication cycle in PC-3 cells when compared to LNCaP cells, suggesting that IFN-stimulated genes are active at multiple steps in PC-3 cells to deter virus replication (25). Indeed, a microarray analysis comparing gene expression changes between PC-3 and LNCaP cells overexpression of antiviral genes in PC-3 cells, and overexpression of the key IFN signaling molecule STAT1 was confirmed by immunoblotting (25).

These studies suggest that during tumor progression, some cancer cells may upregulate their antiviral responses to promote aggression, whereas other cancer cells may downregulate their antiviral responses to promote survival. I hypothesize that the susceptibility of prostate cancer changes during tumor development, at the stages of initiating mutation, invasive adenocarcinoma and castration-resistant adenocarcinoma. This hypothesis was tested using cells derived from a murine model of prostate cancer, the prostate *Pten* knockout mouse. Primary cultures of tumor-derived *Pten* $^{-/-}$ cells contain a mixture of cells that are susceptible and resistant to VSV. Upon castration and tumor evolution, castration-resistant tumors develop susceptibility to VSV. Clonal populations of tumor-derived *Pten* $^{-/-}$ cells in long-term culture poorly support viral gene expression even when infected at high MOI. This is not simply dependent on *Pten* deletion because cells that are deleted for the *Pten* gene *in vitro* (acutely-deleted *Pten* $^{-/-}$ cells) are susceptible to VSV infection and support viral gene expression. In addition, acutely-deleted *Pten* $^{-/-}$ cells were also poorly responsive to IFN treatment and protection from VSV-induced cell death. Tumor-derived *Pten* $^{-/-}$ cells also exhibit resistance to VSV-induced cell death when compared to acutely-deleted *Pten* $^{-/-}$ cells. Tumor-derived *Pten* $^{-/-}$ cells also overexpress STAT1. Together, these data in chapter 1

suggest a model in which prostate epithelial cells are susceptible to VSV and poorly responsive to IFN protection when *Pten* is acutely deleted. During tumor development, prostate cells acquire resistance to VSV infection and thereafter-induced cell death. Upon castration, castration-resistant tumors evolve to regain VSV sensitivity.

The differences susceptibility to VSV may also arise due to the various genetic alterations occuring during prostate carcinogenesis. Dysregulation of oncogenic pathways, such as loss of the tumor suppressor pRb or TAK1, may have consequences on antiviral signaling and affect susceptibility to VSV. The effect of loss of *Rb* was tested in murine prostate epithelial cells. $Rb^{-/-}$ cells were more susceptible to VSV-induced cell death. Downregulation of *Tak1* had very little effect on susceptibility to VSV or response to IFN. Together, these data in chapter 2 suggest that IFN response and susceptibility to VSV may be dependent on the type of genetic alterations occuring during prostate carcinogenesis.

Activated STAT3 have been shown to modulate prostate carcinogenesis, as well as antiviral defense. Chapter 3 explores the effect of activated IL-6/STAT3 signaling on susceptibility to VSV. Tumor-derived $Pten^{-/-}$ cells have constitutively active STAT3 signaling, which is mediated by high levels of IL-6 production. Activated STAT3 has very little effect on activation and expression levels of STAT1. However, IL-6 induced activation of STAT3 plays a small role in mediating antiviral defense against VSV, protecting control $Pten^{L/L}$ cells from VSV infection at low multiplicities of infection.

Materials and Methods

Mice

Prostate-specific *Pten* $^{-/-}$ mice were generated by crossing *Pten* $^{Loxp/Loxp}$ mice with mice of the ARR2Probasin-*Cre* transgenic line PB-Cre4, in which expression of the cre recombinase is under the control of a modified rat prostate-specific probasin promoter, as previously described (74, 138). *Pten* L/L mice were backcrossed to C57BL/6 for 3-5 generations (17). The mice were a generous gift from Dr. Yong Q Chen's laboratory at Wake Forest School of Medicine. DNA was acquired via tail snipping for genotyping. Castration procedure was performed on prostate-specific *Pten* $^{-/-}$ mice at 3 months of age under isoflurane anesthesia. Recovery from the procedure was carefully monitored. All animals were maintained in an isolated environment. Animal care was conducted in compliance with the state and federal Animal Welfare Acts and the standards and policies from the US Department of Health and Human Services. The protocol was approved by the Institutional Animal Care and Use Committee at Wake Forest University.

Cells and Viruses

Primary cultures of epithelial cells were derived from prostates of normal *Pten* $^{L/L}$, tumor *Pten* $^{-/-}$ and castration-resistant *Pten* $^{-/-}$ mice at 3 and 6 months of age. This culture method was first developed by Nandi et al and was modified by Barclay et al (13, 95). Briefly, prostate lobes wre microdissected from the mice and collected into tubes containing HEPES-buffered saline (HBS). The prostate lobes were washed repeatedly in HBS containing 5% penicillin/streptomycin. The prostate lobes were then minced using a sterile razor blade and digested for 2-3 hours using 225U/mL of collagenase (type IV, Worthington). Digestion was considered complete when the organoids were

released from the surrounding stroma. The digested tissue was layered on to a Percoll gradient and the epithelial organoids were separated from the stromal cells and debris by gradient centrifugation (2000rpm, 20 mins). The fraction containing epithelial organoids was isolated and washed repeatedly. The organoids were cultured in Dulbecco's modified Eagle's medium (DMEM)/F12 (1:1) containing 1% fetal bovine serum, 10% bovine serum albumin (Sigma), 10 ng/mL of cholera toxin (BD biosciences), 28 ug/mL of bovine pituitary extract (Hammond Cell Tech), 80 ug/mL of gentamycin, 8 ug/mL of insulin (Gibco), alpha tocopherol (2.3×10^{-6} M), 5 ug/mL of transferrin (Sigma) and trace elements. The organoids were cultured in dishes coated with rat-tail collagen. Cell outgrowths from the organoids formed a confluent monolayer by day 6 of harvest and were used for experiments. Only passage 2 and passage 3 of the cells were used for primary culture experiments.

Long term cultures of *Pten* $^{L/L}$, acutely-deleted *Pten* $^{-/-}$, tumor-derived *Pten* $^{-/-}$, shNC, shTAK1, *Rb* $^{L/L}$ and *Rb* $^{-/-}$ cells were obtained from Dr. Scott Cramer's laboratory and maintained in the aforementioned medium (9, 13, 135). Briefly, *Pten* $^{L/L}$ cells were spontaneously immortalized from prostate epithelial cells of 8 week old *Pten* $^{L/L}$ mice. Acutely-deleted *Pten* $^{-/-}$ cells were derived by transducing *Pten* $^{L/L}$ cells with lentivirus expressing cre recombinase to achieve *Pten* deletion *in vitro*. Tumor-derived *Pten* $^{-/-}$ were obtained by spontaneous immortalizing prostate cells from 16 week old *Pten* $^{-/-}$ mice.

The recombinant viruses, rwt and rM51R, as well as viruses encoding GFP and palmitoylated form of dsred were prepared in BHK cells, by infecting at a low MOI and harvesting the virus after cytopathic effect is observed (69).

Immunofluorescence

Primary cells were seeded on to rat-tail collagen coated imaging plates. Following infection, cells were washed three times with phosphate-buffered saline (PBS) and fixed with 4% paraformaldehyde at room temperature for 15 mins. The cells were permeabilized with PBS containing 0.25% Triton X-100 (PBST) for 15 mins. Cells were washed with PBS and blocked with 1% BSA in PBST for 30 mins. Cells were incubated with anti-pancytokeratin conjugated to the phycoerythrin fluorophore (Sigma) for an hour with constant agitation. Cells were then washed and incubated with 1 ug/mL of DAPI (4',6-Diamidino-2-Phenylindole) to detect DNA.

Microscopy and Imaging Analysis

Long term culture cells were seeded on 6 well tissue culture dishes. Cells were infected at the indicated MOI with VSV-GFP or VSV-dsRed. At 24 hours postinfection, fluorescence and bright field images were captured using Retiga EX 1350 digital camera (QImaging Corp) attached to a Nikon Eclipse TE 300 inverted microscope.

Images of fixed primary cells were acquired using a BD Pathway 855 instrument. Image analysis was performed using BD Attovision software. Briefly, a region of interest (ROI)

was defined using area occupied by DAPI. Each area occupied by DAPI (ROI) denotes a single cell. For each ROI, fluorescence intensity in GFP and PE channels were determined. The number of cells that both express viral protein (GFP) and cytokeratin (PE) were expressed as a percentage of the total number of cells that express cytokeratin (PE). Images shown are merged images of GFP, PE and DAPI channels.

Cell Viability Assay

Cells were grown in 96 well tissue culture dishes until 70% confluence and were then infected with viruses at indicated multiplicities of infection (MOI). At various times postinfection, live cells were measured using MTT assay (cell proliferation kit 1, Roche Diagnostics).

Metabolic Labeling

Cells were grown in 6 well tissue culture dishes until 70-90% confluence and were then infected with viruses at MOI of 10. At indicated times postinfection, cells were pulse-labeled for 20 mins using ^{35}S-methionine at 100 uCi/mL. Cells lysates were harvested in RIPA buffer and resolved on (sodium dodecyl sulfate-polyacrylamide) SDS-PAGE gels. Phosphorescence imaging was used to analyze the gels.

Immunoblotting Analysis

Cells were seeded in 6 well tissue culture dishes until 70-90% confluence and were then mock or virus-infected with various MOIs. At indicated times postinfection, cell lysates

were prepared in RIPA buffer containing 1 mM aprotinin, 1 uM leupeptin, 1 uM E-64 protease inhibitor, 500 uM AEBSF and 1X PhosSTOP (Roche Applied Sciences). Proteins were resolved on SDS-PAGE gels and were transferred on to 0.45 um polyvinyl difluoride (PVDF) membranes. The membranes were blocked for 1 hour in PBS containing 0.1% Tween 20 and 5% nonfat dried milk. Immunoblots were then probed with antibodies against the viral matrix (M) protein, phospho-STAT1 (tyrosine 701; Cell Signaling), STAT1 (Cell Signaling), phospho-STAT3 (tyrosine 705, Cell Signaling) or STAT3 (Cell Signaling). Phosphoproteins were probed before unphosphorylated proteins. Proteins were detected using enhanced chemiluminescence substrate (Thermo Scientific). The intensity of the bands was quantified using ImageJ software.

IFN Responsive Assay

Cells were pretreated with indicated concentrations of universal type I IFN (PBL interferon source). Cells were infected with virus at indicated MOI. At 72 hours postinfection, cells were treated with MTT reagent and cell viability was determined.

Enzyme-Linked Immunosorbet Assay (ELISA)

Cells (5×10^5) were seeded into 6 well tissue culture dishes. After attachment, medium was aspirated. Cells were mock- or VSV-infected in low volume for an hour and then fresh medium was layered on the cells. At indicated times, supernatants were harvested and stored at -20^0C. Supernatants were analyzed for the presence of murine interleukin-6 (IL-6) using BD ELISA detection kit. Briefly, capture Ab was coated on to ELISA plates and incubated overnight. The plates were washed and blocked with assay diluent.

Samples were diluted 100 fold and added to the plate. Following incubation, detection antibody was added. IL-6 concentration was measured against known standards.

Inhibition of IL-6

Tumor-derived *Pten* $^{-/-}$ were incubated with medium containing the indicated concentrations of anti-murine IL-6 antibody (R&D Systems). Cell lysates were prepared at 16, 40 and 64 hours posttreatment to determine phospho- and total STAT1 as well as phospho- and total STAT3 levels.

To determine viral gene expression following inhibition of IL-6, tumor-derived *Pten* $^{-/-}$ were incubated with medium containing the indicated concentrations of anti-murine IL-6 antibody for 16 hours. At 6, 12 and 24 hours postinfection, cell lysates were harvested for immunoblot analysis of viral M protein expression.

IL-6 Treatment

Control *Pten* $^{L/L}$ cells were incubated with medium containing the indicated concentrations of recombinant murine IL-6 (Sigma) cytokine. Cell lysates were prepared at 1, 2, 3 and 6 hours posttreatment to determine phospho- and total STAT1 as well as phospho- and total STAT3 levels.

To determine viral gene expression following IL-6 treatment, control *Pten* $^{L/L}$ cells were incubated with medium containing the indicated concentrations of IL-6 cytokine for 1

hour. Cells were mock-infected or infected with rwt-GFP. At indicated times postinfection, cells were trypsinized from the tissue culture plates using 0.125% trypsin in PBS. The reaction was stopped using trypsin inhibitor (Gibco). Cells were fixed in 4% PFA for 20 mins. GFP fluorescence was analyzed using a Becton Dickinson FACSCaliber flow cytometer.

To determine cell viability following IL-6 treatment, control *Pten* $^{L/L}$ cells were incubated with medium containing the indicated concentrations of IL-6 cytokine for 1 hour. Cells were mock or VSV-infected. At indicated times postinfection, cells were incubated with MTT reagent to determine cell viability.

Statistical Analysis

Statistical analysis of two groups was performed using a student's t-test. One way analysis of variance (ANOVA) was performed on data with two or more groups. Two way ANOVA with Bonferroni post-test was performed for all pairwise multiple comparisons. All statistical analyses were performed with GraphPad Prism software.

Chapter 1

Susceptibility of Prostate Cancer to VSV Oncolysis during Progression of Prostate Cancer

Effects of Infecting Primary Prostate Tumors Cells with VSV

Many cancer cells downregulate their antiviral responses, rendering them susceptible to treatment with oncolytic viruses like VSV. However, individual cancer cell lines vary dramatically in their sensitivity to oncolytic viruses, even when these cancers arise from the same tissue type. For example, human prostate cancer cell lines respond very differently to VSV infection (2, 28). PC-3 cells are resistant to VSV infection whereas LNCaP cells are sensitive. The variability in response of prostate cancer cells to VSV infection may arise due to differences in the initial genetic lesions leading to prostate cancer development. Alternatively, susceptibility to VSV oncolysis may change during cancer progression. Human prostate cancers are heterogeneous in histologic architecture, immunophenotype and genetic diversity (106). This raises the possibility that susceptible and resistant cells may coexist in the same tumor.

These two hypotheses were tested using primary prostate epithelial cell cultures from transgenic Pb-Cre4 x *Pten* $^{loxp/loxp}$ mice. In this mouse model, prostate-specific deletion of the *Pten* gene flanked by loxP sites is achieved by expressing Cre recombinase under the control of a probasin promoter (128). From a single genetic alteration of *Pten* deletion, these transgenic mice develop prostatic lesions from normal prostate epithelium that develop to the stage of invasive adenocarcinoma. Upon castration, these transgenic mice are capable of developing castration-resistant tumors that model castration-resistant adenocarcinoma in humans (128).

Cells cultured from normal mouse prostates or prostate tumors were primarily of epithelial origin as shown by cytokeratin expression. Shown in Fig. 1 are fluorescence images of cells cultured from normal *Pten* $^{L/L}$ prostates, *Pten* $^{-/-}$ prostate tumors, and castration resistant *Pten* $^{-/-}$ prostate tumors. The cells were cultured according to the procedure described by Barclay et. al, in a system that promotes epithelial cell growth (13). Cells were seeded at passage 2 or 3 onto imaging plates and labeled with DAPI as a marker for the nucleus, and immunolabeled for cytokeratins as a marker of epithelial cells. Mouse embryo fibroblasts (MEFs) were used as a negative control for cytokeratin labeling. 85-95% of the cultured prostate cells were positive for cytokeratin, indicating their epithelial origin. In previously published data, these cells also express markers of both luminal and basal epithelium (13).

Figure. 1. Primary cultures of mouse prostate epithelial cells express cytokeratin. Primary cultures of mouse prostate epithelial cells were cultured from normal *Pten* $^{L/L}$ prostates, *Pten* $^{-/-}$ prostate tumors, and castration resistant *Pten* $^{-/-}$ prostate tumors. Cells were seeded into imaging plates and stained with DAPI (blue) as a marker for the nucleus, and immunolabeled for cytokeratin (red) as a marker for epithelial cells. Using the region marked by DAPI to denote a single cell, the number of cells immunolabeled with cytokeratin were counted and shown in the graph. Murine embryonic fibroblasts (MEFs) were used as a negative control for cytokeratin immunolabeling.

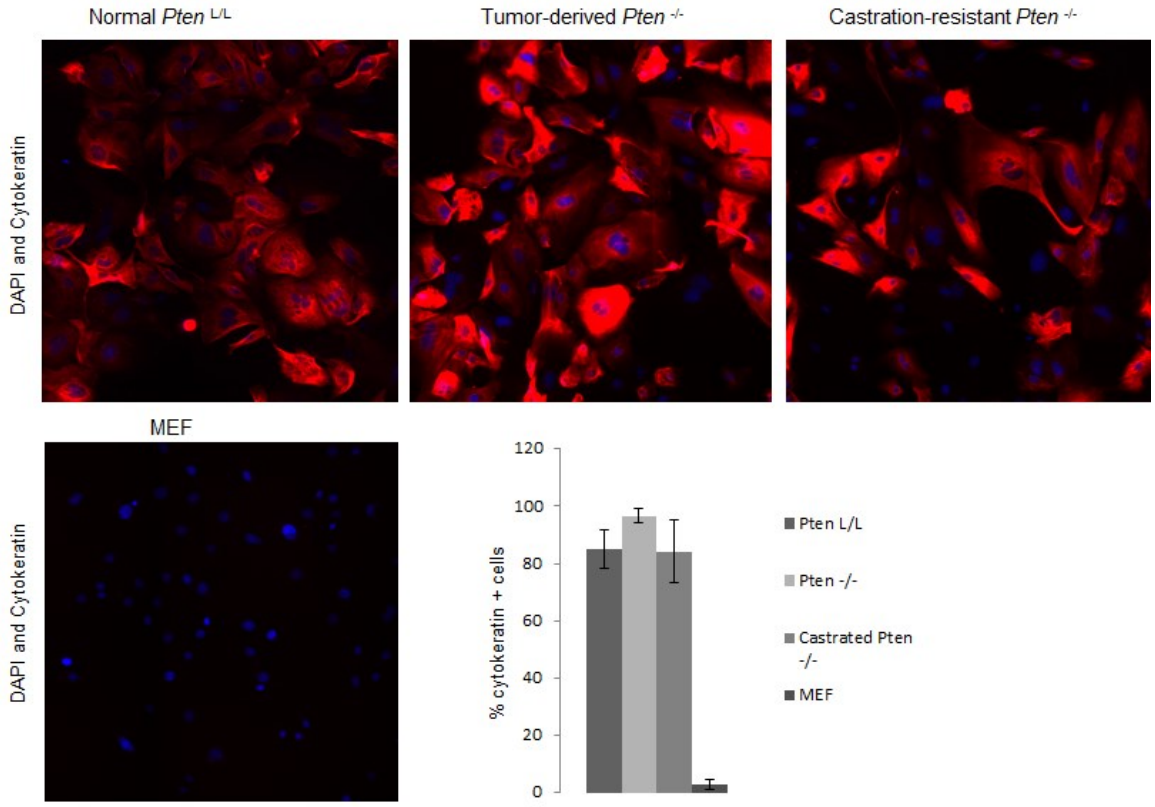

In order to determine whether cells derived from *Pten* $^{-/-}$ prostate tumors are susceptible to VSV infection, primary prostate cells from 3 month old prostate-specific *Pten* $^{-/-}$ mice and their littermate controls were infected with the recombinant virus containing a wt M protein (rwt) and the isogenic M protein mutant virus (rM51R) at MOI of 10 for 16 hours. Both viruses encode the fluorescent protein GFP so that susceptible cells express GFP. Cells were then fixed and stained with DAPI and anti-cytokeratin antibody. Fluorescence images of normal and tumor-derived cells infected with rwt-GFP are shown in Figure. 2A. The numbers of cells that express both GFP and cytokeratin were expressed as a percentage of total cytokeratin positive cells, and data from multiple experiments are shown in Figure. 2B.

When normal *Pten* $^{L/L}$ prostate epithelial cells were infected with rwt virus, most of the epithelial cells (75%) were infected and express GFP. These results are consistent with previous data that normal human prostate epithelial cells are susceptible to VSV (2). In contrast, significantly fewer of the cells in *Pten* $^{-/-}$ prostate tumors (42%) expressed detectable GFP. The number of prostate cells that expressed detectable GFP from the attenuated M protein mutant virus (rM51R) was less than that of cells infected by rwt virus, likely due to the induction of antiviral responses in some of the cells by the M protein mutant virus. Nonetheless, the prostate epithelial cells infected with M protein mutant virus exhibited a similar trend in that fewer cells from *Pten* $^{-/-}$ tumors support GFP expression compared to normal *Pten*$^{L/L}$ prostate epithelial cells. These results indicate that even with a single defined initiating genetic lesion of *Pten* deletion, a heterogeneous response to VSV infection develops in the prostate tumor during carcinogenesis.

Figure. 2. Prostate tumors contain a mixture of resistant and susceptible cells. Primary cultures of prostate epithelial cells were cultured from *Pten* $^{-/-}$ prostate tumors of 3 month old mice and their littermate normal *Pten* $^{L/L}$ controls. Cells were seeded into imaging plates and were infected with rwt-GFP and rM51R-GFP viruses (green). Cells were fixed and immunolabeled for cytokeratin (red) and stained with DAPI as a marker for the nucleus (blue). Representative fluorescence images are shown in A. The number of cells that were positive for GFP and cytokeratin were counted and expressed as a percentage of total cytokeratin positive cells (B). Data shown are average of at least 3 experiments +/- SEM.

A

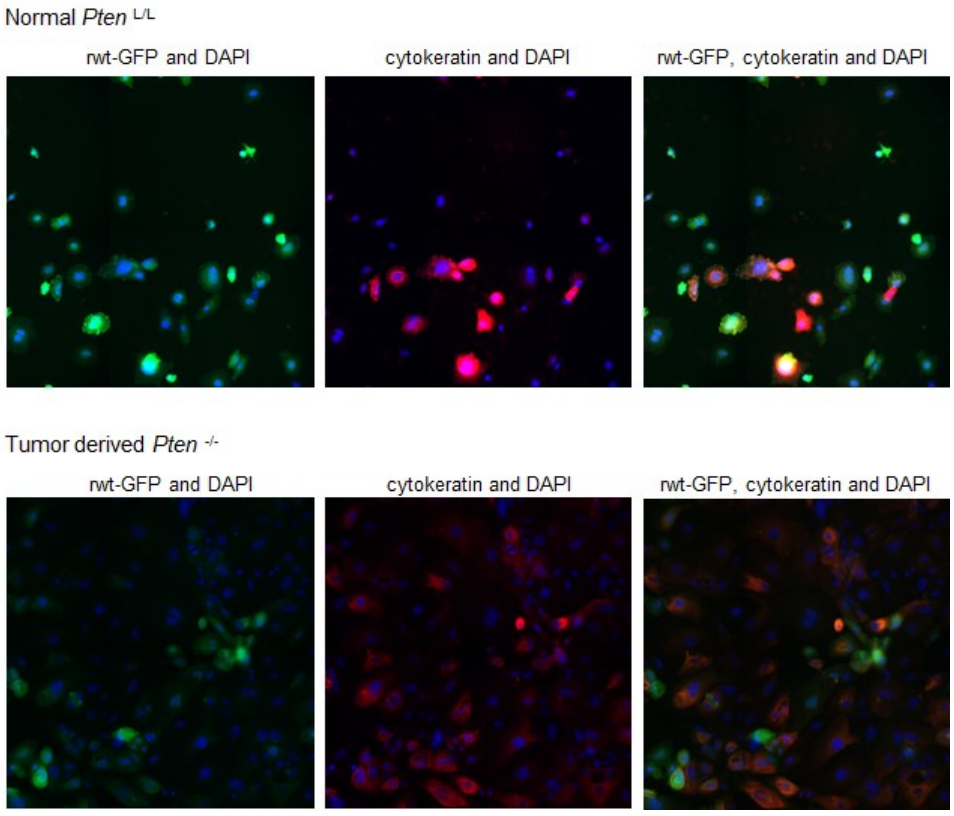

B

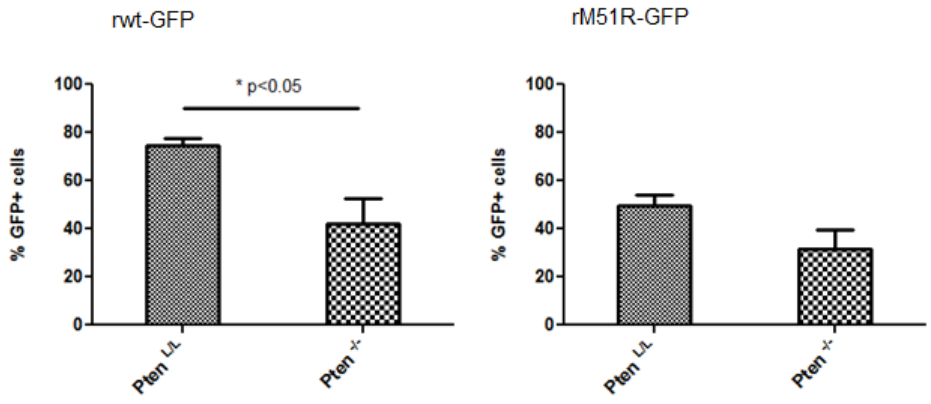

Figure. 2. Prostate tumors contain a mixture of resistant and susceptible cells.

In order to determine the susceptibility of castration resistant *Pten* $^{-/-}$ prostate tumors to VSV infection, transgenic Pb-Cre4 x *Pten* $^{loxp/loxp}$ mice were castrated at 3 months of age, and cells were cultured from castration-resistant *Pten* $^{-/-}$ prostate tumors at 6 months of age. Normal *Pten* $^{L/L}$ prostate cells and *Pten* $^{-/-}$ prostate tumor cells from 6-month-old noncastrated mice served as controls. The cells were infected, stained, and imaged, and subjected to the same analysis as in Figure. 2. Shown in Figure. 3 are images of cells from castration-resistant *Pten* $^{-/-}$ and 6 month old control *Pten* $^{-/-}$ tumors following infection with rwt-GFP virus. Most of the castration-resistant *Pten* $^{-/-}$ prostate tumor cells (approximately 62%) expressed GFP similar to the results with normal Pten$^{L/L}$ cells. In contrast, the cells from control *Pten* $^{-/-}$ mice at 6 months still consisted of a mixture of cells that were primarily resistant cells that support very little viral gene expression, similar to the results with 3 month old mice in Figure. 2.

Figure. 3. Castration resistant tumor cells are susceptible to VSV infection.

Pten $^{-/-}$ mice were castrated at 3 months of age and by 6 months of age developed castration resistant tumors. Primary cultures of prostate epithelial cells were cultured from *Pten* $^{-/-}$ prostate tumors of 6 month old mice, castration resistant tumors, and their littermate normal *Pten* $^{L/L}$ control prostates. Cells were seeded into imaging plates and were infected with rwt-GFP and rM51R-GFP viruses (green). Cells were fixed and immunolabeled for cytokeratin (red) and stained with DAPI as a marker for the nucleus (blue). The fluorescence images captured were shown in A. The total number of cytokeratin positive cells was counted. The number of cells that are positive for GFP and cytokeratin were counted and expressed as a percentage of total cytokeratin positive cells (B). Data shown are average of at least 3 experiments +/- SEM.

A

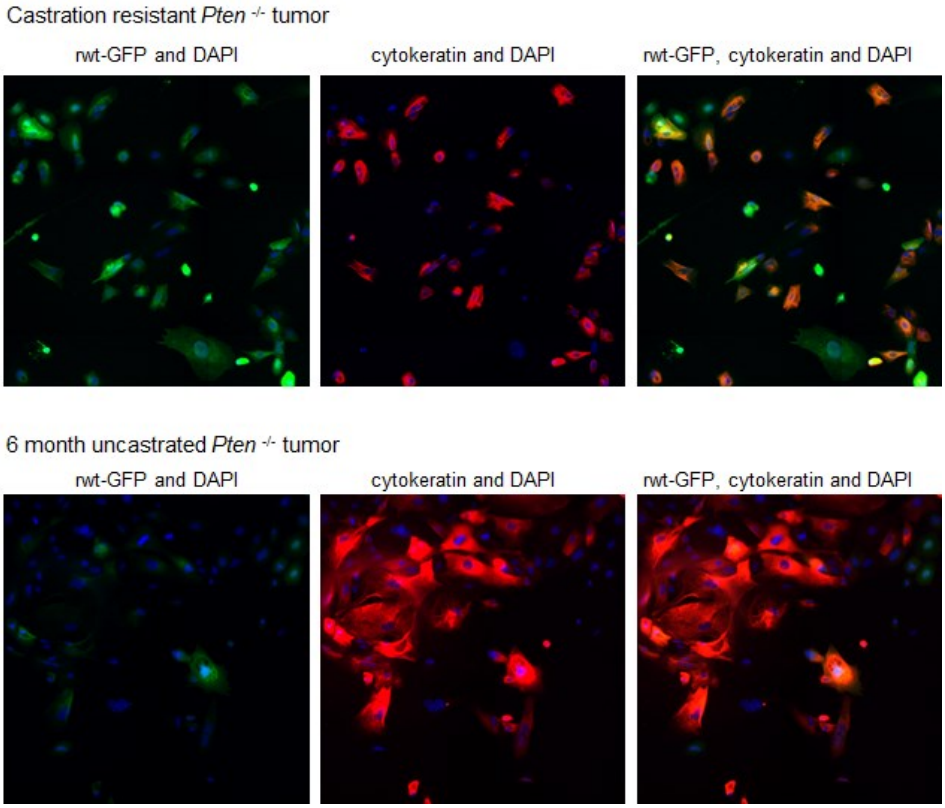

B

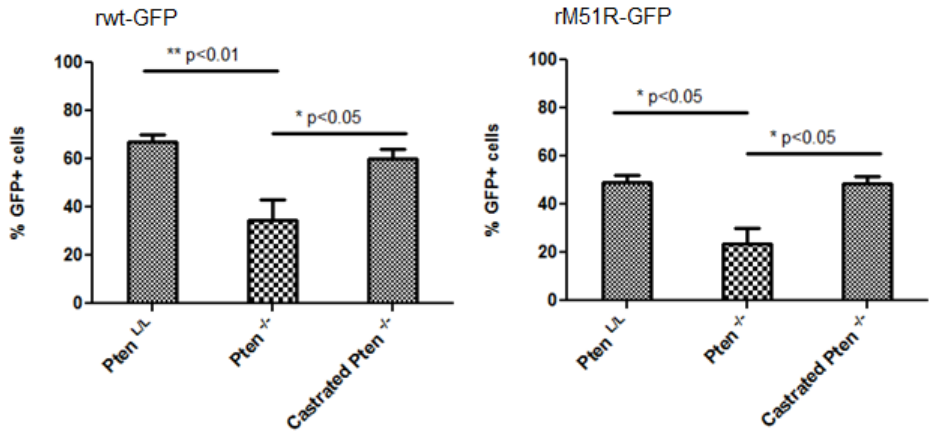

Figure. 3. Castration resistant tumor cells are susceptible to VSV infection.

The observation that *Pten*$^{-/-}$ prostate tumors contain a mixture of VSV-sensitive and VSV-resistant cells (Figure. 2 and Figure. 3) suggests that resistance does not result from *Pten* deletion alone but instead results from cellular changes during tumor progression. To further determine whether resistance to VSV develops from a single genetic lesion of *Pten* deletion or from tumor progression, clonal populations of mouse prostate epithelial cells in long term culture were used. Acute deletion of the *Pten* gene in normal prostate epithelial cells was achieved by transducing *Pten* $^{L/L}$ cells *in vitro* with lentivirus that expresses self-deleting Cre recombinase or with control lentivirus as described (10). Clonal populations of cells derived from tumors of 4 month old *Pten* $^{-/-}$ mice were used to model tumor-derived *Pten*-$^{-/-}$ cells (8).

Control *Pten* $^{L/L}$, acutely-deleted and tumor-derived *Pten* $^{-/-}$ cells were infected with rwt virus that encodes a palmitoylated version of the fluorescent protein dsRed at increasing MOIs. Shown in Fig. 4 are representative bright-field and fluorescence images of these cells at 24 hours postinfection. Both the control *Pten* $^{L/L}$ cells and acutely-deleted *Pten* $^{-/-}$ cells supported viral gene expression at MOI of 1 with slightly more viral gene expression at MOI of 10 or 50. However, tumor-derived *Pten* $^{-/-}$ cells supported very little viral gene expression independently of MOI. This result supports the conclusion that resistance to VSV in prostate tumor cells develops following *Pten* deletion and progression in tumor.

Figure. 4. Tumor-derived *Pten* $^{-/-}$ cells support very little viral gene expression even at high MOI. Control *Pten* $^{L/L}$, acutely-deleted *Pten* $^{-/-}$ (A) and tumor-derived *Pten* $^{-/-}$ cells (B) were infected with rwt-dsRed virus at MOIs of 1, 10 and 50. Bright field and fluorescence images were captured at 24 hpi. Images shown are representative images of at least 2 or 3 experiments.

A

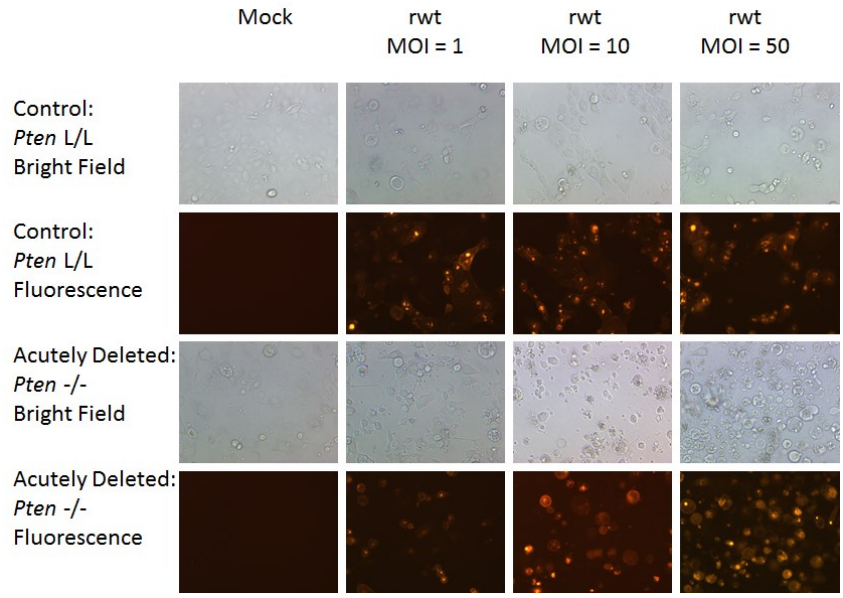

B

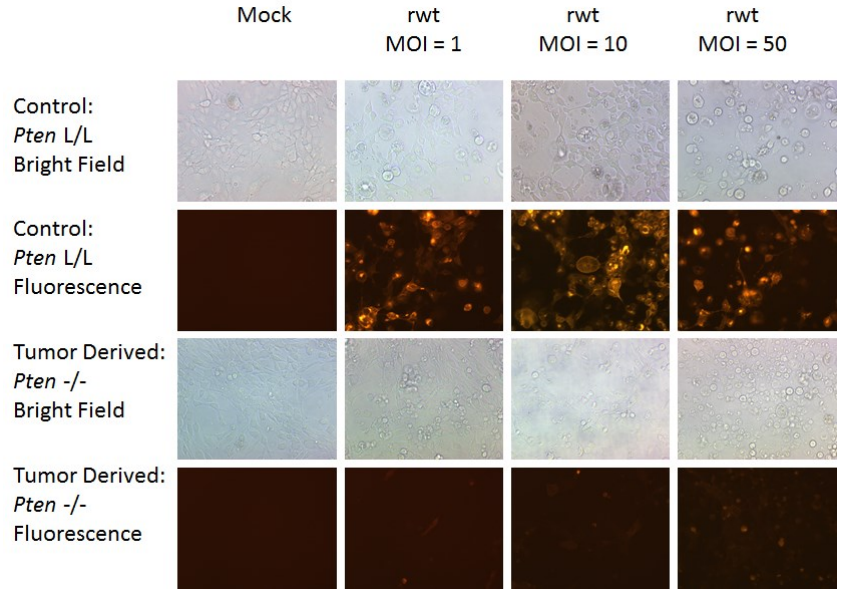

Figure. 4. Tumor-derived *Pten* $^{-/-}$ cells support very little viral gene expression even at high MOI.

The difference in viral gene expression in tumor-derived *Pten*$^{-/-}$ cells versus acutely-deleted or normal prostate epithelial cells was confirmed by radiolabeling infected cells with ^{35}S-methionine and by immunoblot analysis of viral M protein (Figure. 5). Control *Pten* $^{L/L}$, acutely-deleted and tumor-derived *Pten* $^{-/-}$ cells were infected with rwt virus. At 6, 12 and 24 hours postinfection, cells were pulse-labeled with ^{35}S-methioninine, and cell lysates were analyzed by SDS-PAGE and phosphorescence imaging. Shown in Figure. 5A are representative phosphoimages that depict the rate of viral protein synthesis in these cells following virus infection. Control *Pten* $^{L/L}$ and acutely-deleted *Pten* $^{-/-}$ cells infected with rwt virus had a pattern of viral protein synthesis that is typical for permissive cell types, in which viral protein synthesis was detectable as early as 6 hours after infection, and continued from 12-24 hours after infection. However, the ability of tumor-derived *Pten* $^{-/-}$ cells to translate viral proteins was poor at all times postinfection.

Also apparent in Figure. 5A is the inhibition of host protein synthesis by VSV, in which labeling of host proteins visible in mock-infected cells declined during the course of infection. The inhibition of host protein synthesis in tumor-derived *Pten*$^{-/-}$ cells was not notably different from that in control cells, suggesting that these cells do express viral proteins to a level sufficient to inhibit host protein synthesis.

The accumulation of M protein in infected cells was determined by immunoblots. Shown in Figure. 5B is a representative image of the M protein blots. Individual band intensity was quantified and expressed as a percentage of band intensity of control *Pten* $^{L/L}$ cells at 12 hours post infection. There was no significant difference between control *Pten* $^{L/L}$ and acutely-deleted *Pten* $^{-/-}$ cells. In comparison, M protein expression in tumor-derived *Pten* $^{-/-}$ cells was only detectable in longer exposures and was only about 10% of that of control cells.

Figure. 5. Control *Pten* $^{L/L}$ cells and acutely-deleted *Pten* $^{-/-}$ cells support viral gene expression. Tumor-derived *Pten* $^{-/-}$ cells support very little if any viral gene expression. (A) Control *Pten* $^{L/L}$, acutely-deleted *Pten* $^{-/-}$ and tumor-derived *Pten* $^{-/-}$ cells were infected with rwt at MOI of 10 or mock-infected (M). At 6, 12 and 24 hpi, cells were pulse-labeled with ^{35}S-methionine. Cell lysates were harvested and resolved on SDS-PAGE gels. Representative phosphoimages are shown. Viral proteins L, G, N, P and M are indicated on the phosphoimage. (B) Control *Pten* $^{L/L}$, acutely-deleted *Pten* $^{-/-}$ and tumor-derived *Pten* $^{-/-}$ cells were infected with rwt at MOI of 10. Cell lysates were harvested at 6 and 12 hpi and probed for viral matrix protein (M) protein expression by immunoblots. Representative immunoblots of at least 3 experiments are shown. Viral matrix (M) protein expression was quantified and expressed as a percentage of M protein expression in control *Pten* $^{L/L}$ cells at 12 hpi. Graphical summary of the M protein expression in these cells are also shown in (B).

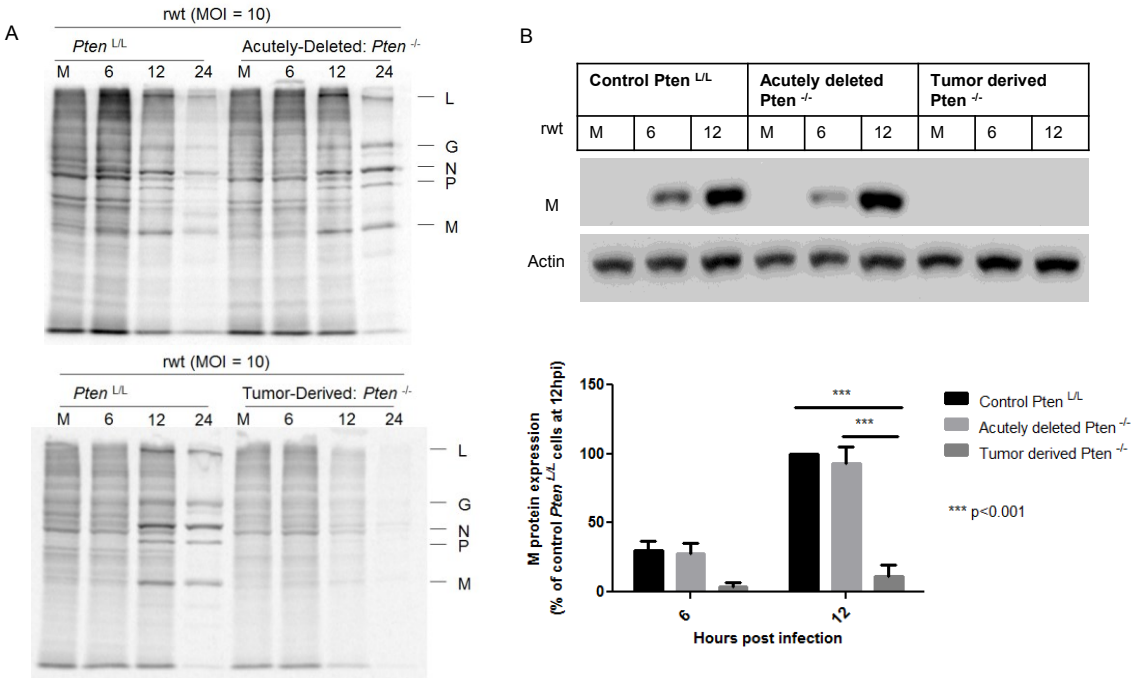

To determine whether the ability to support viral gene expression leads to cell death, cell viability was determined following VSV infection (Figure. 6). Control *Pten* $^{L/L}$, acutely-deleted and tumor-derived *Pten* $^{-/-}$ cells were infected with rwt or rM51R virus at MOI of 10. At various times after infection, cells were incubated with MTT reagent. Cell viability was expressed as a percentage of mock-infected cells at that time point. Following a single cycle infection with rwt or rM51R virus, both control *Pten* $^{L/L}$ and acutely-deleted *Pten* $^{-/-}$ cells were mostly killed by 36-48 hours postinfection (Figure. 6A, B). At 12 and 24 hours post infection, the acutely-deleted *Pten* $^{-/-}$ cells had significantly more viability than control *Pten* $^{L/L}$ cells, which may be due to a delay in induction of cell death in acutely-deleted *Pten* $^{-/-}$ cells. In contrast, tumor-derived *Pten* $^{-/-}$ cells were more resistant to virus-induced cell death with about 50% of tumor-derived *Pten* $^{-/-}$ cells remaining viable by 48 hours postinfection with rwt virus (Figure. 6C) and about 75% remaining viable after infection with rM51R virus (Figure. 6D).

Figure. 6. Control *Pten* $^{L/L}$ and acutely derived *Pten* $^{-/-}$ cells are susceptible to virus-induced cell death. Tumor-derived *Pten* $^{-/-}$ cells are resistant to virus induced cell death. Control *Pten* $^{L/L}$, acutely-deleted (A and B) and tumor-derived *Pten* $^{-/-}$ cells (C and D) were infected with rwt (A and C) and rM51R (B and D) virus at MOI of 10. Cell viability was determined using MTT assay and expressed as a percentage of mock-infected cells. Data shown are average of at least 3 experiments +/- SEM.

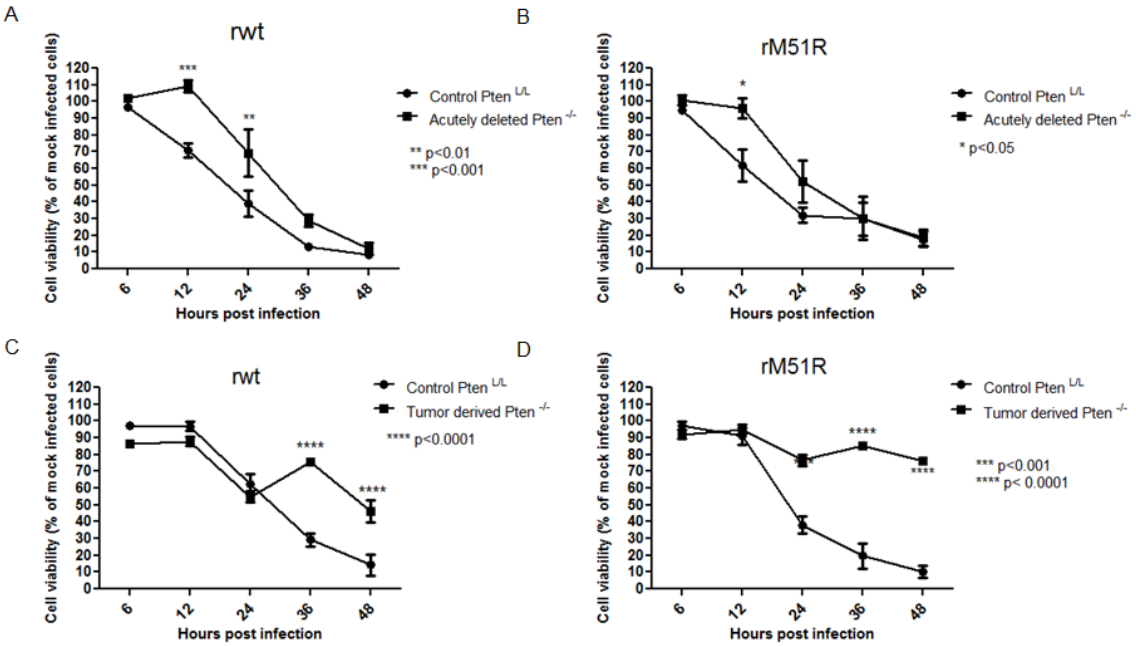

The difference in susceptibility between tumor-derived and acutely-deleted *Pten*$^{-/-}$ or normal cells was even more pronounced in multiple cycle infections (Figure. 7). Cells were infected with rwt or rM51R virus at MOI of 0.1 and cell viability was determined using MTT reagent as in Fig. 6. When control *Pten* $^{L/L}$ and acutely-deleted *Pten* $^{-/-}$ cells were infected with rwt virus at low MOI, the virus was able to infect cells, replicate and spread across the culture. Thus most of the cells were killed by 48 hours post infection (Figure. 7A). When these cells were infected with rM51R virus, spread of virus and induction of cell death was delayed in comparison to rwt virus (Figure. 7B). Tumor-derived *Pten* $^{-/-}$ cells were able to limit the spread of the virus across the culture and most of the cells remained viable at 48 hours postinfection with either virus (Figure. 7C, D).

Figure. 7. In a multiple cycle infection, control *Pten* $^{L/L}$ cells and acutely-deleted *Pten* $^{-/-}$ cells are susceptible to rwt-induced cell death. Tumor-derived *Pten* $^{-/-}$ cells are resistant to rwt- and rM51R-induced cell death. Control *Pten* $^{L/L}$, acutely-deleted (A and B) and tumor-derived *Pten* $^{-/-}$ cells (C and D) were infected with rwt (A and C) and rM51R (B and D) virus at MOI of 0.1. Cell viability was determined using MTT assay and expressed as a percentage of mock-infected cells. Data shown are average of at least 3 experiments +/- SEM.

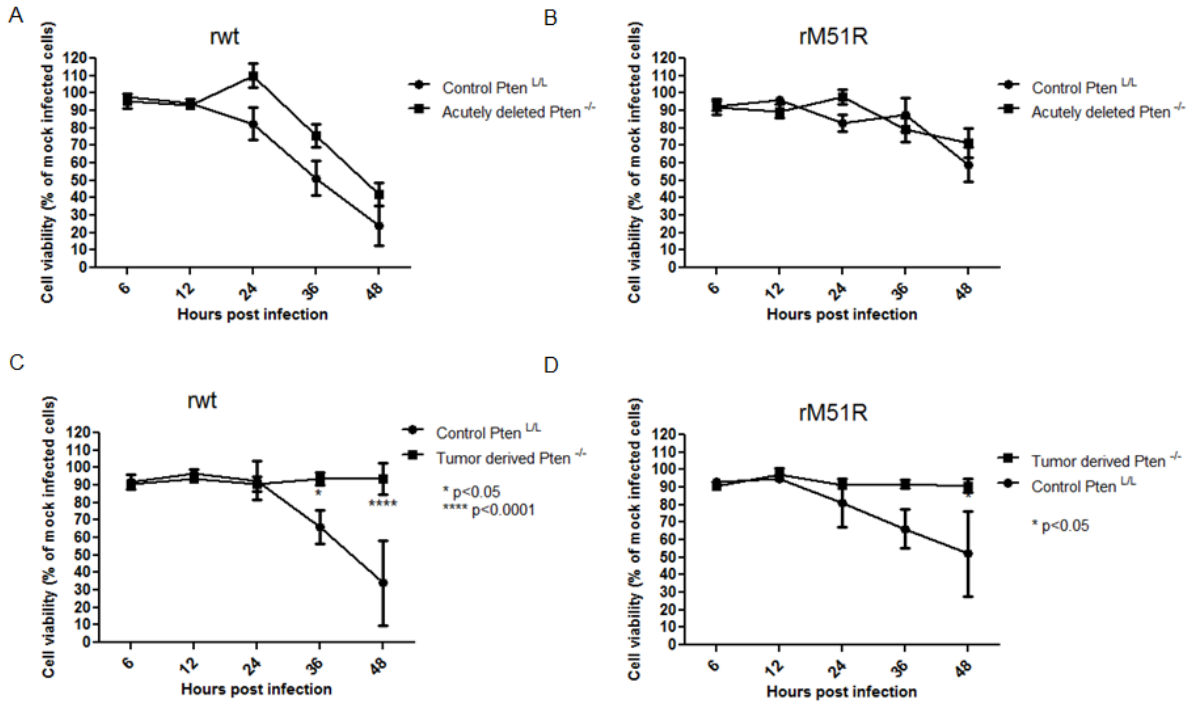

The type I IFN system is an important factor that mediates the resistance of cells to VSV infection. The ability of control *Pten* $^{L/L}$, acutely-deleted and tumor-derived *Pten* $^{-/-}$ cells to activate the key IFN-activated transcription factor STAT1 in response to VSV infection was investigated. Cells were infected with rwt virus at MOI of 10 and cell lysates were harvested at the indicated times post infection. The levels of phospho- and total STAT1 were analyzed using immunoblots and quantified (Figure. 8A). Tumor-derived *Pten* $^{-/-}$ cells constitutively express high levels of total STAT1. This is important, because unphosphorylated STAT1 has been shown to mediate antiviral activity independent of phosphorylated forms of STAT1 (reviewed in (29)). In contrast, control *Pten* $^{L/L}$ and acutely-deleted *Pten* $^{-/-}$ cells constitutively express very little total STAT1. In response to rwt virus infection, tumor-derived *Pten* $^{-/-}$ cells expressed activated, phosphorylated STAT1 as early as 6 hpi, despite the inhibitory activity of the wt M protein. STAT1 expression was also maintained at 12 hpi despite the inhibitory activity of the wt M protein. This data corresponds to data from viral gene expression assay and cell viability analysis. The data suggests that in the presence of wt M protein, tumor-derived *Pten* $^{-/-}$ cells are still capable of phosphorylating and activating antiviral signaling proteins, creating resistance to viral gene expression and thereafter virus-induced cell death. In contrast, control *Pten* $^{L/L}$ and acutely-deleted *Pten* $^{-/-}$ cells were poorly able to activate and upregulate antiviral proteins, and were susceptible to rwt virus infection and thereafter rwt virus-induced cell death.

The ability of control *Pten* $^{L/L}$, acutely-deleted and tumor-derived *Pten* $^{-/-}$ cells to activate STAT1 in response to rM51R virus infection was also investigated. In the presence of rM51R virus, tumor-derived *Pten* $^{-/-}$ cells were still able to phosphorylate and activate STAT1 similar to results with rwt virus infection (Figure. 8B). Total STAT1 expression

was upregulated by 12 hpi in cells infected with M protein mutant virus, in contrast to infection with rwt virus. This upregulation of STAT1 expression may contribute to the greater resistance of tumor-derived *Pten* $^{-/-}$ cells to rM51R virus infection when compared to rwt virus infection. For control *Pten* $^{L/L}$ and acutely-deleted *Pten* $^{-/-}$ cells, these cells were able to activate and upregulate STAT1 upon infection with rM51R virus, unlike infection with rwt virus. However, control *Pten* $^{L/L}$ cells differ from acutely-deleted *Pten* $^{-/-}$ cells in that control *Pten* $^{L/L}$ cells phosphorylated and activated STAT1 to higher levels than acutely-deleted *Pten* $^{-/-}$ cells. Control *Pten* $^{L/L}$ cells also upregulated STAT1 to higher levels than acutely-deleted *Pten* $^{-/-}$ cells by 12 hpi. This data suggests that control *Pten* $^{L/L}$ and acutely-deleted *Pten* $^{-/-}$ cells differ in their antiviral response to virus infection. To determine if this antiviral response creates antiviral effect, the IFN responsive assay was performed.

Figure. 8. Tumor-derived *Pten* $^{-/-}$ cells constitutively express higher levels of antiviral genes. Control *Pten* $^{L/L}$ cells activate and upregulate higher levels of antiviral genes than acutely-deleted *Pten* $^{-/-}$ cells with rM51R infection. Control *Pten* $^{L/L}$, acutely-deleted and tumor-derived *Pten* $^{-/-}$ cells were infected with rwt (A) or rM51R (B) virus at MOI of 10. Cell lysates were harvested at indicated times and probed for phospho- and total STAT1 expression. Shown here are representative immunoblots of at least 3 experiments. Levels of phospho- and total STAT1 were quantified and expressed as a percentage of levels in tumor-derived *Pten* $^{-/-}$ cells at 6 hpi. Data shown are average of at least 3 experiments +/- SEM.

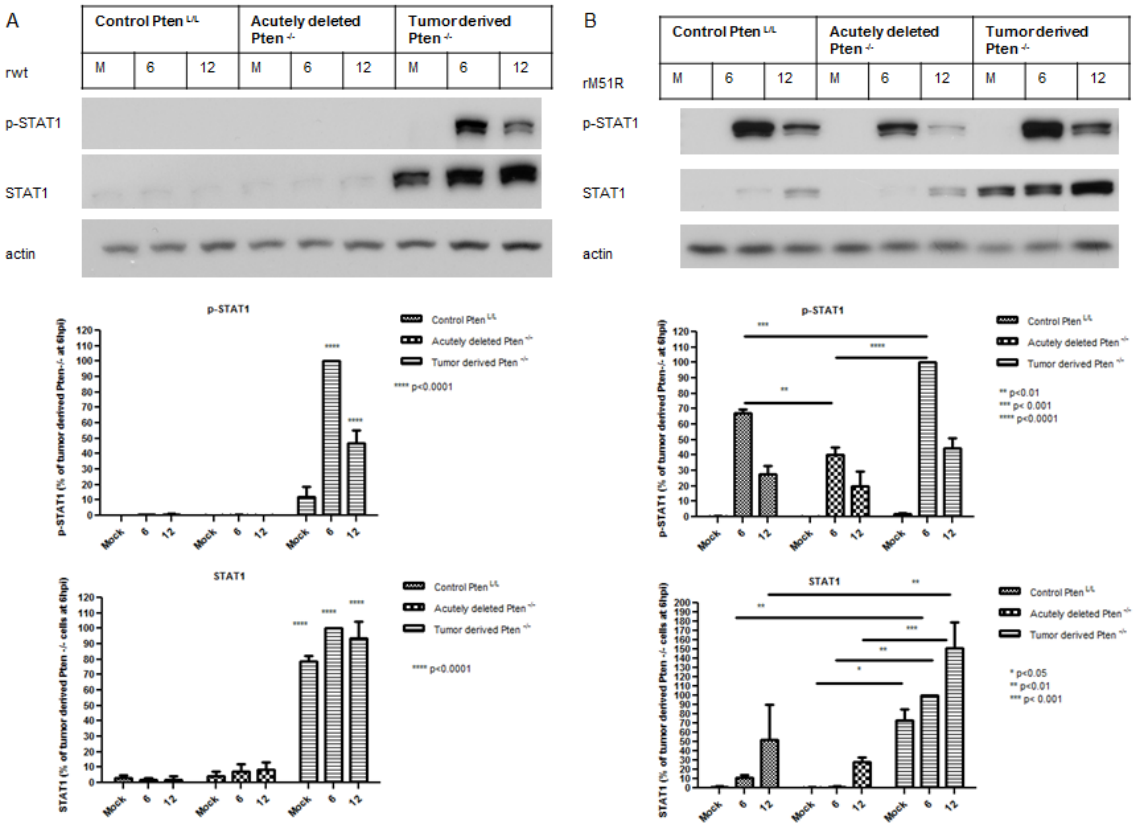

The principle of oncolytic virus therapy suggests that normal cells are typically responsive to IFN and are protected from VSV infection, whereas cancer cells poorly respond to IFN and are susceptible to VSV infection. The IFN responsiveness of control *Pten* $^{L/L}$ and acutely-deleted *Pten* $^{-/-}$ cells was evaluated. The cells were pretreated with the indicated doses of type I IFN for 16 hours. The cells were then infected with rwt virus at MOI of 10. Cell viability was determined at 72 hours. Control *Pten* $^{L/L}$ cells responded to IFN in a dose-dependent manner and were protected from rwt virus infection. In contrast, acutely-deleted *Pten* $^{-/-}$ cells were susceptible to rwt virus infection even at high doses of IFN. In data not shown, acutely-deleted *Pten* $^{-/-}$ cells were just as responsive as control *Pten* $^{L/L}$ cells to IFN when infected with rM51R virus. This suggests that the IFN responsiveness of acutely-deleted *Pten* $^{-/-}$ cells, when assayed by VSV infection, may be dependent on the ability of M protein to inhibit expression of antiviral genes.

Figure. 9. Control *Pten* $^{L/L}$ cells responds to IFN stimulation. Acutely-deleted *Pten* $^{-/-}$ cells poorly respond to IFN stimulation. Control *Pten* $^{L/L}$ and acutely-deleted *Pten* $^{-/-}$ cells were pretreated with increasing concentrations of IFN and infected with rwt at MOI of 10. Cell viability was determined using MTT assay at 72 hpi and expressed as a percentage of mock-infected cells.

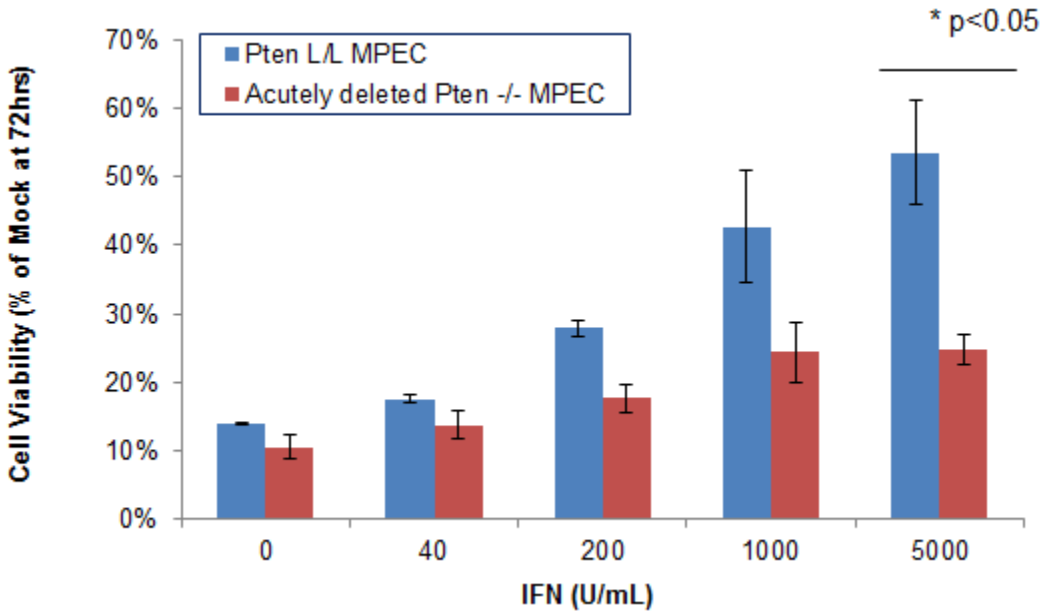

Summary

Together, the data in Chapter 1 of this thesis support a model in which normal prostate epithelial cells are susceptible to VSV infection but retain antiviral responses (Figure. 10). Upon acute loss of tumor suppressor gene, the *Pten* gene, prostate cells lose their ability to respond to IFN and mount an antiviral response. During tumor development, some of the prostate cells acquire resistance to VSV-infection and thereafter-induced cell death. Castration may lead to death of some of the resistant cells, or progression to castration resistance is accompanied by downregulation of antiviral genes, such that castration resistant prostate epithelial cells are mostly susceptible to VSV infection.

Figure. 10. Model for changes in susceptibility to VSV during progression of prostate cancer.

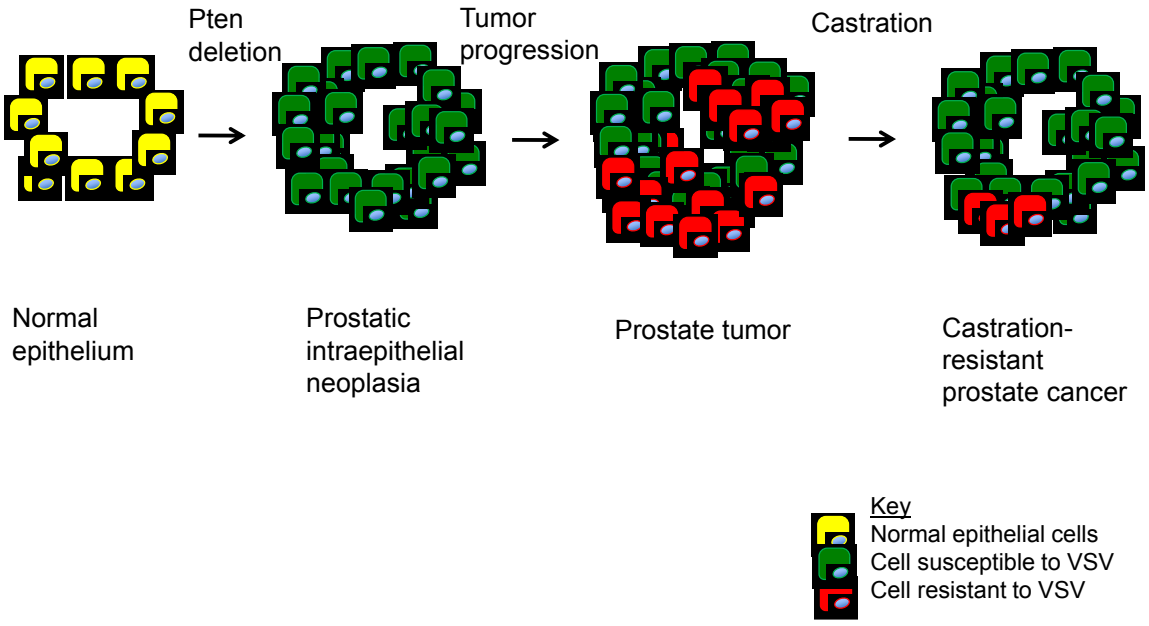

Chapter 2

Effects of *Rb* Deletion or TAK1-Downregulation on Susceptibility to VSV Oncolysis

Effects of Rb Deletion on Susceptibility to VSV-Induced Cell Death

In Chapter 1, the effects of *Pten* deletion on susceptibility to VSV infection were demonstrated. Deleting the *Pten* gene *in vitro* altered IFN-responsiveness of the murine prostate epithelial cells. Given that Rb is an important tumor suppressor in prostate cancer, and that its loss or mutation is frequently associated with advanced prostate tumors, the role of Rb in susceptibility to VSV was investigated. My hypothesis is that loss of Rb increases susceptibility to VSV infection. This hypothesis was tested using murine prostate epithelial cells derived by Barclay et al (13). Long-term cultures of *Rb* $^{L/L}$ cells were derived from prostates of 8-weeks old *Rb* $^{L/L}$ mice, and *Rb* $^{-/-}$ cells were obtained by transducing the *Rb* $^{L/L}$ cells *in vitro* with lentivirus expressing cre recombinase to achieve deletion of the *Rb* gene.

In order to determine the role of Rb in mediating susceptibility to VSV infection, control *Rb* $^{L/L}$ and *Rb* $^{-/-}$ cells were infected with rwt and rM51R viruses. Cell viability was determined at various times postinfection using the MTT assay. In a single cycle infection, *Rb* $^{-/-}$ cells showed greater susceptibility to rwt-induced cell death than control *Rb* $^{L/L}$ cells (Figure. 11A). By 24hpi, 66% of the control *Rb* $^{L/L}$ cells remained viable after rwt-induced cell death, whereas only 29% of *Rb* $^{-/-}$ cells remain viable at this time. By 48 hpi, most of the *Rb* $^{-/-}$ cells are killed by rwt-induced cell death, but 40% of the control *Rb* $^{L/L}$ cells remained viable. In the case of rM51R infection, a similar trend was observed. *Rb* $^{-/-}$ cells were more susceptible to rM51R-induced cell death than control *Rb* $^{L/L}$ cells

(Figure. 11B). When comparing between rwt and rM51R viruses, the rwt virus induces death at a faster rate than the rM51R virus. This is consistent with the idea that wt M protein accelerates induction of cell death in these cells by inhibiting cellular gene expression (67, 68, 70).

Figure. 11. *Rb* $^{-/-}$ mouse prostate epithelial cells show increased susceptibility to VSV-induced cell death. *Rb* $^{L/L}$ and *Rb* $^{-/-}$ cells were infected with rwt (A) and rM51R (B) viruses at MOI of 10. Cell viability was determined using MTT assay at the indicated times. Cell viability was expressed as a percentage of mock-infected cells. Data is an average of at least three experiments +/- SEM.

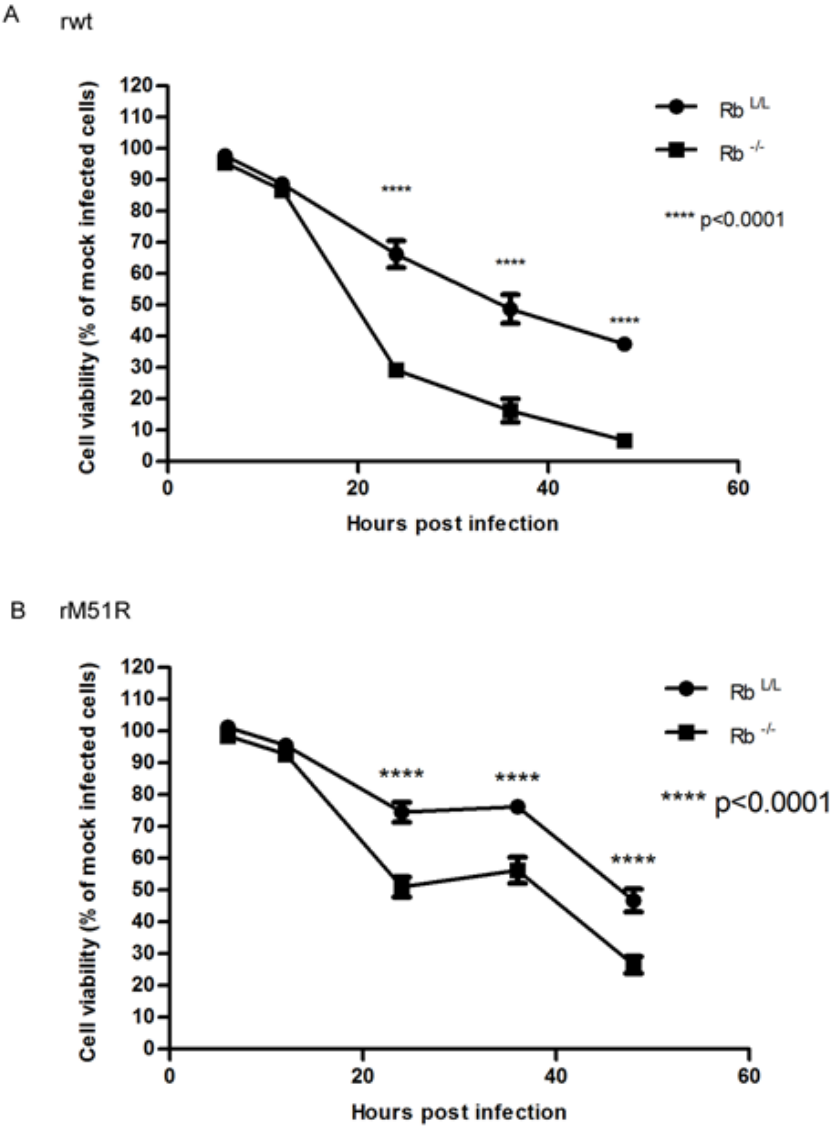

Analysis of cell viability in a multiple cycle infection was used to evaluate the ability of VSV to spread across the culture. Control *Rb* $^{L/L}$ and *Rb* $^{-/-}$ cells were infected with rwt and rM51R viruses at MOI of 0.1. Cell viability was determined at the indicated times postinfection. In a multiple cycle infection, rwt virus-infected *Rb* $^{-/-}$ cells exhibited a similar trend to those infected in a single cycle infection (Figure. 12A). *Rb* $^{-/-}$ cells showed a greater susceptibility to rwt virus-induced cell death when compared to control *Rb* $^{L/L}$ cells. *Rb* $^{-/-}$ cells were not able to deter the rwt virus from infecting, replicating and spreading across the culture, which resulted in death of most of the cells by 48 hpi. In contrast, control *Rb* $^{L/L}$ cells were able to limit rwt virus infection and replication across the culture, thus 54% of the control *Rb* $^{L/L}$ cells remained viable by 48 hpi. In the case of rM51R virus, infection, replication and spread across the culture was delayed compared to the rwt virus for both cell types, which resulted in delayed rate of induction of cell death in both cell types (Figure. 12B). Nonetheless, *Rb* $^{-/-}$ cells still showed a greater susceptibility to rM51R-induced cell death than control *Rb* $^{L/L}$ cells. The difference in cell viability between rwt- and rM51R-induced cell death by 48hpi suggests that the *Rb* $^{-/-}$ cells retain some antiviral response, and this antiviral response is sensitive to inhibition by the rwt virus.

Figure. 13. In a multiple cycle infection, *Rb* $^{-/-}$ mouse prostate epithelial cells show increased susceptibility to VSV-induced cell death. *Rb* $^{L/L}$ and *Rb* $^{-/-}$ cells were infected with rwt (A) and rM51R (B) at MOI of 0.1. Cell viability was determined using MTT assay at the indicated times. Cell viability was expressed as a percentage of mock-infected cells. Data is an average of at least three experiments +/- SEM.

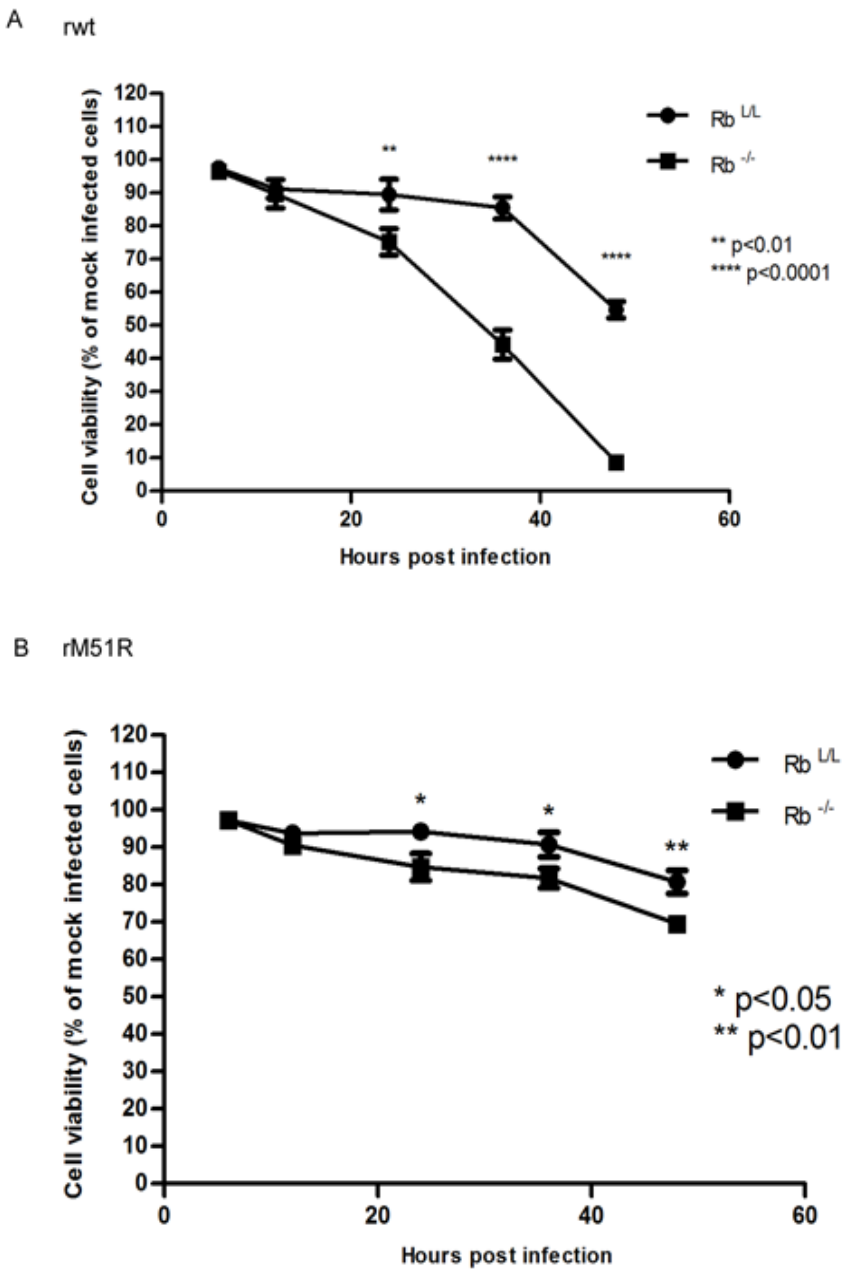

Figure. 12. In a multiple cycle infection, *Rb* $^{-/-}$ mouse prostate epithelial cells show increased susceptibility to VSV-induced cell death.

The ability of control *Rb* $^{L/L}$ and *Rb* $^{-/-}$ cells to respond to IFN and produce an antiviral effect was further evaluated. Control *Rb* $^{L/L}$ and *Rb* $^{-/-}$ cells were pretreated with increasing concentrations of IFN for 16 hours and infected with rwt virus at MOI of 10. Cell viability was determined at 72 hpi. Both *Rb* $^{L/L}$ and *Rb* $^{-/-}$ cells showed responsiveness to IFN and demonstrate an antiviral effect at high concentrations of IFN, about 5000 U/mL (Figure. 13). However, *Rb* $^{-/-}$ cells appeared to require more IFN to create such an antiviral effect. *Rb* $^{-/-}$ cells required 200 U/mL of IFN to achieve 50% of the cells protection from rwt infection. In contrast, *Rb* $^{L/L}$ cells required 5 fold less (40 U/mL) of IFN to achieve 50% protection. This data corresponds to the multicycle infection analysis with rM51R virus that suggest *Rb* $^{-/-}$ cells retain some antiviral response, but not as much as *Rb* $^{L/L}$ cells (Figure. 12B). Together, these data suggest that *Rb* $^{-/-}$ cells are capable of responding to IFN and creating an antiviral effect. However, *Rb* $^{-/-}$ cells require more IFN to create such an antiviral effect. Thus, in a multicycle infection, *Rb* $^{-/-}$ cells are more susceptible to VSV-infection since more IFN is required to delay spread of virus across the culture.

Figure. 13. Control and *Rb* $^{-/-}$ cells are responsive to IFN. *Rb* $^{L/L}$ and *Rb* $^{-/-}$ cells were pretreated with the indicated concentrations of IFN for 16 hours. Cells were infected with rwt at MOI of 10. Cell viability was determined using MTT assay at 72 hpi. Data is an average of two experiments.

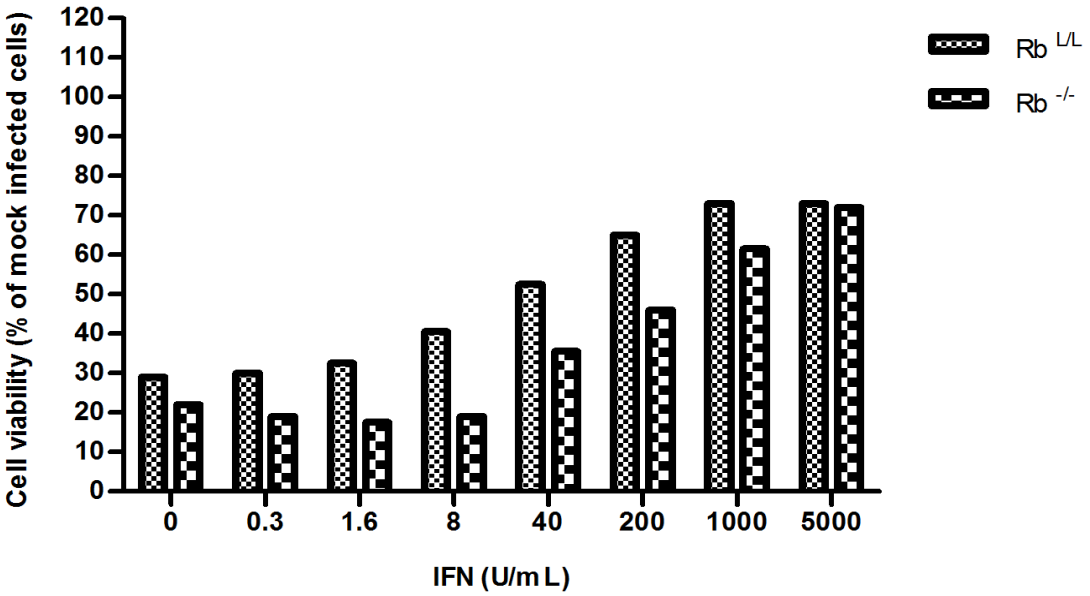

Effects of Tak1-Downregulation on Susceptibility to VSV

Liu et al (81) demonstrated that TAK1 is an important tumor suppressor in prostate cancer, whose deletion is associated with higher Gleason grade prostate cancers. The role of Tak1 as a tumor suppressor was further validated in tissue recombination studies; Tak1-silenced cells developed pathologically-confirmed tumors *in vivo* (135). Tak1 is also a downstream intermediary of immune signaling. Shi et al suggested that Tak1 mediates the activation of antiviral signaling following recognition of VSV by Tlr 13, and this effect was observed in dendritic cells and mouse embryonic fibroblasts (MEFs) (112). Thus, Tak1 may play a role in antiviral signaling and defense following infection with VSV. Alterations in Tak1 may cause changes in susceptibility to VSV infection. I hypothesize that downregulation of the tumor suppressor and immune adaptor molecule Tak1 in prostate epithelial cells would increase susceptibility to VSV infection. This hypothesis was addressed using murine prostate epithelial cells derived by Wu et al (135). Murine prostate epithelial cells were transduced with lentivirus that expresses either shRNA against the Tak1 RNA or control non-targeting shRNA, and individual clones were selected (112).

Murine prostate epithelial cells expressing non-targeting control shRNA (shNC clones 3 and 4) and shTAK1 shRNA (shTAK1 clones 1, 2 and 7) were tested for expression of Tak1 protein by immunoblots. Tak1 expression was measured as a percentage of Tak1 levels in shNC clone 4. Tak1 expression in shNC clone 3, shNC clone 4, shTAK1 clone 1, shTAK1 clone 2 and shTAK1 clone 7 were 74%, 100%, 17%, 22% and 15% respectively. It is unclear why expression of Tak1 would differ between the two non-targeting controls shNC clone 3 and shNC clone 4. However, shRNA silencing of Tak1

was able to achieve downregulation of Tak1 expression, down to 15-22% of shNC clone 4 levels.

In order to determine the role of Tak1 in susceptibility to VSV infection, the ability of shNC and shTAK1 cells to support viral gene expression was determined. shNC clone 3 and shTAK1 clone 1 cells were infected with rwt and rM51R viruses encoding the fluorescent protein GFP. At 24 hpi, bright field and fluorescence images were captured (Figure. 14). In a single cycle infection, most of shNC and shTAK1 cells were infected with virus and were able to support viral gene expression. This was observed for both rwt and rM51R viruses. In a multiple cycle infection, in which cells were infected at MOI of 0.1, the ability of the viruses to infect, replicate and spread across the culture was evaluated. For both shNC and shTAK1 cells, the rwt virus was able to infect and spread across the culture. In the case of the M protein mutant virus, rM51R virus, GFP expression was observed in both cell types. This suggests that there is very little difference between shNC clone 3 and shTAK1 clone 1 cells in their ability to support rM51R viral gene expression and spread across the culture over time. Together, these data suggest that both control and Tak1-downregulated cells are susceptible to VSV infection.

Figure. 14. Control and *Tak1*-downregulated cells support viral gene expression.

Control and *Tak1*-downregulated cells were infected with rwt and rM51R at MOI of 10 and 0.1. Bright field and fluorescence images were captured at 24 hpi.

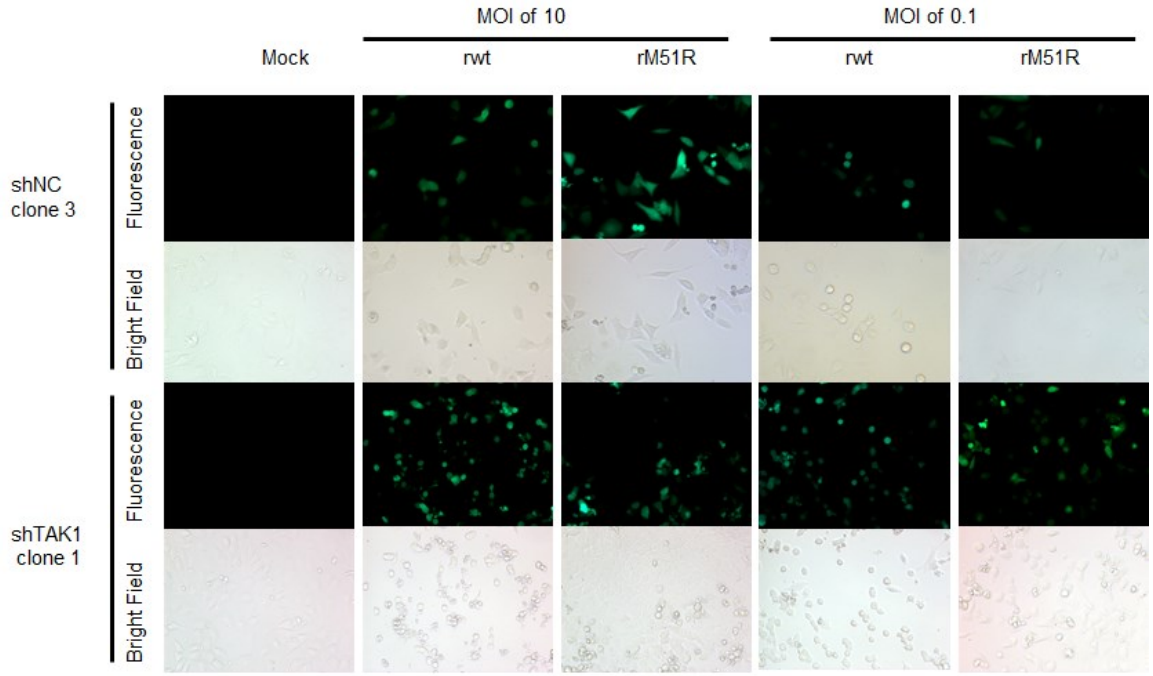

Given that both control and Tak1-downregulated cells support viral gene expression, the ability of the expressed viral genes to induce cell death was determined. shNC and shTAK1 cells were infected with rwt and rM51R viruses at MOI of 10. Cell viability was determined using the MTT assay at various times post infection. In a single cycle infection by rwt virus, both control and Tak1-downregulated cells were susceptible to virus-induced cell death and were mostly killed by 36 to 48 hpi (Figure. 15A). For a single cycle infection with rM51R virus, both control and Tak1-downregulated cells were susceptible to rM51R-induced cell death as well (Figure. 15B). The rate of induction of cell death was slower in cells infected with rM51R versus rwt virus. However, It appears that there is very little difference between control and Tak1-downregulated cells in susceptibility to VSV-induced cell death.

Figure. 15. Control and *Tak1*-downregulated cells are susceptible to VSV-induced cell death. Control and *Tak1*-downregulated cells were infected with rwt (A) and rM51R (B) at MOI of 10. Cell viability was determined using MTT assay at the indicated times. Cell viability was expressed as a percentage of mock-infected cells.

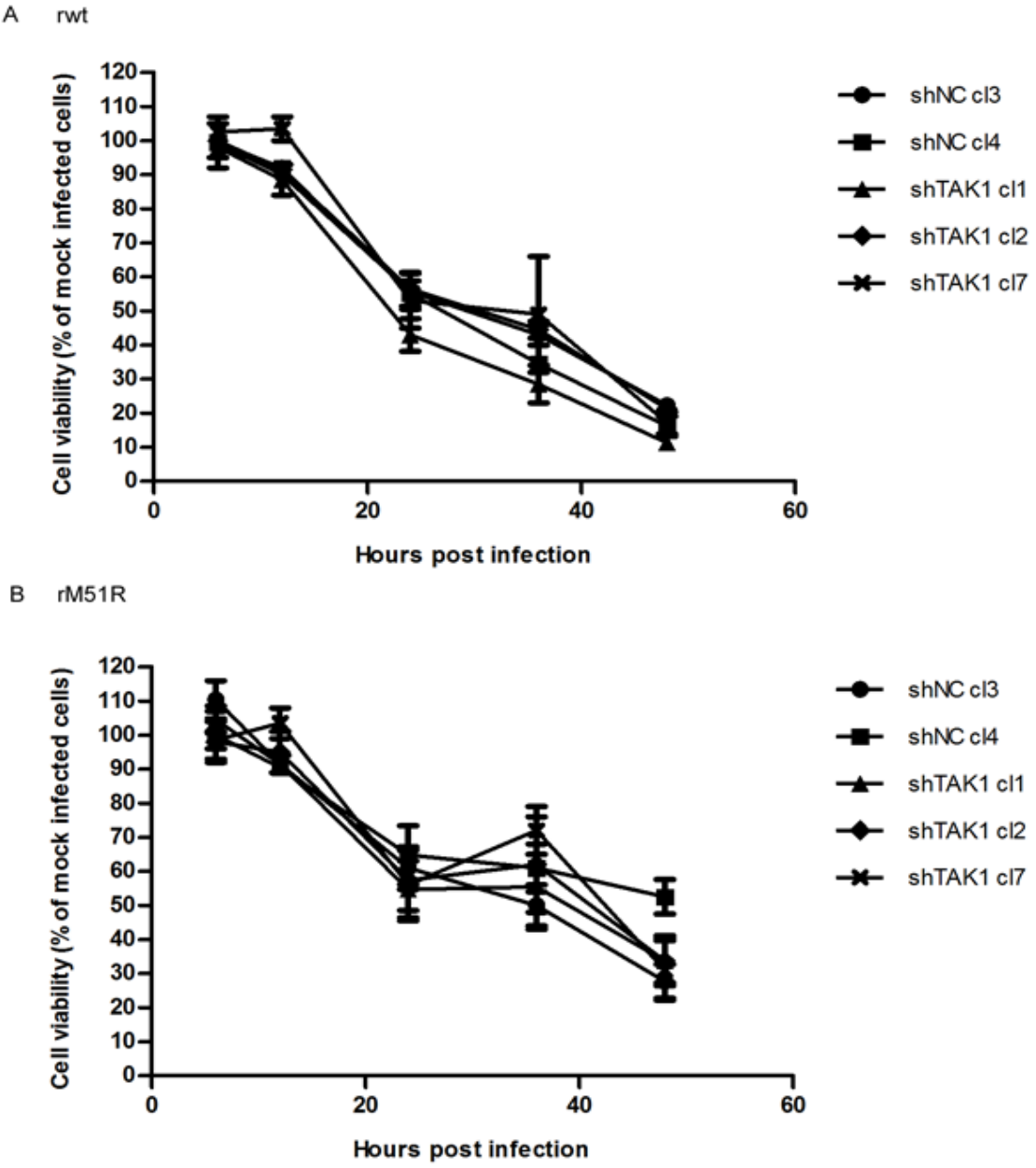

In a multiple cycle infection in which cells were infected at a low MOI of 0.1, the ability of the viruses to spread to surrounding cells was evaluated in these cell types. shNC and shTAK1 cells infected with rwt at MOI of 0.1 showed very little difference in susceptibility to rwt virus-induced cell death (Figure. 16A). By 48 hpi, both control and Tak1-downregulated cells exhibited similar cell viability (30-40% of mock-infected cells). This data suggests that the rwt virus is just as efficient in infecting, shutting-off host gene expression, replicating and infecting surrounding in control cells as Tak1-downregulated cells. There is also very little difference between shNC and shTAK1 cells in rate of cell death following infection with rM51R virus at MOI 0.1, suggesting that the rM51R virus is just as effective in spreading across shNC cells as shTAK1 cells. Again, the rate of induction of cell death in rM51R virus-infected cells was slower than rwt virus-infected cells (Figure. 16B), corresponding to the slower rate of induction of cell death in a single cycle infection (Figure. 15). This data also indicates that there is very little difference in antiviral defense between shNC and shTAK1 cells.

Figure. 16. In a multiple cycle infection, control and *Tak1-downregulated* cells are susceptible to VSV-induced cell death. Control and *Tak1*-downregulated cells were infected with rwt (A) and rM51R (B) at MOI of 0.1. Cell viability was determined using MTT assay at the indicated times. Cell viability was expressed as a percentage of mock-infected cells.

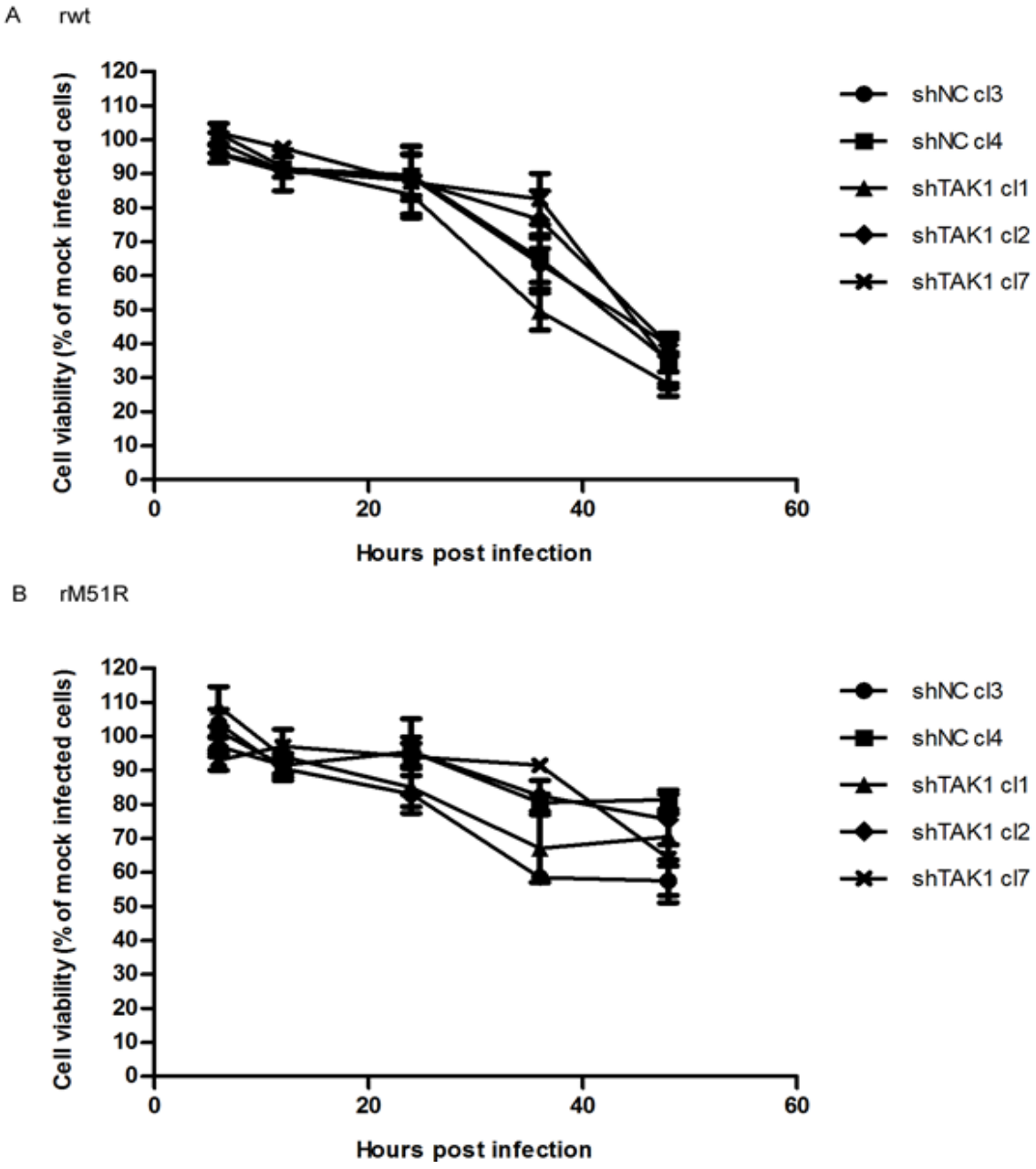

Figure. 16. In a multiple cycle infection, control and *Tak1*-downregulated cells are susceptible to VSV-induced cell death.

The difference in antiviral responses between shNC and shTAK1 was further evaluated using IFN responsive assay. Cells were treated with increasing concentrations of IFN. Cells were then infected with rwt at MOI of 10 and cell viability was determined at 72 hpi. In this assay, the IFN responsiveness between the two control cell lines shNC clone 3 and clone 4 were somewhat different (Figure. 17). shNC clone 4 cells required approximately 8 U/mL of IFN to achieve 50% protective effect from VSV-induced cell death. shNC clone 3 cells required 200 U/mL of IFN to achieve similar effects. This difference could be due to the 26% difference in Tak1 expression levels between the two cell lines. However, shTAK1 cells required a lower amount of IFN, 40 U/mL, to achieve 50% protective effect. Given the difference in IFN-responsiveness between the two controls, it is difficult to conclude whether downregulation of Tak1 alters IFN responsiveness of the murine prostate epithelial cells. All these data suggest that downregulation of Tak1 does not alter susceptibility to VSV infection. It is possible that the remaining 15-22% of Tak1 in Tak1-downregulated cells may mediate changes in sensitivity to VSV infection. Thus, this hypothesis can be further tested in cells that have constitutive deletion of the *Tak1* gene.

Figure. 17. Control and *Tak1*-downregulated cells are responsive to IFN. Control and *Tak1*-downregulated cells were pretreated with the indicated concentrations of IFN for 16 hours. Cells were infected with rwt at MOI of 10. Cell viability was determined using MTT assay at 72 hpi.

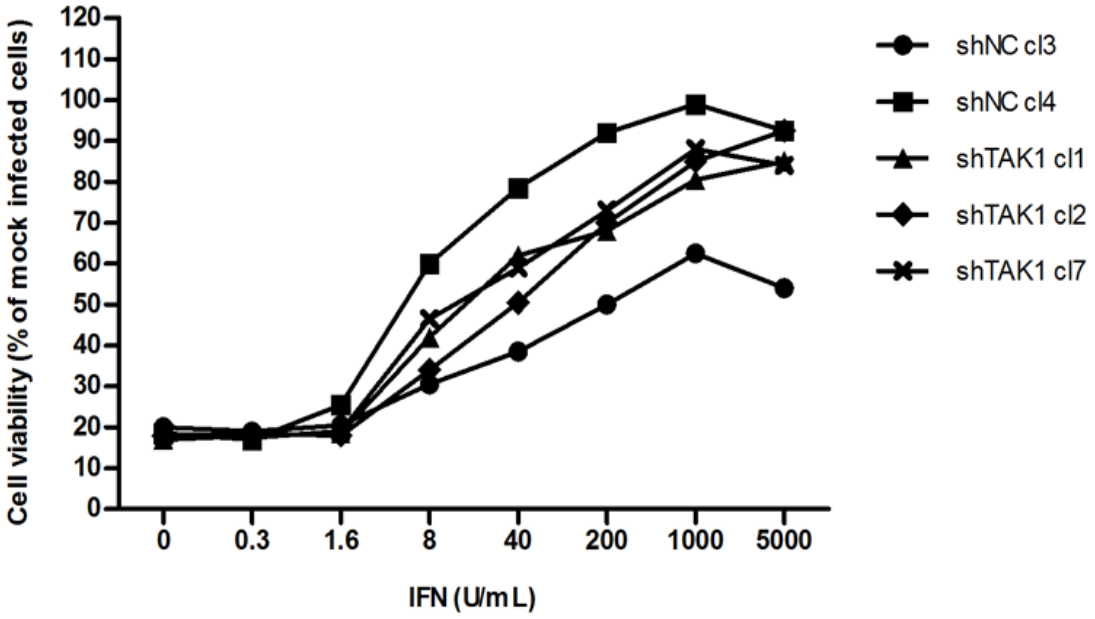

Chapter 3

Activation of IL-6/STAT3 Pathway in Murine Prostate Cancer Cells

Expression of IL-6 in Tumor-Derived *Pten* $^{-/-}$ cells

The resistance of tumor-derived *Pten* $^{-/-}$ cells to VSV was demonstrated in Chapter 1. One mechanism of resistance for tumor-derived *Pten* $^{-/-}$ cells to VSV is the constitutive activation and upregulation of STAT1, a key signaling molecule for the type I IFN system. Constitutive activation of the type I IFN system contributes to antiviral defense against VSV in human prostate cancer cell lines, such as DU-145 and PC3 cells. These cells also have constitutively active IL-6/STAT3 pathway, and activation of this pathway leads to expression of anti-apoptotic genes that promote survival in cancer cells. Crosstalk between the STAT3 pathway and STAT1 pathway may be mediated by Jak kinases that activate both trancription factors (Figure. 18). In some cell types, activated IL-6/STAT3 pathway also demonstrates antiviral activity against viruses such as Theiler's murine encephalitis virus or hepatitis C virus. The IL-6/STAT3 pathway provides antiviral activity against these viruses by directly interfering with the intracellular virus replication or by activating the type I IFN system. I hypothesize that tumor-derived *Pten* $^{-/-}$ cells have activated IL-6/STAT3 pathway, and that activation of this pathway contributes to antiviral activity against these cells.

Figure. 18. Model for crosstalk between the IL-6-STAT3 axis and the STAT1 pathway

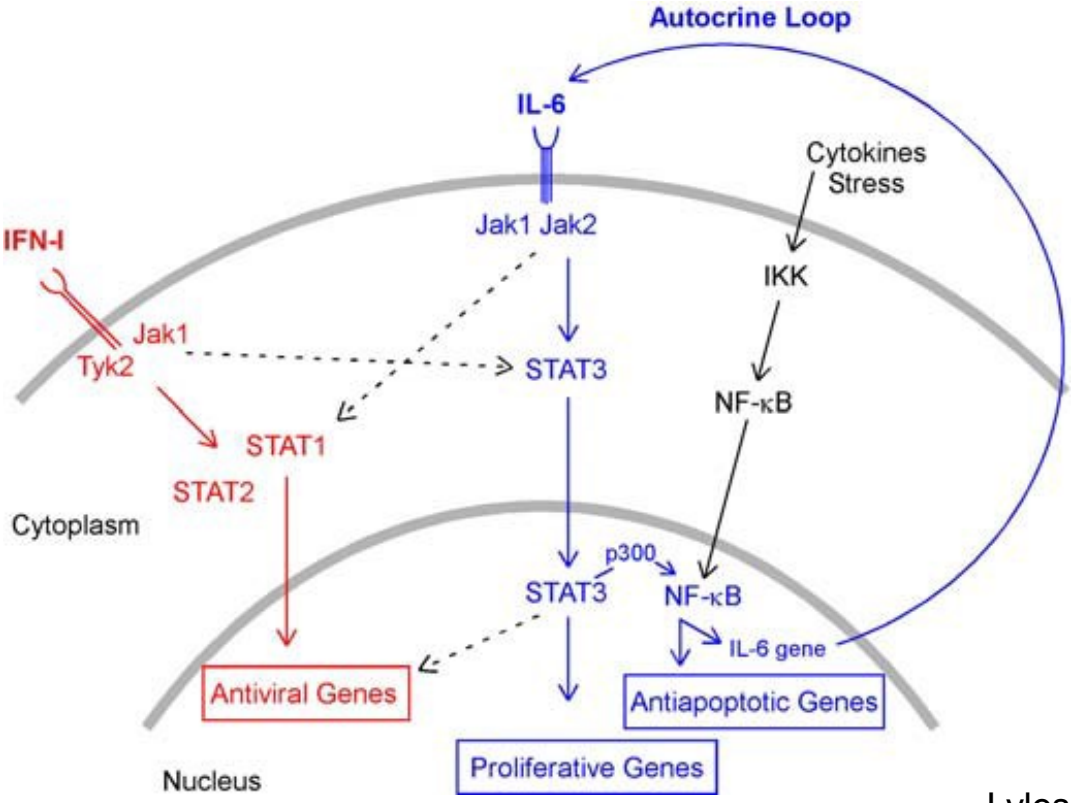

Lyles DS

To determine whether tumor-derived *Pten* $^{-/-}$ cells have activated IL-6/STAT3 pathway, their ability to express IL-6 was evaluated compared to control *Pten* $^{L/L}$ and acutely-deleted *Pten* $^{-/-}$ cells. Control *Pten* $^{L/L}$, acutely-deleted *Pten* $^{-/-}$ and tumor-derived *Pten* $^{-/-}$ cells were cultured overnight in their respective media, and then the medium was changed to determine the time course of IL-6 production. At indicated times, culture supernatants were harvested, and IL-6 concentrations in the supernatants were measured using ELISA. As shown in Figure. 19, tumor-derived *Pten* $^{-/-}$ cells produced higher levels of IL-6 when compared to control *Pten* $^{L/L}$ and acutely-deleted *Pten* $^{-/-}$ cells. The higher level of IL-6 produced in tumor-derived *Pten* $^{-/-}$ cells can be first observed at 6 hours and accumulates to 10 ng/mL by 24 hours. In contrast, control *Pten* $^{L/L}$ and acutely-deleted *Pten* $^{-/-}$ cells constitutively expressed very little IL-6. Together, these data suggest that IL-6 expression by tumor cells is not due solely to Pten deletion but instead suggest that progression to tumor is required for cellular changes that promote IL-6 production.

Figure. 19. Tumor-derived *Pten* $^{-/-}$ cells constitutively express high levels of IL-6.

Control *Pten* $^{L/L}$, acutely-deleted *Pten* $^{-/-}$ and tumor-derived *Pten* $^{-/-}$ cells were cultured in their respective media overnight. Following attachment, fresh medium was layered on the cells. At indicated times, culture supernatants were harvested. IL-6 concentration (ng/mL) in the supernatants were measured using ELISA. The data shown is an average of at least three experiments +/- standard error of mean.

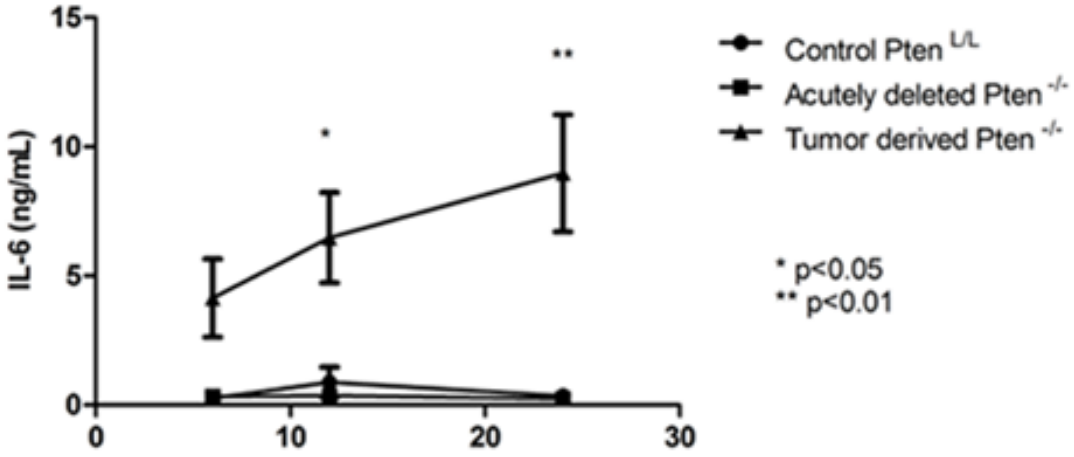

Effects of rwt virus infection on IL-6 expression

As a mechanism to suppress host antiviral responses, the M protein in rwt virus shuts off host gene expression. It is evident from ^{35}S-methionine radiolabeling analysis that the rwt virus is able to shut off host gene expression on control *Pten* $^{L/L}$, acutely-deleted *Pten* $^{-/-}$ and tumor-derived *Pten* $^{-/-}$ cells. Thus, the effects of rwt virus infection on IL-6 production were determined. Tumor-derived *Pten* $^{-/-}$ cells infected with rwt virus at MOI of 0.1 or 10 (Figure. 20A and B, respectively) produced similar amounts of IL-6 as uninfected controls (Figure. 19), approximately 10ng/mL by 24 hours after infection. This data suggests that IL-6 production in tumor-derived *Pten* $^{-/-}$ cells may be resistant to inhibition of host gene expression by the rwt virus. Infecting control *Pten* $^{L/L}$ cells and acutely-deleted *Pten* $^{-/-}$ cells with rwt at MOI of 0.1 or 10 also did not significantly alter the IL-6 levels in culture (Figure. 19 and Figure. 20A, B).

Figure. 20. Control *Pten* $^{L/L}$, acutely-deleted *Pten* $^{-/-}$ and tumor-derived *Pten* $^{-/-}$ cells were either mock infected, or infected with rwt MOI = 0.1 (A), or infected with rwt MOI = 10 (B). At indicated times, culture supernatants were harvested. IL-6 concentration (ng/mL) in the supernatants was measured using ELISA. The data shown is an average of at least three experiments +/- standard error of mean.

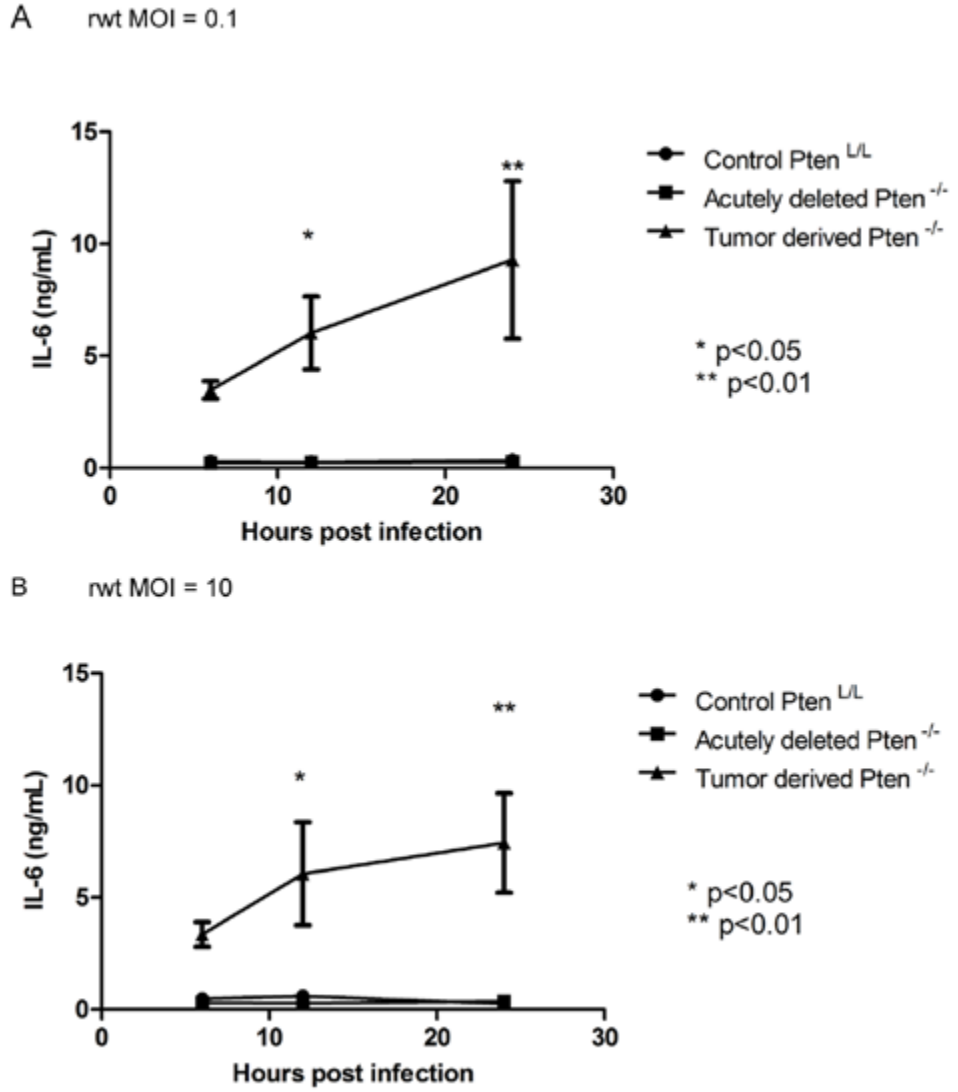

Effects of rM51R Virus Infection on IL-6 Production

The rM51R virus is a mutant virus that is defective in its ability shut-off of host gene expression. Virus replication is detected by PRRs, which typically leads to activation of NF-kB. IL-6 expression may also be regulated by NF-kB activity. Thus, in cells that are responsive to NF-kB activation, IL-6 is produced as a consequence of virus infection. Because rM51R virus is defective in its ability to inhibit host gene expression, infection of these cells typically induces production of IL-6. The effects of rM51R infection on control *Pten* $^{L/L}$, acutely-deleted *Pten* $^{-/-}$ and tumor-derived *Pten* $^{-/-}$ cells were evaluated. The control *Pten* $^{L/L}$ cells produced very little IL-6 constitutively, and infection with rM51R virus at MOI of 0.1 or 10 had very little effect on IL-6 levels (Figure. 21A and B). Although rM51Rvirus infection at MOI of 10 at 24 hpi had higher levels of IL-6 (1.24 ng/mL) than mock-infected cells (0.36 ng/mL) in these cells, these were not statistically significant differences. A similar small increase in production of IL-6 was observed for rM51R virus-infected acutely-deleted *Pten* $^{-/-}$ cells but this was also not a statistically signficant difference. Together, these data suggest that VSV infection in mouse prostate epithelial cells produced very little IL-6.

In contrast, tumor-derived *Pten* $^{-/-}$ cells responded dramatically to rM51R virus infection by enhancing the production of IL-6. In an asynchronous infection with rM51R virus at MOI 0.1 (Figure. 21A), tumor-derived *Pten* $^{-/-}$ cells produced about 25 ng/mL of IL-6 at 24 hpi when compared to 9 ng/mL in mock-infected cells (Figure. 21B). Synchronous infection of tumor-derived *Pten* $^{-/-}$ cells with rM51R virus at MOI 10 resulted in a significant increase in IL-6 in the supernatant, particularly at 6 and 12 hpi with up to 48 ng/mL at 24 hpi (Figure. 21B). This data suggests that IL-6 production in tumor-derived

Pten $^{-/-}$ cells is extremely responsive to virus stimulation, such that the presence of the virus resulted in greater IL-6 production than mock-infected cells. The data also suggests that when compared to the other cells, tumor-derived *Pten* $^{-/-}$ cells are more responsive to rM51R infection, as indicated by greater IL-6 production in tumor-derived *Pten* $^{-/-}$ cells.

Figure. 21. Tumor-derived *Pten* $^{-/-}$ cells dramatically upregulate IL-6 production in response to rM51R infection. Control *Pten* $^{L/L}$, acutely-deleted *Pten* $^{-/-}$ and tumor-derived *Pten* $^{-/-}$ cells were either mock infected, or infected with rM51R virus at MOI of 0.1 (A), or MOI of 10 (B). At indicated times, culture supernatants were harvested. IL-6 concentration (ng/mL) in the supernatants was measured using ELISA. The data shown is an average of at least three experiments +/- standard error of mean (SEM).

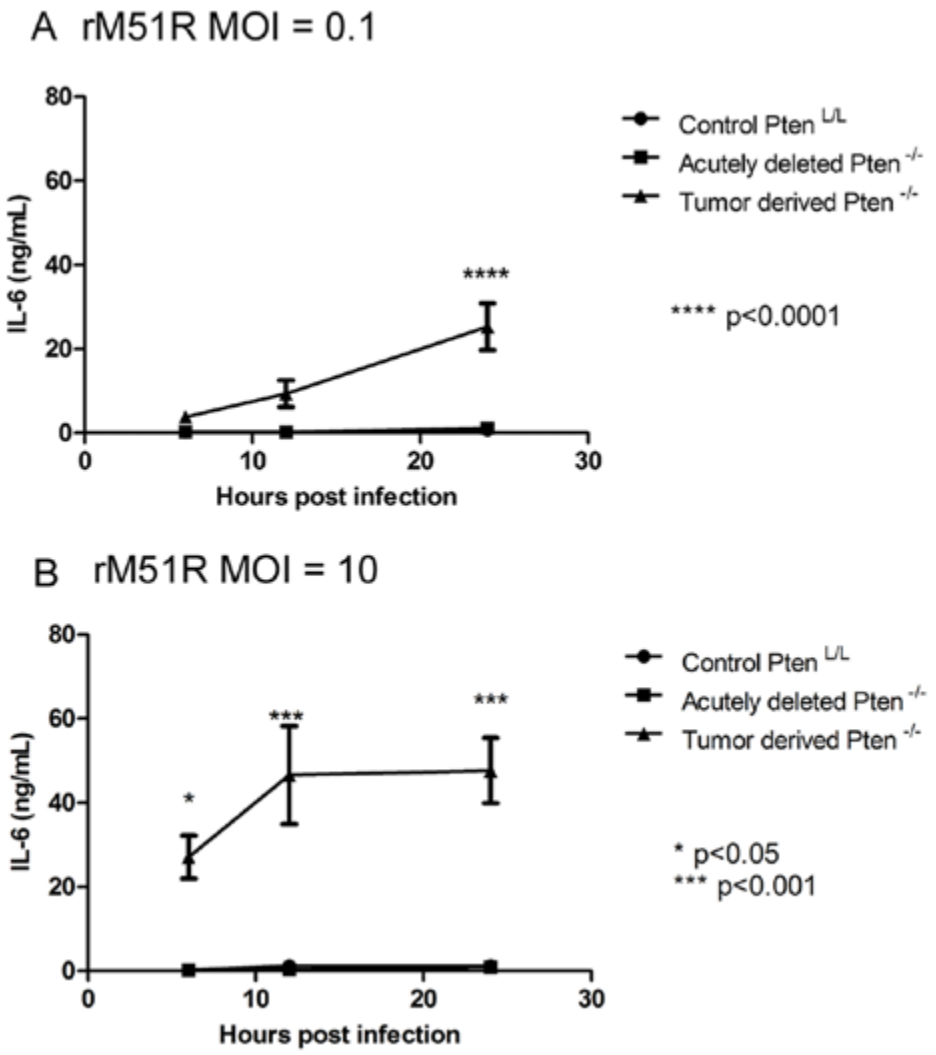

Figure. 21. Tumor-derived *Pten* $^{-/-}$ cells dramatically upregulate IL-6 production in response to rM51R infection.

Activation of STAT3 in Tumor-Derived *Pten* $^{-/-}$ Cells

The IL-6/STAT3 pathway uses activated forms of STAT3 to propagate pro-inflammatory signals necessary for tumor progression. Antiviral signaling through STAT3 is also known to be mediated through the activated form of STAT3. STAT3 is activated by phosphorylation at tyrosine 705 residue, which allows it to dimerize and transduce signals to the nucleus and regulate expression of downstream effector genes. To determine whether control *Pten* $^{L/L}$, acutely-deleted *Pten* $^{-/-}$ and tumor-derived *Pten* $^{-/-}$ cells have activated STAT3, cells were either mock infected, or infected with rwt virus at MOI of 10. Cell lysates were harvested at the indicated times after infection. Immunoblotting was performed to probe for total and phospho-STAT3 (Figure. 22A). The levels of STAT3 were not significantly different among control *Pten* $^{L/L}$, acutely-deleted *Pten* $^{-/-}$ and tumor-derived *Pten* $^{-/-}$ cells (Figure. 22A and B). This is not surprising, as presence of STAT3 is necessary for maintaining cell growth. rwt infection also did not significantly alter STAT3 expression levels in any of these cells. The ratio of phospho-STAT3 to total STAT3 is significantly different among these cells (Figure. 22C). In control *Pten* $^{L/L}$ and acutely-deleted *Pten* $^{-/-}$ cells, the ratio of p-STAT3 to STAT3 is approximately 0.16 and 0.13 respectively. Since the control *Pten* $^{L/L}$ and acutely-deleted *Pten* $^{-/-}$ cells have similar levels of total STAT3 (Figure. 22A and B), the ratio indicates that these cells have similar amounts of phosphorylated form of STAT3 within the cell. This low level of STAT3 activation corresponds to the very low levels of IL-6 produced by these cells. In contrast, the ratio of p-STAT3/STAT3 in tumor-derived *Pten* $^{-/-}$ cells were significantly higher than the other cells (0.81), indicating that more of the STAT3 in tumor-derived *Pten* $^{-/-}$ cells were activated than other cells. This large population of activated STAT3 likely occurred due to the high amounts of IL-6 produced in these cells, and feeds back into production of more IL-6 in these cells. Together, this data suggests

that activation of STAT3 occurs during progression in tumor. Infection with rwt at MOI of 10 did not significantly alter the levels of phospho-STAT3 in control *Pten* $^{L/L}$ and acutely-deleted *Pten* $^{-/-}$ cells (Figure. 22A) and this corresponds to the ELISA analysis of IL-6 production in these cells following rwt infection. rwt infection neither induced nor inhibited the limited amounts of IL-6 produced by these cells, and correspondingly, no significant changes in phospho-STAT3 levels were observed. The levels of phospho-STAT3 in tumor-derived *Pten* $^{-/-}$ cells were not altered by rwt infection. This also corresponds to the ELISA analysis, in which rwt infection did not alter the production of IL-6 in tumor-derived *Pten* $^{-/-}$ cells. This high level of IL-6 can then maintain activation of STAT3 in the presence of rwt infection (Figure. 22A and B).

Figure. 22. Tumor-derived *Pten* $^{-/-}$ cells have constitutively activated STAT3. Control *Pten* $^{L/L}$, acutely-deleted *Pten* $^{-/-}$ and tumor-derived *Pten* $^{-/-}$ cells were either mock infected, or infected with rwt at MOI of 10. Cell lysates were harvested and at the indicated times after infection. Immunoblotting was performed to probe for total and phospho-STAT3 and actin was included as a loading control. (A) shows a representative image of the experiment. Protein expression levels were quantified using densitometry analysis and normalized to loading control levels. STAT3 levels were quantified and expressed as a percentage of tumor-derived *Pten* $^{-/-}$ cells at 12hpi (B). Ratio of p-STAT3/STAT3 is shown in (C). Data shown is an average +/- SEM of 3 experiments.

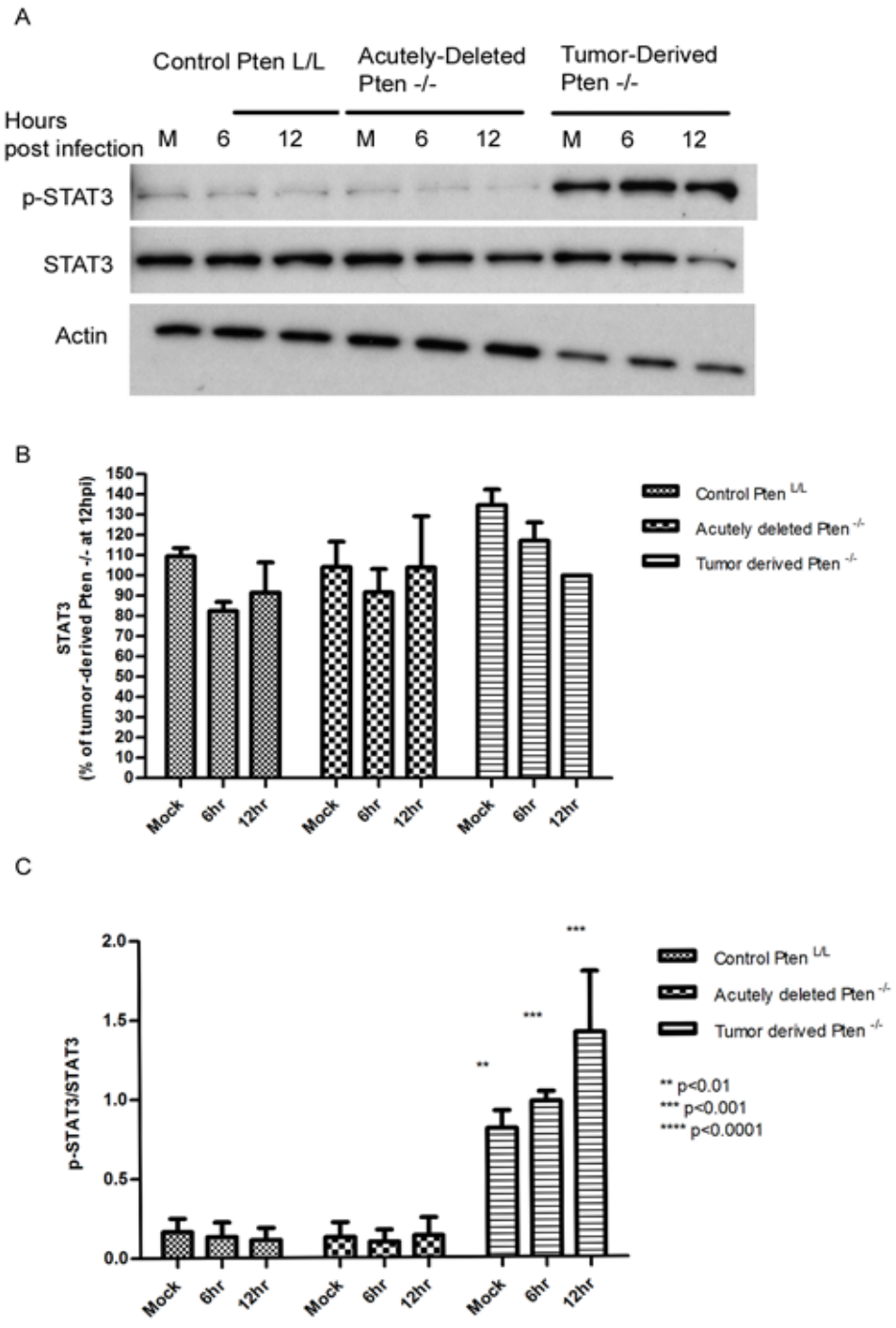

Figure. 22. Tumor-derived *Pten* $^{-/-}$ cells have constitutively activated STAT3.

Effects of Inhibiting IL-6 on STAT3 Activation

Constitutive IL-6 production is likely responsible for STAT3 activation in tumor-derived *Pten* $^{-/-}$ cells (Figure. 19 and Figure. 21), although STAT3 activation may be mediated by factors other than IL-6. Some of these factors include IFN-α and γ. To determine whether activation of STAT3 is mediated by IL-6, tumor-derived *Pten* $^{-/-}$ cells were treated with anti-IL-6 antibody at increasing concentrations. Cell lysates were harvested at indicated times after treatment and immunoblotting was performed to probe for total and phospho-STAT3 levels. At 16 hours after treatment with anti-IL-6 antibody, tumor-derived *Pten* $^{-/-}$ cells demonstrated a dose-dependent response to anti-IL-6 treatment (Figure. 23A and B). At 5 ng/mL of anti-IL-6 antibody, levels of p-STAT3 were about 28% of untreated controls. High levels of anti-IL-6 antibody (5000 ng/mL) achieved almost complete inhibition of STAT3 activation, such that the p-STAT3 level was about 2% of untreated controls. The effectiveness of anti-IL-6 inhibition of STAT3 activation decreased over time, such that by 64 hours after treatment, 50 ng/mL of anti-IL-6 antibody was necessary to achieve 50% inhibition of STAT3 activation. This could be due to antibody degradation in culture, or due to accumulation of IL-6 expressed by tumor-derived *Pten* $^{-/-}$ cells. Together, these data demonstrate that STAT3 activation in tumor-derived *Pten* $^{-/-}$ cells is mediated by the IL-6 cytokine.

The levels of total STAT3 expression did not demonstrate any observable dose-dependent relationship with amounts of anti-IL-6 antibody treated (Figure. 23C). The levels of total STAT3 also did not demonstrate any correlation with the levels of p-STAT3. However, STAT3 levels in cells treated with anti-IL-6 antibody were slightly less than those in untreated cells, about 60-80% of untreated controls. Inhibiting IL-6 may

decrease the positive feedback that IL-6 provides on the IL-6/STAT3 pathway, thereby downregulating STAT3 expression to this extent.

Figure. 23. IL-6 mediates activation of STAT3 in tumor-derived *Pten* $^{-/-}$ cells.

Tumor-derived *Pten* $^{-/-}$ cells were treated with anti-IL-6 antibody at concentrations of 5, 50, 500 and 5000 ng/mL. Cell lysates were harvested at indicated times after treatment and immunoblotting was performed to probe for total and phospho-STAT3 levels. (A) shows a representative image of two independent experiments. . p-STAT3 (B) and STAT3 (C) levels were quantified and expressed as a percentage of untreated controls of tumor-derived *Pten* $^{-/-}$ cells. Data shown are average of two experiments +/- SEM.

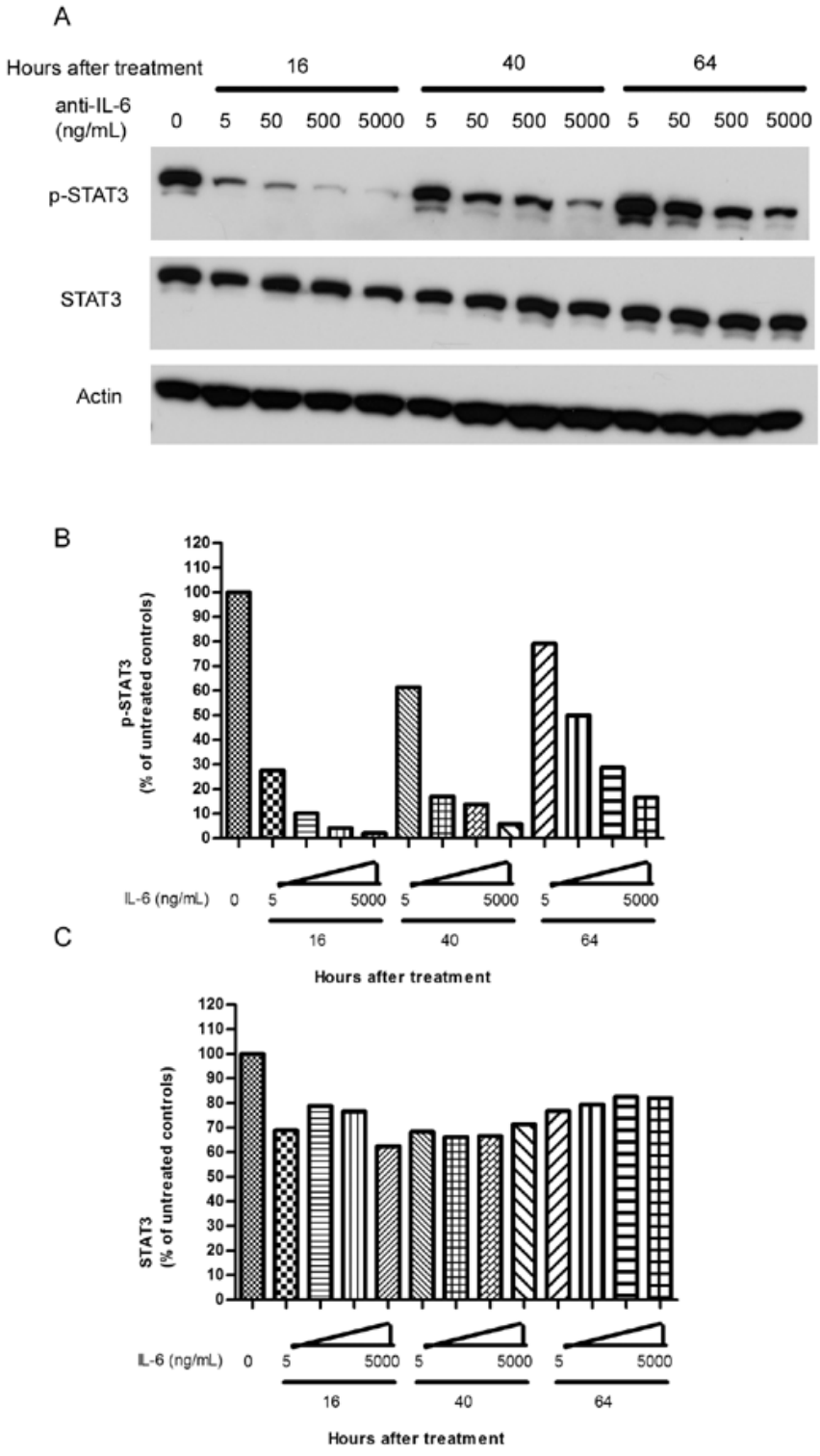

Figure. 23. IL-6 mediates activation of STAT3 in tumor-derived *Pten* $^{-/-}$ cells.

Effects of Inhibiting IL-6 on Activation and Expression of STAT1 in Tumor-Derived *Pten* $^{-/-}$ cells

There is significant cross-talk between the type I IFN system and the IL-6/STAT3 pathway reported in literature. In some systems, activation of the IL-6/STAT3 pathway leads to activation of type I IFN system, which promotes phosphorylation and upregulation of STAT1 and creates an antiviral effect. In other systems, the role of STAT3 in negatively regulating the type I IFN system has been demonstrated. Therefore, the effect of inhibiting STAT3 activation on STAT1 signaling in tumor-derived *Pten* $^{-/-}$ cells was investigated. The same lysates from the previous analysis were analyzed for p-STAT1 and STAT1 levels using immunoblotting (Figure. 24A). The levels of total STAT1 were analyzed in this experiment. Unphosphorylated STAT1 has been shown to have IFN responsiveness and antiviral activity by itself. There does not appear to be a dose-dependent relationship between amount of anti-IL6 antibody and total STAT1 levels. However, at 16 hours post treatment with 5000 ng/mL of anti-IL-6 antibody, a condition in which the greatest inhibition of phospho-STAT3 was achieved, total STAT1 levels were about 43% of untreated controls. But, by 64 hours post treatment, the levels of total STAT1 at any given concentration are higher than untreated controls. There was no observable dose-dependent relationship between the ratio of p-STAT1/STAT1 and amount of anti-IL-6 antibody (Figure. 24A and C). However, at the concentrations in which greatest p-STAT3 inhibition was observed (5000ng/mL), the ratio of p-STAT1/STAT1 were 1.2, 0.5 and 0.5 at 16, 40 and 64 hours after treatment respectively. In addition, at 40 hours post treatment, the ratio of p-STAT1/STAT1 are lower than untreated controls at any given concentration.

Thus, there was no discernible pattern in change in p-STAT1 or STAT1 levels following inhibition of STAT3 activation. Nonetheless, change in p-STAT1 or STAT1 levels was observed after treating with anti-IL-6 antibody. This suggests that there is a more complicated mechanism of regulation of type I IFN signaling by IL-6/STAT3 pathway that is more than just simply positive or negative regulation.

Figure. 24. Anti-IL-6 antibody has very little effect on activation and expression of STAT1 in tumor-derived *Pten* $^{-/-}$ cells. Tumor-derived *Pten* $^{-/-}$ cells were treated with anti-IL-6 antibody at concentrations of 5, 50, 500 and 5000 ng/mL. Cell lysates were harvested at indicated times after treatment and immunoblotting was performed to probe for total and phospho-STAT1 levels. (A) shows a representative image of two independent experiments. STAT1 levels were quantified and expressed as a percentage of untreated controls of tumor-derived *Pten* $^{-/-}$ cells (B). The ratio of p-STAT1/STAT1 is shown in (C). Data shown are average of two experiments.

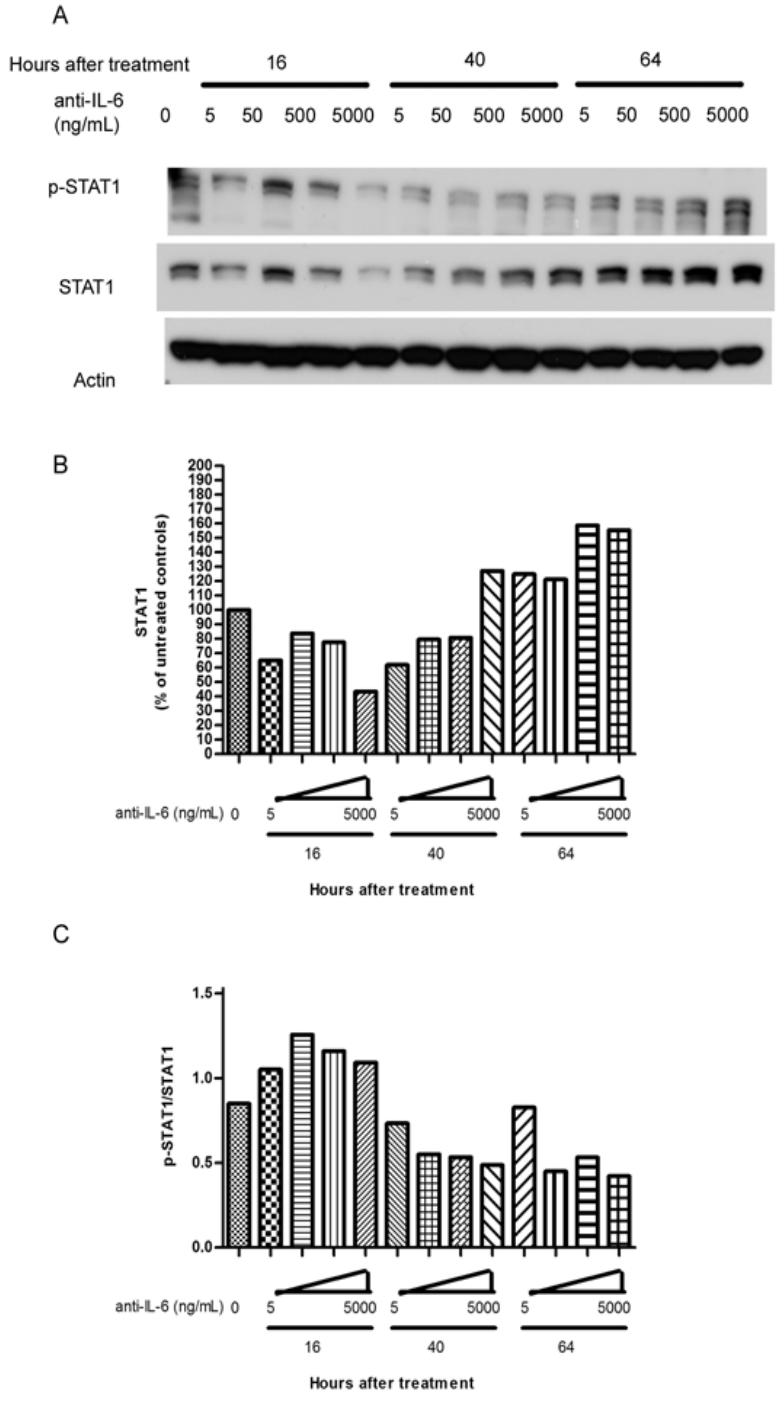

Figure. 24. Anti-IL-6 antibody has very little effect on activation and expression of STAT1 in tumor-derived *Pten* $^{-/-}$ cells.

Effects of Inhibiting STAT3 Activation on Viral Gene Expression in Tumor-Derived *Pten* $^{-/-}$ cells

In order to determine whether the IL-6/STAT3 pathway has an antiviral effect, the ability of tumor-derived *Pten* $^{-/-}$ cells to support viral gene expression was evaluated. Tumor-derived *Pten* $^{-/-}$ cells were cultured in media containing indicated concentrations of anti-IL-6 antibody for 16 hours. Cells were infected with rwt virus at MOI of 10, and cell lysates were analyzed by immunoblotting. M protein expression was analyzed as a measure of viral gene expression and calculated as a percentage of untreated controls at 24 hpi. The dose response to anti-IL-6 treatment was analyzed in two separate series of experiments at low doses (0, 5 and 50 ng/mL, Figure. 25A) and high doses (0, 500 and 5000 ng/mL, Figure. 25B). If inhibiting STAT3 activation increases susceptibility to VSV infection, viral gene expression would increase as a result of inhibiting STAT3 activation. However, there was very little difference in M protein levels in infected cells treated with either low levels of anti-IL-6 antibody (Figure. 25A) or high levels (Figure. 25B). Together, this data suggests that Inhibiting STAT3 activation has very little effect on viral gene expression in tumor-derived *Pten* $^{-/-}$ cells cells.

Figure. 25. Inhibiting STAT3 activation has very little effect on viral gene expression in tumor-derived *Pten* $^{-/-}$ cells. Tumor-derived *Pten* $^{-/-}$ cells were cultured in media containing indicated concentrations of anti-IL-6 antibody for 16hrs. Cells were mock-infected or infected with rwt MOI = 10 for the indicated times. Cells were maintained in media containing anti-IL-6 antibody during infection. Cell lysates were harvested at indicated times after infection. Immunoblotting was performed to determine viral M protein expression. Actin protein expression levels were included as loading controls. Data shown are representative images of two experiments. (A) shows images of tumor-derived *Pten* $^{-/-}$ cells treated in 0, 5 and 50 ng/mL of anti-IL-6 antibody and the graph is a quantification of M protein expression expressed as a percentage of untreated controls at 24hpi. (B) shows images of tumor-derived *Pten* $^{-/-}$ cells treated in 0, 500 and 5000 ng/mL of anti-IL-6 antibody and the graph is a quantification of M protein expression expressed as a percentage of untreated controls at 24hpi. Data shown are average of two experiments.

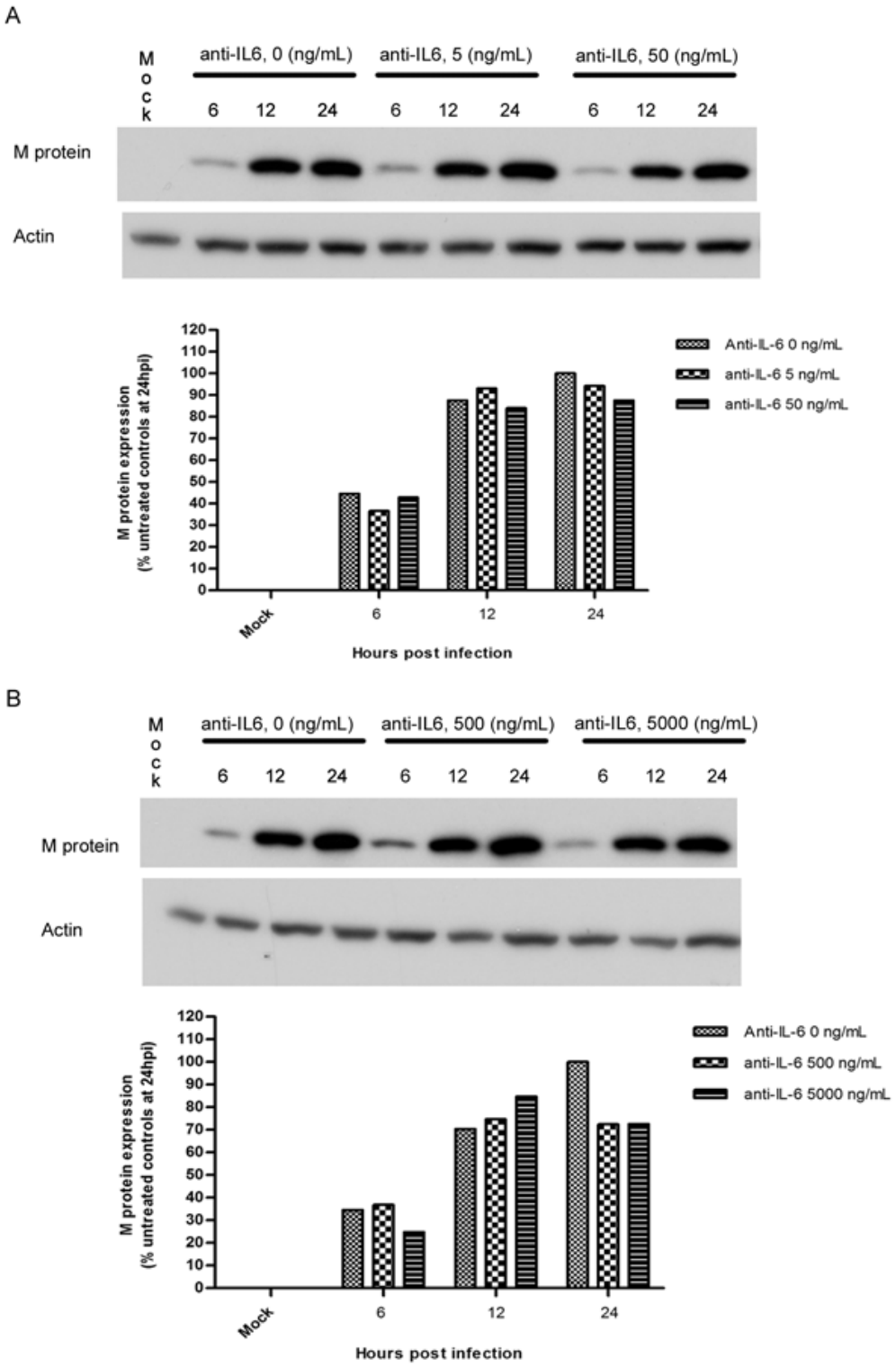

Figure. 25. Inhibiting STAT3 activation has very little effect on viral gene expression in tumor-derived *Pten* $^{-/-}$ cells.

Effects of IL-6 Treatment on Control *Pten* $^{L/L}$ cells

In order to further examine the effect of IL-6/STAT3 pathway on prostate epithelial cells, I determined whether normal *Pten* $^{L/L}$ cells can be protected from VSV infection by treatment with IL-6. Control *Pten* $^{L/L}$ cells were first treated with IL-6 to examine whether the IL-6/STAT3 system can be activated in these cells. These cells were treated with varying concentrations of IL-6 and cell lysates were harvested at the indicated times after infection. Immunoblotting was performed to examine levels of p-STAT3 and STAT3 (Figure. 26). 0.1 ng/mL of IL-6 was not sufficient to stimulate p-STAT3. A ten-fold increase in IL-6 (1 ng/mL) was able to achieve some activation of STAT3 at later times of treatment (6 hours post treatment), but 10 ng/mL of IL-6 achieved robust STAT3 activation as early as 1 hour after treatment, and this activation was sustained for up to 6 hours after treatment. This amount of STAT3 activation was at least as high as the level in tumor-derived derived *Pten* $^{-/-}$ cells, which served as a positive control in the immunoblot (Figure. 26A). Cells stimulated with high amounts of IL-6 (10ng/mL) have lower levels of total STAT3 (Figure. 26C), suggesting that there is a shift in STAT3 protein population from total to phosphorylated forms. Together, this data indicates that upon IL-6 stimulation, *Pten* $^{L/L}$ cells rapidly activate STAT3 and this activation is maintained over time.

Figure. 26. IL-6 induces activation of STAT3 in control *Pten* $^{L/L}$ cells. Control *Pten* $^{L/L}$ cells were serum-starved for 24hrs and were then treated with indicated concentrations of IL-6 cytokine. Cell lysates were harvested at various times after treatment. Total STAT3 protein expression and STAT3 phosphorylation status were detected using total and phospho-specific antibodies. The positive control for phospho-STAT3 and STAT3 were lysates from tumor-derived *Pten* $^{-/-}$ cells. (A) shows a representative image of the experiment. (B) shows a quantification of p-STAT3 levels expressed as a percentage of cells treated with IL-6 at 10 ng/mL for 6 hours. (C)) shows a quantification of STAT3 levels expressed as a percentage of cells treated with IL-6 at 10 ng/mL for 6 hours

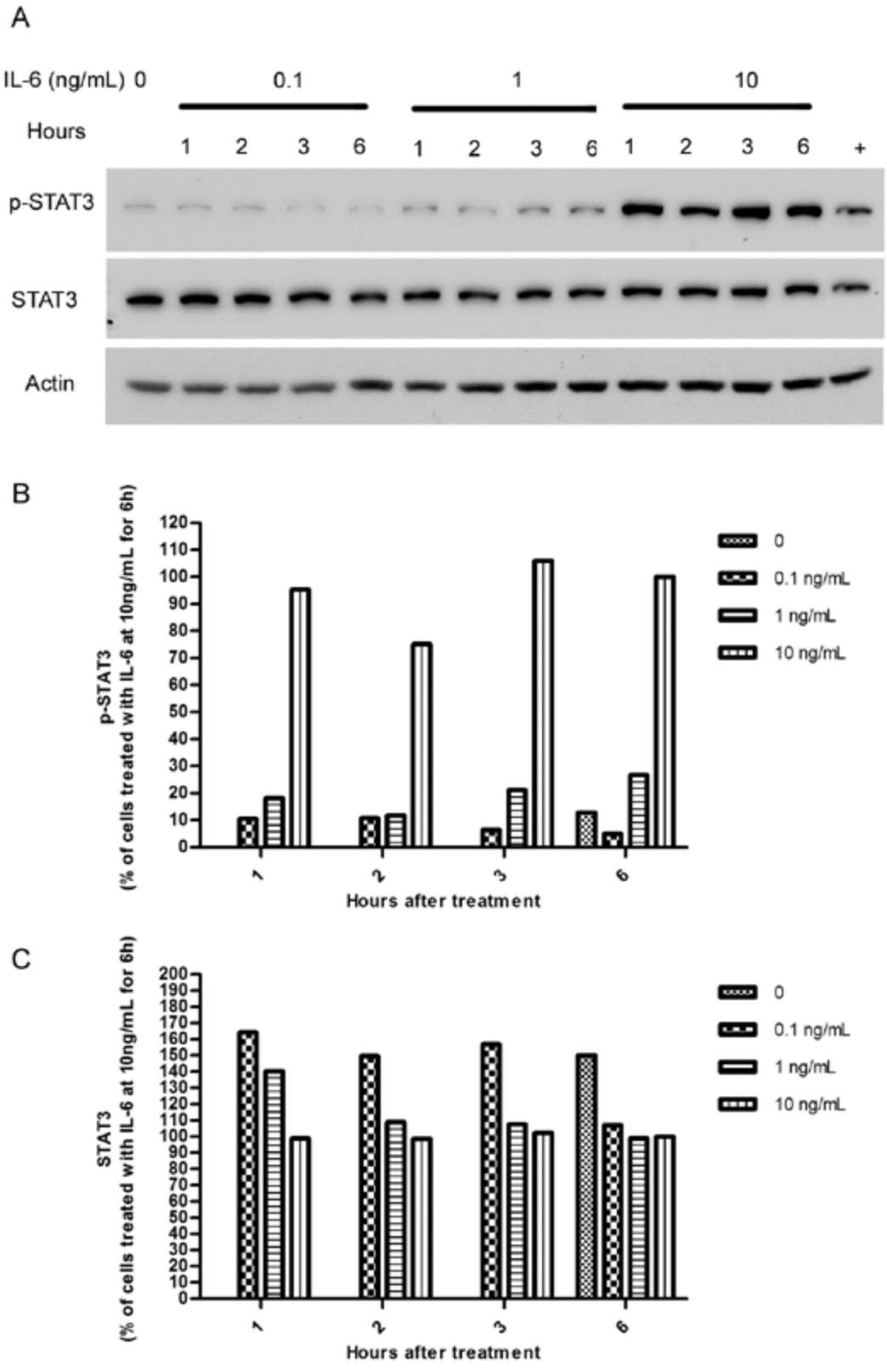

Figure. 26. IL-6 induces activation of STAT3 in control *Pten* $^{L/L}$ cells.

Effects of IL-6 Stimulation on Activation and Upregulation of STAT1 in Control *Pten* $^{L/L}$ Cells

In order to determine whether the activation of IL-6/STAT3 has an effect on activation of STAT1, control *Pten* $^{L/L}$ cells were stimulated with IL-6 and probed for p-STAT1 and STAT1 (Figure. 27). Very little if any p-STAT1 was observed upon stimulation with varying concentrations of IL-6 over 6 hours of stimulation. Levels of STAT1 expression were quantified and a modest upregulation of STAT1 was observed in cells treated with 10 ng/mL of IL-6 (Figure. 27B), particularly at the 3 hr time point. This corresponds with some observations in the literature that suggest modulation of the type I IFN system by IL-6 may be small and transient (51).

Figure. 27. IL-6 induces very little activation or upregulation of STAT1 in control *Pten* $^{L/L}$ cells. Control *Pten* $^{L/L}$ cells were serum-starved for 24hrs and were then treated with indicated concentrations of IL-6 cytokine. Cell lysates were harvested at various times after treatment. Total STAT1 protein expression and STAT1 phosphorylation status were detected using total and phospho-specific antibodies. The positive control for phospho-STAT1 and STAT1 were lysates from tumor-derived *Pten* $^{-/-}$ cells infected with rM51R virus. (A) shows a representative image of the experiment. (B) shows a graphical summary of levels of STAT1 expressed as a percentage of cells treated with IL-6 at 10 ng/mL for 6 hours.

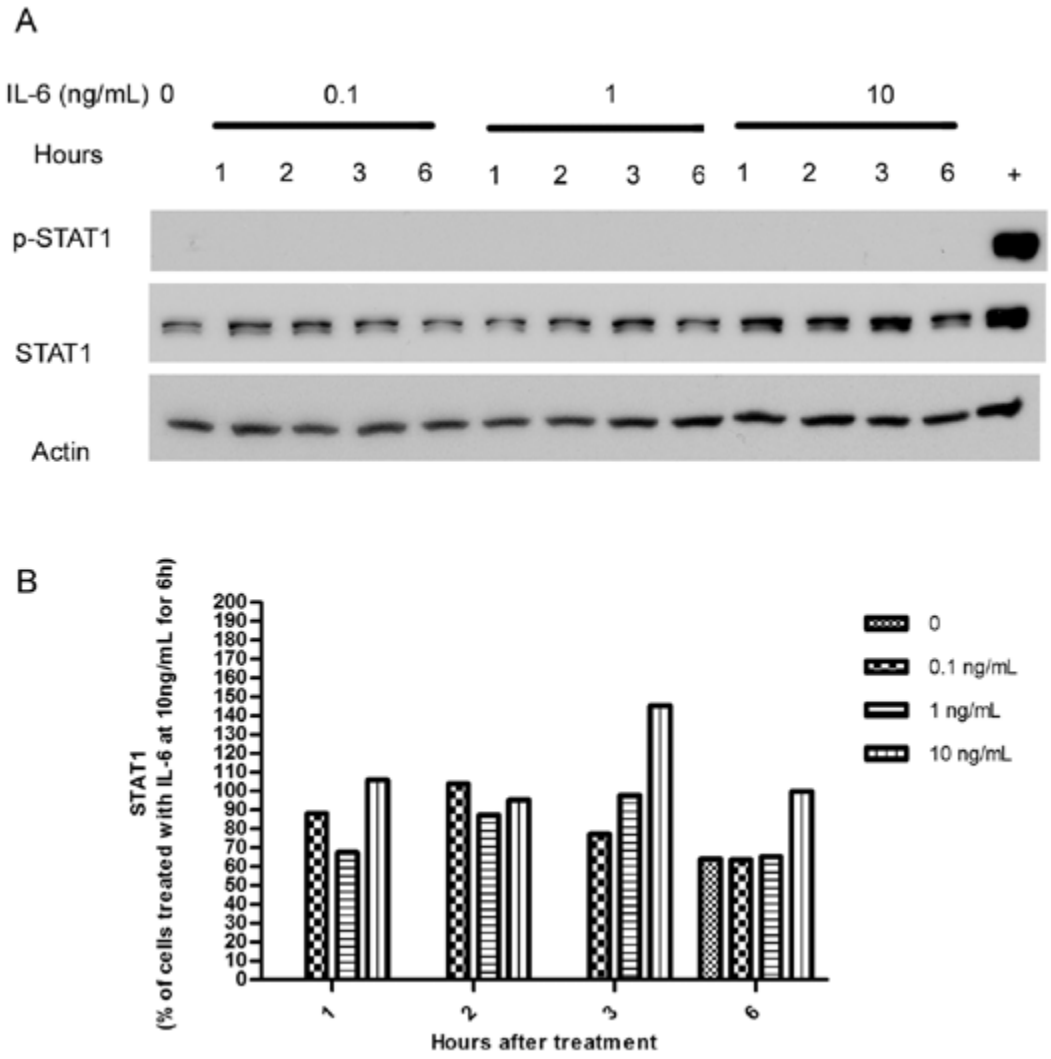

Figure. 27. IL-6 induces very little activation or upregulation of STAT1 in control *Pten* $^{L/L}$ cells.

Effects of IL-6 on Viral Gene Expression

In order to determine whether IL-6 alters susceptibility to VSV infection, cells were treated with various concentrations of IL-6 for 1 hr and infected with rwt-GFP virus. The ability of the cells to support viral gene expression was evaluated by flow cytometry. Figure. 28A shows histograms of cells treated with varying concentrations of IL-6 and infected with rwt-GFP virus at MOI of 0.1. A graphical summary of geometric mean fluorescence (MFI) intensity is shown alongside. When compared to mock-infected cells (Figure. 28C), most of the cells infected with rwt-GFP virus at MOI of 0.1 remain in the first (negative) decade by 6 hpi, but a majority of the cells shifted past the first decade by 12 hpi as expected in a multiple cycle infection (Figure. 28A). The amount of cells in the low GFP expressing population was reduced slightly by treatment with IL-6. Analysis of geometric MFI showed that at 12 hpi, treatment with IL-6 decreased GFP fluorescence intensity at MOI of 0.1. However, this effect is very small. At MOI of 10, there was no reproducible decrease in MFI. Together, this data suggests that IL-6 activation of STAT3 has a very modest effect on delaying VSV infection at low MOI.

Figure. 28. Treating control *Pten* $^{L/L}$ cells with IL-6 has a modest effect on decreasing viral gene expression. Control *Pten* $^{L/L}$ cells were serum-starved for 24hrs and were then treated with indicated concentrations of IL-6 cytokine for 1hr. Cells were infected with rwt-GFP at MOI of 0.1 (A), or at MOI of 10 (B), or were mock-infected (C). GFP expression was analyzed by flow cytometry. Data shown are histograms of cells expressing GFP. Geometric mean fluorescence intensity was obtained as shown. Data are average of two experiments.

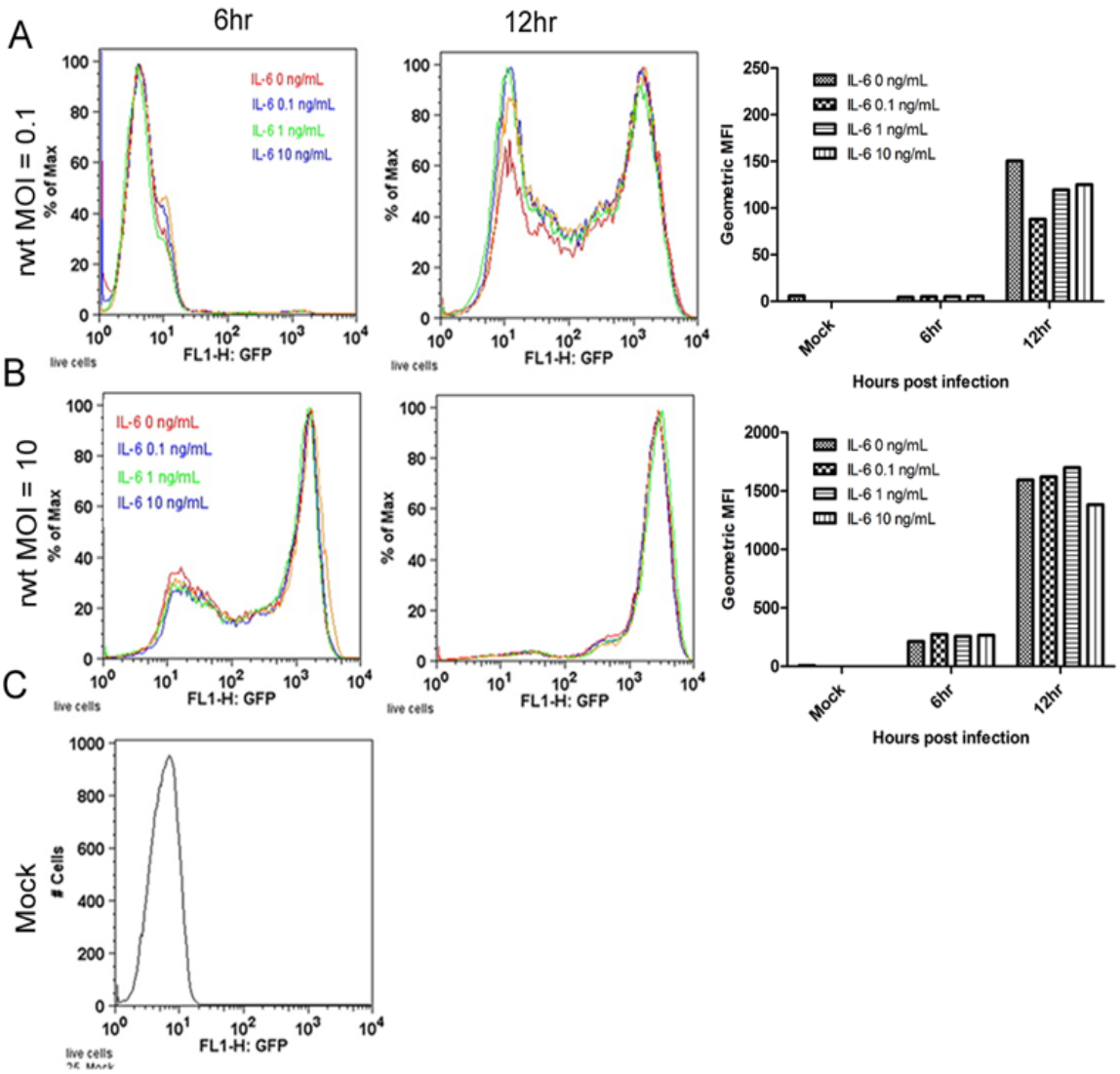

Figure. 28. Treating control *Pten* $^{L/L}$ cells with IL-6 has a modest effect on decreasing viral gene expression.

Effects of IL-6 on VSV-Induced Cell Death

The antiviral effects of IL-6/STAT3 pathway were further examined by treating control *Pten* $^{L/L}$ cells with IL-6, infecting with rwt and rM51R viruses, and analyzing cell viability by MTT assay. In rwt virus-infected cells, protection from VSV-induced cell death was only observed at MOI of 0.1 at 24 hpi (Figure. 29A). This data corresponds to data from the viral gene expression assay, in which IL-6 treatment modestly decreased viral gene expression at low MOI (Figure. 28A). This protective effect was transient, as the cells treated with IL-6 (10ng/mL) were eventually killed by 48 hpi (Figure. 29C). IL-6 treatment offered very little, if any protective effect on cells that were infected at higher MOIs of 1 and 10 (Figure. 29A and C). This data suggests IL-6 may provide some protection to VSV infection at low MOI, such that IL-6 delays the spread of the virus across the culture, but has very little effect in providing immediate protection from virus infection at high MOI. This delay in virus spread across the culture was not observed for rM51R virus at any MOI. Because the rM51R virus does not inhibit host gene expression, and induces low levels of IL-6 production in these cells, the actual levels of IL-6 in these cultures may not be at the levels in which these cells were treated. Thus, it appears that exogenous IL-6 treatment does not have any observable effect in protecting these cells from rM51R virus-induced cell death.

Figure. 29. IL-6 provides a small amount of protection to control *Pten* $^{L/L}$ cells from rwt-induced cell death at low MOI. Control *Pten* $^{L/L}$ cells were serum-starved for 24hrs and were then treated with indicated concentrations of IL-6 cytokine for 1hr. Cells were infected with rwt (A and C) and rM51R (B and D). Cell viability was determined using MTT reagent at 24 (A and B) or 48 hours after infection (C and D). Cell viability was expressed as a percentage of mock-infected cells. Data shown are average of at least three experiments +/- SEM.

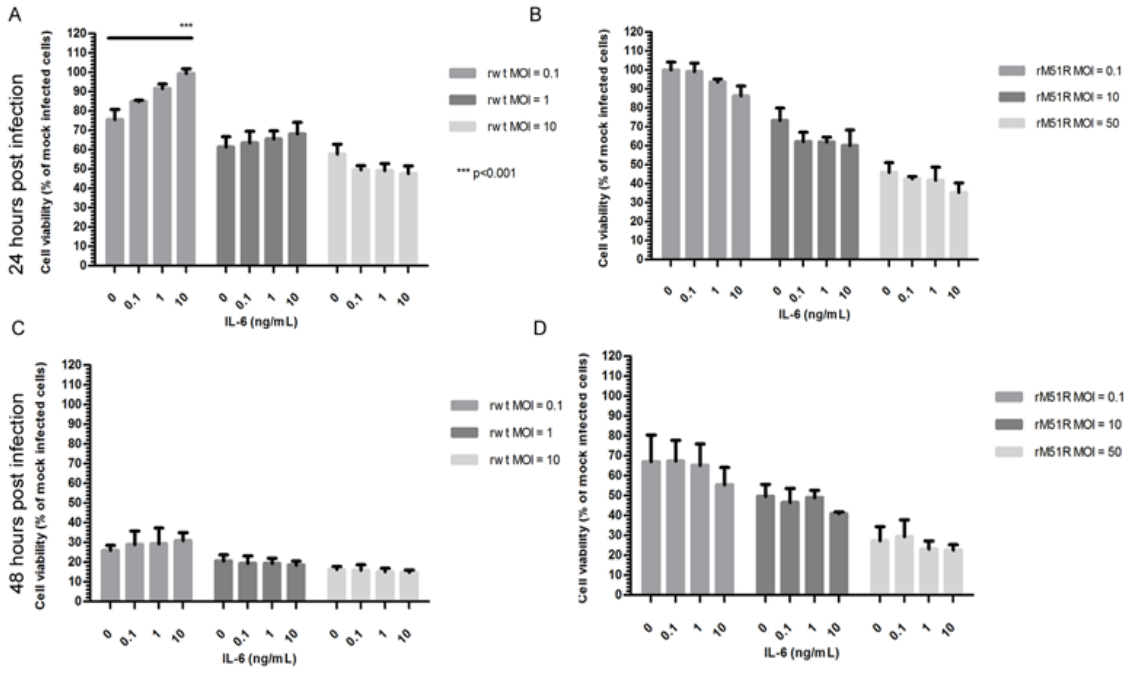

Figure. 29. IL-6 provides a small amount of protection to control *Pten* $^{L/L}$ cells from rwt-induced cell death at low MOI.

Discussion

Vesicular stomatitis virus is an attractive candidate oncolytic virus. To date, the virus has been tested as an oncolytic agent against a myriad of cancer cell types, ranging from glioblastomas, head and neck cancers, pancreatic adenocarcinomas, hepatocellular carcinomas to breast and prostate cancers, to name a few (6, 26, 27, 90, 133). Even more excitingly, VSV has recently moved to phase I clinical trials for treatment of patients with liver cancer. However, the common trend observed in the literature is that some cell lines are susceptible to VSV oncolysis, whereas other cell lines are resistant to VSV oncolysis, despite originating from the same tissue type. In human prostate cancer cell lines, Ahmed et al found that LNCaP cells are sensitive, whereas PC-3 cells are susceptible to VSV infection (2) . A follow-up analysis by Carey et al found that PC-3 cells constitutively activate and upregulate antiviral proteins that may contribute to their resistance to VSV(26). LNCaP and PC-3 cells represent two widely studied cell lines in prostate cancer and vary in many aspects of their biology, including their responsiveness to IFN to amount antiviral defense. The question arises, whether this difference in susceptibility to VSV infection stems from evolution of the tumor. I hypothesized that susceptibility to VSV changes during progression of prostate cancer, from the stage of initiating mutation, to advanced adenocarcinoma and castration-resistant prostate cancer. Primary and long-term cultures of cells derived from the murine prostate-specific *Pten*-deletion tumor model were used to test this hypothesis.

A surprising finding from my experiments is that advanced prostate adenocarcinomas from the murine prostate-specific *Pten*-deletion tumor model contained a mixture of cells

susceptible and resistant to VSV (Figures 2 and 3). This finding is interesting, and suggests that susceptibility of cancer cells to VSV is not only dependent on the type of initiating mutation, since these tumor cells arise from a single genetic mutation of *Pten* deletion. Instead, susceptible and resistant cells can evolve within the same tumors due to heterogeneity in tumor evolution. The role of *Pten* in sensitivity to VSV infection was further investigated using long-term cultures of murine prostate cells. Acutely-deleted *Pten* $^{-/-}$ cells were derived by deleting the Pten gene *in vitro*. Tumor-derived *Pten* $^{-/-}$ cells were obtained by spontaneously immortalizing *Pten* -/- cells from tumors developed in the murine prostate-specific *Pten*-deletion model. My experiments demonstrated that acutely-deleted *Pten* $^{-/-}$ cells were poorly responsive to IFN stimulation, and were susceptible to VSV infection (Figures 4-7, 9). This suggests that in the early stages of tumor development, cells destined to become prostate cancer are primarily sensitive to VSV. In comparison, tumor-derived *Pten* $^{-/-}$ cells constitutively expressed higher levels of antiviral proteins, activated STAT1 in response to VSV infection, and were correspondingly resistant to VSV infection (Figures 4-8). These results indicate that simply deleting the *Pten* gene in vitro causes decreased IFN responsiveness and susceptibility to VSV infection, but deleting the *Pten* gene and subsequent evolution in tumor leads to development of some cells that are resistant to VSV infection. This is a novel result that indicates susceptibility to VSV infection is not only dependent on the type of initiating mutation for prostate cancer.

The observation that acute deletion of the *Pten* gene leads to poor IFN responsiveness and susceptibility to VSV is consistent with studies that investigated the crosstalk between PTEN/AKT pathway and the JAK-STAT pathway. The PTEN/AKT pathway interacts with the JAK-STAT pathway at multiple levels, one of which is at the level of

glycogen synthase kinase-3β (GSK-3β). GSK-3β is a serine/threonine kinase whose activity is inhibited through phosphorylation by AKT. Activated GSK-3β removes the inhibition of SHP2 on STAT1 (124). Tseng et al demonstrated that activation of AKT following PTEN loss leads to downregulation of STAT1, and this occurs through inhibition of GSK-3β activity (125). Moussavi et al also demonstrated that a murine cell line derived from *Pten* $^{-/-}$ prostate tumors was poorly responsive to IFN treatment and was susceptible to VSV infection (92). Together, these studies support my observations that an acute loss of Pten decreases the protective effect of IFN against VSV infection.

The effect of acute Pten loss does not account for the difference in susceptibility between LNCaP and PC-3 cells, as neither of these two cell lines have functional Pten protein, and both have constitutively active AKT pathway (137). Moreover, primary cultures of tumor cells derived from mice with prostate-specific deletion of the Pten gene contained a heterogeneous mix of cells susceptible and resistant to VSV infection (Figures 2 and 3). Clonal populations of tumor-derived *Pten* $^{-/-}$ cells also exhibited resistance to VSV-infection (Figures 4-7). Together, these data indicate that evolution within tumors changes the susceptibility to VSV infection. What could be the cause of this resistance? Tumor-derived *Pten* $^{-/-}$ cells overexpress STAT1 proteins (Figure 8), and overexpression of these proteins has an antiviral effect (29). Thus, changes must have occurred during tumor evolution to promote antiviral gene expression. During tumor progression, activated AKT pathway may a different role in antiviral defense.

In addition to the observation that GSK-3β activates STAT1, activated AKT has been demonstrated to interact with JAK-STAT pathway at other levels to give a completely different phenotype, a phenotype that promotes IFN responsiveness and antiviral

defense. This occurs at the level of one downstream effector of AKT, protein kinase C-δ (PKC- δ). PKC- δ is activated by treatment with type I IFNs and associates with STAT1 to phosphorylate and activate STAT1 (reviewed in (96)). Inhibiting PKC- δ reduced the responsiveness of HeLa cells to IFN and greatly diminished IFN-mediated protective antiviral activity against VSV (98). Another downstream substrate of Akt is EMSY, a transcriptional repressor that in conjunction with other binding partners binds to ISRE and repress transcription of IFN-stimulated genes (40). AKT activates EMSY and removes this repressive activity from ISREs, which allows transcription of antiviral genes that protect from VSV infection (40). More recently, Kaur et al demonstrated that AKT mediates translation of interferon stimulated transcripts, through activating the mTOR arm of AKT (63). Inactivating or inhibiting the mTOR branch of AKT diminishes IFN responsiveness and increases susceptibility to VSV infection *in vitro* as well as *in vivo*. Thus, activation of AKT pathway can have antiviral effects. The widely opposing antiviral effects of AKT in the literature reflect the complexity in regulation of IFN and antiviral response by AKT. Because AKT regulates interferon responses at multiple levels, it is unclear which level dominates over the other, thus the overall effect of activated AKT pathway on antiviral responses may be dependent on cell type, and in the case of the cells I have studied, the effect must depend on other genetic and epigenetic changes that occur in prostate cancer evolution.

As mentioned in the introduction, AKT-independent effects of PTEN loss have been observed. JNK signaling is activated following PTEN loss (127). Chu et al demonstrated that JNK2 is required for activation of IFN activity following stimulation by either dsRNA or VSV (32). Activation of IFN activity could result from JNK-mediated phosphorylation of STAT1 (144). Thus, accumulation of cellular changes following

PTEN loss and tumor development, could lead to activation of IFN responses and antiviral defense thereby promoting resistance of tumor-derived *Pten* $^{-/-}$ cells to VSV infection.

Observations from my experiments differ from those made by Moussavi et al (92). Moussavi et al treated prostate-specific *Pten* $^{-/-}$ mice with a mutant strain of VSV (AV3) that is defective in inhibiting host antiviral responses, similar to rM51R virus. Intraprostatic administration of AV3 in prostate-specific *Pten* $^{-/-}$ mice yielded robust viral gene expression compared to control mice. This was demonstrated using recombinant AV3 encoding luciferase gene: following injection with AV3-luciferase, luciferin was administered. Bioluminescence was measured as readout for viral gene expression. By this assay, bioluminescence in prostate-specific *Pten* $^{-/-}$ mice was robust immediately following infection, rose to high levels by 6 hpi and was barely detectable by 96 hpi. Similarly, viral titers to determine amount of replicating virus in the prostates of prostate-specific *Pten* $^{-/-}$ mice were higher than control mice, and follows the same time frame as the viral gene expression assay. These experiments suggest that cells in prostate-specific *Pten* $^{-/-}$ mice are primarily susceptible to VSV (AV3) infection. Nonetheless, by 96 hpi, at time when most of the virus replication is complete, the number of Ki67+ cells in prostate-specific *Pten* $^{-/-}$ mice were still higher than control mice, indicating that highly proliferative cells still exist in the tumor following virus infection, but virus titers are barely detectable by this time. There could be several explanations for this difference between my observations (Figures 2 and 3) and those made by Moussavi et al. My experimental design involves infection of primary cell derived from the tumor with rwt and rM51R at MOI of 10. Infection in this *ex vivo* scenario at this MOI would achieve a synchronous infection in a permissive cell type, such that most of the cell would express

viral genes. Synchronous infection was observed for cells derived from control *Pten* $^{L/L}$ prostates, but not for tumor-derived *Pten* $^{-/-}$ cells. In fact, only some of the cells expressed viral proteins (Figures 2 and 3). This observation was supported by clonal populations of tumor-derived *Pten* $^{-/-}$ cells, that synchronous infection was not achieved even at MOI of 50 (Figure 4), demonstrating a resistance to infection independent of MOI. If cells could not be infected in an ex vivo scenario at MOI of 10 or 50, the likelihood that these cells are infected in vivo (in which fewer viruses infect each cell) are not high. Thus it is very likely that although some of the cells in *Pten* $^{-/-}$ prostate tumors supported viral gene expression, others did not in Moussavi et al's experiments, such that by 96 hpi when viral genes or viral titers was barely detectable, proliferative Ki67+ cell were still observed. Another possibility is that my *ex vivo* primary cultures of tumor-derived *Pten* $^{-/-}$ cells consisted primarily of epithelial cells (Figure 1), and analysis of susceptibility to infection in was performed on epithelial cells in my experiments. Normal and tumorous murine prostates contain epithelial and stromal cells, and it is possible that non-epithelial cells in *Pten* $^{-/-}$ prostate tumors robustly supported viral gene expression (92). To conclusively demonstrate the susceptibility of *Pten* $^{-/-}$ prostate tumors to VSV, tumor size reduction and disease free survival of the mice should be measured. These experiments were not performed by either Moussavi et al or me, due to the extensive mouse breeding that these experiments would entail.

An interesting finding from my data is that castration-resistant *Pten* $^{-/-}$ tumor cells are primarily susceptible to virus infection (Figure 3). At least two possibilities that are not mutually exclusive could contribute to this effect. One possibility is that cells that are IFN-responsive and resistant to VSV-infection are extremely sensitive to effects of androgen withdrawal. As a result, the cells that remain and undergo clonal expansion

are castration-resistant and susceptible to virus. Alternatively, androgen withdrawal induces apoptosis of tumor cells irrespective of their IFN-responsiveness and sensitivity to virus infection, however, the progression of surviving cells to castration resistance is accompanied by downregulation of antiviral genes. Both of these scenarios suggest a relationship between androgen signaling and antiviral response. There are few reports that implicate this relationship. In many castration-resistant prostate cancers, androgen receptor (AR) activation and signaling remains sustained through a variety of mechanisms (reviewed in (111)) , such as amplification of AR gene copy number, gain of function mutations in the AR gene, and alternative splice isoforms that encode constitutively active AR variants. Bettoun et al demonstrated crosstalk between interferon and androgen signaling pathways, and this crosstalk may be mediated in part by Rnase L (18). Androgen-responsive transcription activity was observed in cells treated with androgen, but this transcriptional activity was abrogated in the presence of IFN-stimulated Rnase L activity (18). Silencing AR stimulated IFN-induced STAT1 expression (18). These observations suggest that androgen signaling and IFN signaling may be antagonistic. In a system in which AR signaling predominates, IFN responses are attenuated. These observations would support my result that castration resistance increases susceptibility to VSV infection by increasing AR sensitivity to low levels of androgen. Another regulator of androgen signaling and the JAK-STAT pathway is the protein inhibitor of activated STAT (PIAS). Proteins in the PIAS family interact with AR and can act as AR transcriptional coactivators or corepressors, depending on the particular member of the family (50). PIAS1 is an AR coactivator and promotes AR-dependent transcriptional activity (50, 71). PIAS1 inhibits STAT1-mediated gene activation by preventing the DNA binding activity of STAT1 (80). This inhibitory action occurs when PIAS1 interacting with phosphorylated dimerized form of STAT1, preventing STAT1 from binding to DNA (78). It is possible, that in castration-resistant

prostate cancer, PIAS1 is overexpressed and inhibits antiviral signaling (76). However, it is also possible that only castration-resistant tumor cells with *Pten* $^{-/-}$ initiating mutations develop susceptibility to VSV infection. An analysis of gene expression changes in castration-resistant cell lines revealed that these cell lines express different levels of PIAS1 and STAT1, and suggests other factors may play a role in regulation the crosstalk between JAK-STAT and androgen signaling(79). Given these relationships between androgen signaling and IFN response, future experiments investigating the role of androgen signaling in susceptibility to VSV infection may prove to be informative of the mechanism of susceptibility. One such experiment would be to stimulate LNCaP cells with androgen and determine STAT1 expression and upregulation. This could be followed-up with analysis viral gene expression and cell viability under androgen stimulated conditions. Similarly, LNCaP or murine prostate cancer cells could be treated with androgen antagonists to determine the effect on sensitivity to VSV.

Prostate cancer is a heterogeneous disease, and this heterogeneity arises in part due to the different initiating mutations. The question arises, whether susceptibility to VSV infection is dependent on the type of cancer initiating mutation. The role of one of these initiating mutations, deletion of the tumor suppressor *Rb*, on susceptibility to VSV infection was investigated. *Rb* $^{-/-}$ cells showed increased susceptibility to VSV infection in a single cycle infection with both rwt and rM51R viruses when compared to control *Rb* $^{L/L}$ cells (Figure 10). In a multiple cycle infection assessing the spread of the viruses across the culture, infection with rwt and rM51R viruses resulted in a faster rate of death in *Rb* $^{-/-}$ cells when compared to the control *Rb* $^{L/L}$ cells (Figure 11). This indicates that *Rb* $^{-/-}$ cells were poorly able to restrict the spread of the virus when compared to the control cells, and also suggests that *Rb* $^{-/-}$ cells may have defective antiviral responses.

Antiviral response was further assessed using the IFN-responsive assay (Figure 12). *Rb* $^{-/-}$ cells were capable of responding to IFN and were protected from VSV-induced cell death at high concentrations of IFN, but required more IFN than control *Rb* $^{L/L}$ cells to achieve protection in 50% of the cells (Figure 12). This confirms the observations made in multiple cycle infections, suggesting that *Rb* $^{-/-}$ cells retain IFN responsiveness and antiviral defenses, but have decreased antiviral defenses when compared to control *Rb* $^{L/L}$ cells. These results indicate that a tumor-initiating mutation, specifically deletion of tumor suppressor *Rb*, alters susceptibility to VSV infection.

My observations are consistent with reports in literature that suggest a relationship between innate immune signaling and pRb signaling. Garcia et al demonstrated that *Rb* $^{-/-}$ MEFs are more sensitive to VSV infection than control cells (46). Nuclear translocation of NF-kB following infection was only observed in control cells but not *Rb* $^{-/-}$ MEFs. As a result, control cells were able to produce higher levels of IFN-β following NF-kB translocation, promoting anti-VSV defense (46). Recently, Taura et al found that Rb may regulate antiviral signaling at a level upstream to activating NF-kB (122). Rb is involved in TLR3 expression; Rb prevents E2F1 from repressing transcription at the TLR3 promoter. Thus, decreased Rb expression leads to downregulation of TLR3, and decreases in the viral detector may present challenges for detecting the presence of the virus and initiating antiviral response (122).

Results from my study and previous studies certainly show promise for using VSV as a treatment for prostate cancer cells with dysregulated Rb/E2F signaling. But because susceptibility to VSV may change during progression of tumor, as observed in the

prostate *Pten* $^{-/-}$ tumor model, future studies investigating the susceptibility of tumor-derived Rb $^{-/-}$ cells to VSV will be important. Prostate *Rb*-null mouse models develop prostate adenocarcinomas inefficiently (55, 86), but Rb deletion appears to play a greater role in promoting castration resistance (108, 109). Future experiments determining whether castration-resistant tumor-derived *Rb* $^{-/-}$ cells are sensitive to VSV infection would be of interest.

The role of STAT3 activation in propagating prostate cancer survival and invasion has been previously demonstrated. However, the role of IL-6/STAT3 pathway in antiviral defense and susceptibility to VSV infection is poorly understood. My experiments demonstrated that that following *Pten* deletion and tumor progression, tumor-derived *Pten* $^{-/-}$ cells constitutively activate STAT3 (Figure 20). This constitutively activated STAT3 is mediated by high levels of IL-6 produced by tumor-derived *Pten* $^{-/-}$ cells (Figure 22). Inhibiting IL-6 in tumor-derived *Pten* $^{-/-}$ cells had very little effect on STAT1 activation and upregulation, and had very little effect on viral protein expression following VSV infection (Figures 22 and 23). These results suggest that despite inhibiting the activation of STAT3, activation and upregulation of STAT1 is still observed. Given that the type I IFN system is still active in tumor-derived *Pten* $^{-/-}$ cells, it is likely that the effects of IL-6/STAT3 pathway on susceptibility to VSV-infection are less apparent. STAT1-mediated antiviral responses likely played a major role in controling virus infection in tumor-derived *Pten* $^{-/-}$ cells and masked the effects of IL-6/STAT3 pathway.

The role of IL-6/STAT3 in mediating the susceptibility to VSV-infection was further tested in control *Pten* $^{L/L}$ cells. Treatment with exogenous IL-6 activated STAT3 in these cells,

but very little activation or upregulation of STAT1 was observed (Figures 24 and 25). The effects of IL-6 on STAT1 activation and upregulation may be transient and inefficient when compared to IFN treatment (51). Haan et al showed that members IL-6 family of cytokines, including oncostatin M and IL-6, stimulated STAT1 activation and dimerization as early as 5 mins after treatment, but activation lasted for only 30 mins after treatment (51). Nonetheless, treatment of IL-6 had a small effect in reducing viral gene expression and protection of VSV-induced cell death at low MOI (Figures 26 and 27). This protective effect was transient, and most of the cells died by 48 hpi. These results support the antiviral protective role of IL-6/STAT3, albeit a small role in murine prostate epithelial cells.

Yang et al provided evidence that activated STAT3 may have a role in antiviral response (139). In Daudi cells that have IFN receptors, activated STAT1-STAT2 dimers and undergo IFN-stimulated gene transcription, these demonstrate poor IFN responsiveness in antiviral activity and growth inhibition. These Daudi cells have mutant STAT3 that cannot be phosphorylated. Transduction of these cells with with a gene encoding STAT3 promoted STAT1 DNA binding activity, and subsequent antiviral defense in response to IFN (139). This study suggests that STAT3 enhances antiviral defense. The protective effect of IL-6/STAT3 axis has been observed in other viruses, such as Theiler's murine encephalitis virus (TMEV) (91). IL-6 treatment protected macrophages from TMEV infection: TMEV RNA was reduced to 50% of untreated controls. This protective effect is presumably due to activation of both STAT1 and STAT3 in macrophages by IL-6 (91). IL-6 also suppressed hepatitis B virus replication in hepatocytes, as observed in in moderate reduction in HBV genome-containing nucleocapsids. This reduction in hepatitis B virus replication is independent of IFN

activity (72). Together with my observations, it appears the IL-6 activation of type I IFN responses is dependent on the cell context. However, even when activation and upregulation of STAT1 is barely detectable, some protection from the virus infection upon IL-6 treatment is observed.

It is interesting to note however, that oncostatin M, a member of the IL-6 family of cytokines, may stimulate STAT1 activity more efficiently that IL-6 itself. Oncostatin M has a slightly different structure than IL-6; its alpha helices are more kinked that those of IL-6 (reviewed in (53). Oncostatin M also engages a different nonsignaling-alpha receptor from IL-6, but shares the signaling receptor gp130 with IL-6 ((53). Oncostatin M is just as efficient as IL-6 in activating STAT3, but produces more efficient and long-lasting activation of STAT1 when compared to IL-6 (51). A recent study by Larrea et al found that oncostatin M had a greater effect in reducing viral gene expression of the hepatitis C virus than IL-6 (73). Oncostatin M-stimulated hepatocarcinoma cells upregulated downstream antiviral genes to higher levels than IL-6. Upregulation of antiviral proteins was further enhanced by low concentrations of IFN (73). These studies demonstrate that members of the IL-6 family of cytokines activate the type I IFN system, but the efficiency varies. This family of cytokines may also cooperate with IFN to enhance antiviral defense. Given these observations, a study that compares efficiency of IL-6 family of cytokines in providing antiviral defense to VSV would shed insight into antiviral cytokines and VSV replication.

My studies enhanced the understanding of mechanisms of susceptibility and resistance of prostate epithelial cells to VSV infection. The data in this thesis demonstrated that a

single initiating mutation alters sensitivity to prostate cancer. Loss of the tumor suppressor pRb and Pten decreased IFN responsiveness and increased susceptibility to VSV infection. Following tumor progression, some of the cells in prostate *Pten* $^{-/-}$ tumors developed resistance to VSV. This may be due to constitutively overexpressed STAT1. Advanced *Pten* $^{-/-}$ tumors also have constitutively activated IL-6/STAT3 pathway, which contributes to the survival of the cells, but has little effect on the STAT1 pathway or sensitivity to VSV infection. Castration of advanced *Pten* $^{-/-}$ tumors promotes sensitivity to VSV infection. These results support the use of VSV as an oncolytic agent in castration resistant prostate cancer patients that have *PTEN* loss.

References

1. **Abdulghani, J., L. Gu, A. Dagvadorj, J. Lutz, B. Leiby, G. Bonuccelli, M. P. Lisanti, T. Zellweger, K. Alanen, T. Mirtti, T. Visakorpi, L. Bubendorf, and M. T. Nevalainen.** 2008. Stat3 promotes metastatic progression of prostate cancer. Am J Pathol **172:**1717-28.
2. **Ahmed, M., S. D. Cramer, and D. S. Lyles.** 2004. Sensitivity of prostate tumors to wild type and M protein mutant vesicular stomatitis viruses. Virology **330:**34-49.
3. **Ahmed, M., and D. S. Lyles.** 1998. Effect of vesicular stomatitis virus matrix protein on transcription directed by host RNA polymerases I, II, and III. J Virol **72:**8413-9.
4. **Ahmed, M., M. O. McKenzie, S. Puckett, M. Hojnacki, L. Poliquin, and D. S. Lyles.** 2003. Ability of the matrix protein of vesicular stomatitis virus to suppress beta interferon gene expression is genetically correlated with the inhibition of host RNA and protein synthesis. J Virol **77:**4646-57.
5. **Ahmed, M., S. Puckett, and D. S. Lyles.** 2010. Susceptibility of breast cancer cells to an oncolytic matrix (M) protein mutant of vesicular stomatitis virus. Cancer Gene Ther **17:**883-92.
6. **Ahmed, M., S. Puckett, and D. S. Lyles.** 2010. Susceptibility of breast cancer cells to an oncolytic matrix (M) protein mutant of vesicular stomatitis virus. Cancer gene therapy **17:**883-92.
7. **Andreoiu, M., and L. Cheng.** 2010. Multifocal prostate cancer: biologic, prognostic, and therapeutic implications. Hum Pathol **41:**781-93.
8. **Axanova, L. S.** 2010. 1α,25(OH)2-VITAMIN D3 IN PROSTATE: INTERSECTION WITH AKT/PTEN AXIS AND ROLE IN SENESCENCE. WAKE FOREST UNIVERSITY GRADUATE SCHOOL OF ARTS AND SCIENCES, Winston-Salem,.
9. **Axanova, L. S., Y. Q. Chen, T. McCoy, G. Sui, and S. D. Cramer.** 2010. 1,25-dihydroxyvitamin D(3) and PI3K/AKT inhibitors synergistically inhibit growth and induce senescence in prostate cancer cells. The Prostate **70:**1658-71.
10. **Axanova, L. S., Y. Q. Chen, T. McCoy, G. Sui, and S. D. Cramer.** 2010. 1,25-dihydroxyvitamin D(3) and PI3K/AKT inhibitors synergistically inhibit growth and induce senescence in prostate cancer cells. Prostate **70:**1658-71.
11. **Bander, N. H., D. Yao, H. Liu, Y. T. Chen, M. Steiner, W. Zuccaro, and P. Moy.** 1997. MHC class I and II expression in prostate carcinoma and modulation by interferon-alpha and -gamma. Prostate **33:**233-9.
12. **Barber, G. N.** 2005. VSV-tumor selective replication and protein translation. Oncogene **24:**7710-9.
13. **Barclay, W. W., and S. D. Cramer.** 2005. Culture of mouse prostatic epithelial cells from genetically engineered mice. The Prostate **63:**291-8.
14. **Barik, S., and A. K. Banerjee.** 1992. Phosphorylation by cellular casein kinase II is essential for transcriptional activity of vesicular stomatitis virus phosphoprotein P. Proc Natl Acad Sci U S A **89:**6570-4.
15. **Barik, S., and A. K. Banerjee.** 1992. Sequential phosphorylation of the phosphoprotein of vesicular stomatitis virus by cellular and viral protein kinases is essential for transcription activation. J Virol **66:**1109-18.
16. **Barton, B. E., J. G. Karras, T. F. Murphy, A. Barton, and H. F. Huang.** 2004. Signal transducer and activator of transcription 3 (STAT3) activation in prostate cancer: Direct STAT3 inhibition induces apoptosis in prostate cancer lines. Mol Cancer Ther **3:**11-20.

17. **Berquin, I. M., Y. Min, R. Wu, J. Wu, D. Perry, J. M. Cline, M. J. Thomas, T. Thornburg, G. Kulik, A. Smith, I. J. Edwards, R. D'Agostino, H. Zhang, H. Wu, J. X. Kang, and Y. Q. Chen.** 2007. Modulation of prostate cancer genetic risk by omega-3 and omega-6 fatty acids. The Journal of clinical investigation **117:**1866-75.
18. **Bettoun, D. J., A. Scafonas, S. J. Rutledge, P. Hodor, O. Chen, C. Gambone, R. Vogel, S. McElwee-Witmer, C. Bai, L. Freedman, and A. Schmidt.** 2005. Interaction between the androgen receptor and RNase L mediates a cross-talk between the interferon and androgen signaling pathways. The Journal of biological chemistry **280:**38898-901.
19. **Black, B. L., G. Brewer, and D. S. Lyles.** 1994. Effect of vesicular stomatitis virus matrix protein on host-directed translation in vivo. J Virol **68:**555-60.
20. **Black, B. L., and D. S. Lyles.** 1992. Vesicular stomatitis virus matrix protein inhibits host cell-directed transcription of target genes in vivo. J Virol **66:**4058-64.
21. **Black, B. L., R. B. Rhodes, M. McKenzie, and D. S. Lyles.** 1993. The role of vesicular stomatitis virus matrix protein in inhibition of host-directed gene expression is genetically separable from its function in virus assembly. J Virol **67:**4814-21.
22. **Blumenthal, G. M., and P. A. Dennis.** 2008. PTEN hamartoma tumor syndromes. Eur J Hum Genet **16:**1289-300.
23. **Boorjian, S. A., R. J. Karnes, L. J. Rangel, E. J. Bergstralh, and M. L. Blute.** 2008. Mayo Clinic validation of the D'amico risk group classification for predicting survival following radical prostatectomy. J Urol **179:**1354-60; discussion 1360-1.
24. **Burkhart, D. L., and J. Sage.** 2008. Cellular mechanisms of tumour suppression by the retinoblastoma gene. Nat Rev Cancer **8:**671-82.
25. **Carey, B. L., M. Ahmed, S. Puckett, and D. S. Lyles.** 2008. Early steps of the virus replication cycle are inhibited in prostate cancer cells resistant to oncolytic vesicular stomatitis virus. J Virol **82:**12104-15.
26. **Carey, B. L., M. Ahmed, S. Puckett, and D. S. Lyles.** 2008. Early steps of the virus replication cycle are inhibited in prostate cancer cells resistant to oncolytic vesicular stomatitis virus. Journal of virology **82:**12104-15.
27. **Cary, Z. D., M. C. Willingham, and D. S. Lyles.** 2011. Oncolytic vesicular stomatitis virus induces apoptosis in U87 glioblastoma cells by a type II death receptor mechanism and induces cell death and tumor clearance in vivo. Journal of virology **85:**5708-17.
28. **Cary, Z. D., M. C. Willingham, and D. S. Lyles.** 2011. Oncolytic Vesicular Stomatitis Virus Induces Apoptosis in U87 Glioblastoma Cells by a Type II Death Receptor Mechanism and Induces Cell Death and Tumor Clearance In Vivo. J Virol **85:**5708-17.
29. **Cheon, H., J. Yang, and G. R. Stark.** 2011. The functions of signal transducers and activators of transcriptions 1 and 3 as cytokine-inducible proteins. Journal of interferon & cytokine research : the official journal of the International Society for Interferon and Cytokine Research **31:**33-40.
30. **Chin, Y. E., M. Kitagawa, K. Kuida, R. A. Flavell, and X. Y. Fu.** 1997. Activation of the STAT signaling pathway can cause expression of caspase 1 and apoptosis. Mol Cell Biol **17:**5328-37.
31. **Choo, M. K., H. Sakurai, K. Koizumi, and I. Saiki.** 2006. TAK1-mediated stress signaling pathways are essential for TNF-alpha-promoted pulmonary metastasis of murine colon cancer cells. Int J Cancer **118:**2758-64.

32. **Chu, W. M., D. Ostertag, Z. W. Li, L. Chang, Y. Chen, Y. Hu, B. Williams, J. Perrault, and M. Karin.** 1999. JNK2 and IKKbeta are required for activating the innate response to viral infection. Immunity **11:**721-31.
33. **Connor, J. H., and D. S. Lyles.** 2002. Vesicular stomatitis virus infection alters the eIF4F translation initiation complex and causes dephosphorylation of the eIF4E binding protein 4E-BP1. J Virol **76:**10177-87.
34. **Cureton, D. K., R. H. Massol, S. P. Whelan, and T. Kirchhausen.** 2010. The length of vesicular stomatitis virus particles dictates a need for actin assembly during clathrin-dependent endocytosis. PLoS Pathog **6:**e1001127.
35. **Dai, C., and S. B. Krantz.** 1999. Interferon gamma induces upregulation and activation of caspases 1, 3, and 8 to produce apoptosis in human erythroid progenitor cells. Blood **93:**3309-16.
36. **DeWeese, T. L., H. van der Poel, S. Li, B. Mikhak, R. Drew, M. Goemann, U. Hamper, R. DeJong, N. Detorie, R. Rodriguez, T. Haulk, A. M. DeMarzo, S. Piantadosi, D. C. Yu, Y. Chen, D. R. Henderson, M. A. Carducci, W. G. Nelson, and J. W. Simons.** 2001. A phase I trial of CV706, a replication-competent, PSA selective oncolytic adenovirus, for the treatment of locally recurrent prostate cancer following radiation therapy. Cancer Res **61:**7464-72.
37. **Dunn, G. P., K. C. Sheehan, L. J. Old, and R. D. Schreiber.** 2005. IFN unresponsiveness in LNCaP cells due to the lack of JAK1 gene expression. Cancer Res **65:**3447-53.
38. **Durbin, J. E., R. Hackenmiller, M. C. Simon, and D. E. Levy.** 1996. Targeted disruption of the mouse Stat1 gene results in compromised innate immunity to viral disease. Cell **84:**443-50.
39. **Elankumaran, S., D. Rockemann, and S. K. Samal.** 2006. Newcastle disease virus exerts oncolysis by both intrinsic and extrinsic caspase-dependent pathways of cell death. J Virol **80:**7522-34.
40. **Ezell, S. A., C. Polytarchou, M. Hatziapostolou, A. Guo, I. Sanidas, T. Bihani, M. J. Comb, G. Sourvinos, and P. N. Tsichlis.** 2012. The protein kinase Akt1 regulates the interferon response through phosphorylation of the transcriptional repressor EMSY. Proceedings of the National Academy of Sciences of the United States of America **109:**E613-21.
41. **Fensterl, V., J. L. Wetzel, S. Ramachandran, T. Ogino, S. A. Stohlman, C. C. Bergmann, M. S. Diamond, H. W. Virgin, and G. C. Sen.** 2012. Interferon-induced Ifit2/ISG54 protects mice from lethal VSV neuropathogenesis. PLoS Pathog **8:**e1002712.
42. **Ferran, M. C., and J. M. Lucas-Lenard.** 1997. The vesicular stomatitis virus matrix protein inhibits transcription from the human beta interferon promoter. J Virol **71:**371-7.
43. **Finkelshtein, D., A. Werman, D. Novick, S. Barak, and M. Rubinstein.** 2013. LDL receptor and its family members serve as the cellular receptors for vesicular stomatitis virus. Proc Natl Acad Sci U S A **110:**7306-11.
44. **Fresno Vara, J. A., E. Casado, J. de Castro, P. Cejas, C. Belda-Iniesta, and M. Gonzalez-Baron.** 2004. PI3K/Akt signalling pathway and cancer. Cancer Treat Rev **30:**193-204.
45. **Fueyo, J., C. Gomez-Manzano, R. Alemany, P. S. Lee, T. J. McDonnell, P. Mitlianga, Y. X. Shi, V. A. Levin, W. K. Yung, and A. P. Kyritsis.** 2000. A mutant oncolytic adenovirus targeting the Rb pathway produces anti-glioma effect in vivo. Oncogene **19:**2-12.
46. **Garcia, M. A., P. Gallego, M. Campagna, J. Gonzalez-Santamaria, G. Martinez, L. Marcos-Villar, A. Vidal, M. Esteban, and C. Rivas.** 2009.

Activation of NF-kB pathway by virus infection requires Rb expression. PLoS One **4:**e6422.

47. **Ge, P., J. Tsao, S. Schein, T. J. Green, M. Luo, and Z. H. Zhou.** 2010. Cryo-EM model of the bullet-shaped vesicular stomatitis virus. Science **327:**689-93.
48. **George R. Stark, I. M. K., Bryan R. G. Williams, Robert H. Silverman, and Robert D. Schreiber.** 1998. How cells respond to interferon. Annual Review Biochemistry **67:**227-264.
49. **Georgel, P., Z. Jiang, S. Kunz, E. Janssen, J. Mols, K. Hoebe, S. Bahram, M. B. Oldstone, and B. Beutler.** 2007. Vesicular stomatitis virus glycoprotein G activates a specific antiviral Toll-like receptor 4-dependent pathway. Virology **362:**304-13.
50. **Gross, M., B. Liu, J. Tan, F. S. French, M. Carey, and K. Shuai.** 2001. Distinct effects of PIAS proteins on androgen-mediated gene activation in prostate cancer cells. Oncogene **20:**3880-7.
51. **Haan, S., J. F. Keller, I. Behrmann, P. C. Heinrich, and C. Haan.** 2005. Multiple reasons for an inefficient STAT1 response upon IL-6-type cytokine stimulation. Cellular signalling **17:**1542-50.
52. **Heinrich, P. C., I. Behrmann, S. Haan, H. M. Hermanns, G. Muller-Newen, and F. Schaper.** 2003. Principles of interleukin (IL)-6-type cytokine signalling and its regulation. Biochem J **374:**1-20.
53. **Heinrich, P. C., I. Behrmann, S. Haan, H. M. Hermanns, G. Muller-Newen, and F. Schaper.** 2003. Principles of interleukin (IL)-6-type cytokine signalling and its regulation. The Biochemical journal **374:**1-20.
54. **Her, L. S., E. Lund, and J. E. Dahlberg.** 1997. Inhibition of Ran guanosine triphosphatase-dependent nuclear transport by the matrix protein of vesicular stomatitis virus. Science **276:**1845-8.
55. **Hill, R., Y. Song, R. D. Cardiff, and T. Van Dyke.** 2005. Heterogeneous tumor evolution initiated by loss of pRb function in a preclinical prostate cancer model. Cancer research **65:**10243-54.
56. **Hill, R., Y. Song, R. D. Cardiff, and T. Van Dyke.** 2005. Heterogeneous tumor evolution initiated by loss of pRb function in a preclinical prostate cancer model. Cancer Res **65:**10243-54.
57. **Hix, L. M., J. Karavitis, M. W. Khan, Y. H. Shi, K. Khazaie, and M. Zhang.** 2013. Tumor STAT1 transcription factor activity enhances breast tumor growth and immune suppression mediated by myeloid-derived suppressor cells. J Biol Chem **288:**11676-88.
58. **Howlader N, N. A., Krapcho M, Neyman N, Aminou R, Waldron W, Altekruse SF, Kosary CL, Ruhl J, Tatalovich Z, Cho H, Mariotto A, Eisner MP, Lewis DR, Chen HS, Feuer EJ, Cronin KA, Edwards BK (eds).** 2011, posting date. SEER Cancer Statistics Review 1975-2008. [Online.]
59. **Hsieh, A. C., Y. Liu, M. P. Edlind, N. T. Ingolia, M. R. Janes, A. Sher, E. Y. Shi, C. R. Stumpf, C. Christensen, M. J. Bonham, S. Wang, P. Ren, M. Martin, K. Jessen, M. E. Feldman, J. S. Weissman, K. M. Shokat, C. Rommel, and D. Ruggero.** 2012. The translational landscape of mTOR signalling steers cancer initiation and metastasis. Nature **485:**55-61.
60. **Hu, J. C., R. S. Coffin, C. J. Davis, N. J. Graham, N. Groves, P. J. Guest, K. J. Harrington, N. D. James, C. A. Love, I. McNeish, L. C. Medley, A. Michael, C. M. Nutting, H. S. Pandha, C. A. Shorrock, J. Simpson, J. Steiner, N. M. Steven, D. Wright, and R. C. Coombes.** 2006. A phase I study of OncoVEXGM-CSF, a second-generation oncolytic herpes simplex virus expressing granulocyte

macrophage colony-stimulating factor. Clinical cancer research : an official journal of the American Association for Cancer Research **12:**6737-47.

61. **Inokuchi, S., T. Aoyama, K. Miura, C. H. Osterreicher, Y. Kodama, K. Miyai, S. Akira, D. A. Brenner, and E. Seki.** 2010. Disruption of TAK1 in hepatocytes causes hepatic injury, inflammation, fibrosis, and carcinogenesis. Proc Natl Acad Sci U S A **107:**844-9.
62. **Jemal, A., R. Siegel, J. Xu, and E. Ward.** 2010. Cancer statistics, 2010. CA Cancer J Clin **60:**277-300.
63. **Kaur, S., A. Sassano, B. Dolniak, S. Joshi, B. Majchrzak-Kita, D. P. Baker, N. Hay, E. N. Fish, and L. C. Platanias.** 2008. Role of the Akt pathway in mRNA translation of interferon-stimulated genes. Proceedings of the National Academy of Sciences of the United States of America **105:**4808-13.
64. **Kim, M. J., R. D. Cardiff, N. Desai, W. A. Banach-Petrosky, R. Parsons, M. M. Shen, and C. Abate-Shen.** 2002. Cooperativity of Nkx3.1 and Pten loss of function in a mouse model of prostate carcinogenesis. Proc Natl Acad Sci U S A **99:**2884-9.
65. **Kirby, M., C. Hirst, and E. D. Crawford.** 2011. Characterising the castration-resistant prostate cancer population: a systematic review. Int J Clin Pract **65:**1180-92.
66. **Kluth, M., J. Hesse, A. Heinl, A. Krohn, S. Steurer, H. Sirma, R. Simon, P. S. Mayer, U. Schumacher, K. Grupp, J. R. Izbicki, K. Pantel, E. Dikomey, J. O. Korbel, C. Plass, G. Sauter, T. Schlomm, and S. Minner.** 2013. Genomic deletion of MAP3K7 at 6q12-22 is associated with early PSA recurrence in prostate cancer and absence of TMPRSS2:ERG fusions. Mod Pathol.
67. **Kopecky, S. A., and D. S. Lyles.** 2003. The cell-rounding activity of the vesicular stomatitis virus matrix protein is due to the induction of cell death. J Virol **77:**5524-8.
68. **Kopecky, S. A., and D. S. Lyles.** 2003. Contrasting effects of matrix protein on apoptosis in HeLa and BHK cells infected with vesicular stomatitis virus are due to inhibition of host gene expression. J Virol **77:**4658-69.
69. **Kopecky, S. A., and D. S. Lyles.** 2003. Contrasting effects of matrix protein on apoptosis in HeLa and BHK cells infected with vesicular stomatitis virus are due to inhibition of host gene expression. Journal of virology **77:**4658-69.
70. **Kopecky, S. A., M. C. Willingham, and D. S. Lyles.** 2001. Matrix protein and another viral component contribute to induction of apoptosis in cells infected with vesicular stomatitis virus. J Virol **75:**12169-81.
71. **Kotaja, N., S. Aittomaki, O. Silvennoinen, J. J. Palvimo, and O. A. Janne.** 2000. ARIP3 (androgen receptor-interacting protein 3) and other PIAS (protein inhibitor of activated STAT) proteins differ in their ability to modulate steroid receptor-dependent transcriptional activation. Molecular endocrinology **14:**1986-2000.
72. **Kuo, T. M., C. P. Hu, Y. L. Chen, M. H. Hong, K. S. Jeng, C. C. Liang, M. L. Chen, and C. Chang.** 2009. HBV replication is significantly reduced by IL-6. Journal of biomedical science **16:**41.
73. **Larrea, E., R. Aldabe, I. Gonzalez, V. Segura, P. Sarobe, I. Echeverria, and J. Prieto.** 2009. Oncostatin M enhances the antiviral effects of type I interferon and activates immunostimulatory functions in liver epithelial cells. Journal of virology **83:**3298-311.
74. **Lesche, R., M. Groszer, J. Gao, Y. Wang, A. Messing, H. Sun, X. Liu, and H. Wu.** 2002. Cre/loxP-mediated inactivation of the murine Pten tumor suppressor gene. Genesis **32:**148-9.

75. **Li, J., C. Yen, D. Liaw, K. Podsypanina, S. Bose, S. I. Wang, J. Puc, C. Miliaresis, L. Rodgers, R. McCombie, S. H. Bigner, B. C. Giovanella, M. Ittmann, B. Tycko, H. Hibshoosh, M. H. Wigler, and R. Parsons.** 1997. PTEN, a putative protein tyrosine phosphatase gene mutated in human brain, breast, and prostate cancer. Science **275:**1943-7.
76. **Li, P., X. Yu, K. Ge, J. Melamed, R. G. Roeder, and Z. Wang.** 2002. Heterogeneous expression and functions of androgen receptor co-factors in primary prostate cancer. The American journal of pathology **161:**1467-74.
77. **Li, X. L., J. A. Blackford, and B. A. Hassel.** 1998. RNase L mediates the antiviral effect of interferon through a selective reduction in viral RNA during encephalomyocarditis virus infection. J Virol **72:**2752-9.
78. **Liao, J., Y. Fu, and K. Shuai.** 2000. Distinct roles of the NH2- and COOH-terminal domains of the protein inhibitor of activated signal transducer and activator of transcription (STAT) 1 (PIAS1) in cytokine-induced PIAS1-Stat1 interaction. Proceedings of the National Academy of Sciences of the United States of America **97:**5267-72.
79. **Linja, M. J., K. P. Porkka, Z. Kang, K. J. Savinainen, O. A. Janne, T. L. Tammela, R. L. Vessella, J. J. Palvimo, and T. Visakorpi.** 2004. Expression of androgen receptor coregulators in prostate cancer. Clinical cancer research : an official journal of the American Association for Cancer Research **10:**1032-40.
80. **Liu, B., J. Liao, X. Rao, S. A. Kushner, C. D. Chung, D. D. Chang, and K. Shuai.** 1998. Inhibition of Stat1-mediated gene activation by PIAS1. Proceedings of the National Academy of Sciences of the United States of America **95:**10626-31.
81. **Liu, W., B. L. Chang, S. Cramer, P. P. Koty, T. Li, J. Sun, A. R. Turner, C. Von Kap-Herr, P. Bobby, J. Rao, S. L. Zheng, W. B. Isaacs, and J. Xu.** 2007. Deletion of a small consensus region at 6q15, including the MAP3K7 gene, is significantly associated with high-grade prostate cancers. Clin Cancer Res **13:**5028-33.
82. **Loblaw, D. A., K. S. Virgo, R. Nam, M. R. Somerfield, E. Ben-Josef, D. S. Mendelson, R. Middleton, S. A. Sharp, T. J. Smith, J. Talcott, M. Taplin, N. J. Vogelzang, J. L. Wade, 3rd, C. L. Bennett, and H. I. Scher.** 2007. Initial hormonal management of androgen-sensitive metastatic, recurrent, or progressive prostate cancer: 2006 update of an American Society of Clinical Oncology practice guideline. J Clin Oncol **25:**1596-605.
83. **Lodish, H. F., and M. Porter.** 1980. Translational control of protein synthesis after infection by vesicular stomatitis virus. J Virol **36:**719-33.
84. **Lund, J. M., L. Alexopoulou, A. Sato, M. Karow, N. C. Adams, N. W. Gale, A. Iwasaki, and R. A. Flavell.** 2004. Recognition of single-stranded RNA viruses by Toll-like receptor 7. Proc Natl Acad Sci U S A **101:**5598-603.
85. **Lyles, D., Rupprecht, CE.** 2006. *Rhabdoviridae*, Fields Virology.
86. **Maddison, L. A., B. W. Sutherland, R. J. Barrios, and N. M. Greenberg.** 2004. Conditional deletion of Rb causes early stage prostate cancer. Cancer research **64:**6018-25.
87. **Maddison, L. A., B. W. Sutherland, R. J. Barrios, and N. M. Greenberg.** 2004. Conditional deletion of Rb causes early stage prostate cancer. Cancer Res **64:**6018-25.
88. **Majumder, P. K., J. J. Yeh, D. J. George, P. G. Febbo, J. Kum, Q. Xue, R. Bikoff, H. Ma, P. W. Kantoff, T. R. Golub, M. Loda, and W. R. Sellers.** 2003. Prostate intraepithelial neoplasia induced by prostate restricted Akt activation:

the MPAKT model. Proceedings of the National Academy of Sciences of the United States of America **100:**7841-6.
89. **Matlin, K. S., H. Reggio, A. Helenius, and K. Simons.** 1982. Pathway of vesicular stomatitis virus entry leading to infection. J Mol Biol **156:**609-31.
90. **Moerdyk-Schauwecker, M., N. R. Shah, A. M. Murphy, E. Hastie, P. Mukherjee, and V. Z. Grdzelishvili.** 2013. Resistance of pancreatic cancer cells to oncolytic vesicular stomatitis virus: role of type I interferon signaling. Virology **436:**221-34.
91. **Moore, T. C., K. L. Bush, L. Cody, D. M. Brown, and T. M. Petro.** 2012. Control of early Theiler's murine encephalomyelitis virus replication in macrophages by interleukin-6 occurs in conjunction with STAT1 activation and nitric oxide production. Journal of virology **86:**10841-51.
92. **Moussavi, M., L. Fazli, H. Tearle, Y. Guo, M. Cox, J. Bell, C. Ong, W. Jia, and P. S. Rennie.** 2010. Oncolysis of prostate cancers induced by vesicular stomatitis virus in PTEN knockout mice. Cancer research **70:**1367-76.
93. **Muller, U., U. Steinhoff, L. F. Reis, S. Hemmi, J. Pavlovic, R. M. Zinkernagel, and M. Aguet.** 1994. Functional role of type I and type II interferons in antiviral defense. Science **264:**1918-21.
94. **Murphy, A. M., D. M. Besmer, M. Moerdyk-Schauwecker, N. Moestl, D. A. Ornelles, P. Mukherjee, and V. Z. Grdzelishvili.** 2012. Vesicular stomatitis virus as an oncolytic agent against pancreatic ductal adenocarcinoma. J Virol **86:**3073-87.
95. **Nandi, S., W. Imagawa, Y. Tomooka, M. F. McGrath, and M. Edery.** 1984. Collagen gel culture system and analysis of estrogen effects on mammary carcinogenesis. Archives of toxicology **55:**91-6.
96. **Platanias, L. C.** 2005. Mechanisms of type-I- and type-II-interferon-mediated signalling. Nature reviews. Immunology **5:**375-86.
97. **Rajani, K. R., E. L. Pettit Kneller, M. O. McKenzie, D. A. Horita, J. W. Chou, and D. S. Lyles.** 2012. Complexes of vesicular stomatitis virus matrix protein with host Rae1 and Nup98 involved in inhibition of host transcription. PLoS Pathog **8:**e1002929.
98. **Reich, N. C., and L. M. Pfeffer.** 1990. Evidence for involvement of protein kinase C in the cellular response to interferon alpha. Proceedings of the National Academy of Sciences of the United States of America **87:**8761-5.
99. **Roche, S., S. Bressanelli, F. A. Rey, and Y. Gaudin.** 2006. Crystal structure of the low-pH form of the vesicular stomatitis virus glycoprotein G. Science **313:**187-91.
100. **Roche, S., F. A. Rey, Y. Gaudin, and S. Bressanelli.** 2007. Structure of the prefusion form of the vesicular stomatitis virus glycoprotein G. Science **315:**843-8.
101. **Sakurai, H.** 2012. Targeting of TAK1 in inflammatory disorders and cancer. Trends Pharmacol Sci **33:**522-30.
102. **Salmena, L., A. Carracedo, and P. P. Pandolfi.** 2008. Tenets of PTEN tumor suppression. Cell **133:**403-14.
103. **Sangfelt, O., S. Erickson, J. Castro, T. Heiden, A. Gustafsson, S. Einhorn, and D. Grander.** 1999. Molecular mechanisms underlying interferon-alpha-induced G0/G1 arrest: CKI-mediated regulation of G1 Cdk-complexes and activation of pocket proteins. Oncogene **18:**2798-810.
104. **Schlee, M., A. Roth, V. Hornung, C. A. Hagmann, V. Wimmenauer, W. Barchet, C. Coch, M. Janke, A. Mihailovic, G. Wardle, S. Juranek, H. Kato, T. Kawai, H. Poeck, K. A. Fitzgerald, O. Takeuchi, S. Akira, T. Tuschl, E. Latz, J. Ludwig, and G. Hartmann.** 2009. Recognition of 5' triphosphate by RIG-I

helicase requires short blunt double-stranded RNA as contained in panhandle of negative-strand virus. Immunity **31:**25-34.
105. **Schultz, J., D. Koczan, U. Schmitz, S. M. Ibrahim, D. Pilch, J. Landsberg, and M. Kunz.** 2010. Tumor-promoting role of signal transducer and activator of transcription (Stat)1 in late-stage melanoma growth. Clin Exp Metastasis **27:**133-40.
106. **Shah, R. B., R. Mehra, A. M. Chinnaiyan, R. Shen, D. Ghosh, M. Zhou, G. R. Macvicar, S. Varambally, J. Harwood, T. A. Bismar, R. Kim, M. A. Rubin, and K. J. Pienta.** 2004. Androgen-independent prostate cancer is a heterogeneous group of diseases: lessons from a rapid autopsy program. Cancer Res **64:**9209-16.
107. **Sharma, A., C. E. Comstock, E. S. Knudsen, K. H. Cao, J. K. Hess-Wilson, L. M. Morey, J. Barrera, and K. E. Knudsen.** 2007. Retinoblastoma tumor suppressor status is a critical determinant of therapeutic response in prostate cancer cells. Cancer Res **67:**6192-203.
108. **Sharma, A., C. E. Comstock, E. S. Knudsen, K. H. Cao, J. K. Hess-Wilson, L. M. Morey, J. Barrera, and K. E. Knudsen.** 2007. Retinoblastoma tumor suppressor status is a critical determinant of therapeutic response in prostate cancer cells. Cancer research **67:**6192-203.
109. **Sharma, A., W. S. Yeow, A. Ertel, I. Coleman, N. Clegg, C. Thangavel, C. Morrissey, X. Zhang, C. E. Comstock, A. K. Witkiewicz, L. Gomella, E. S. Knudsen, P. S. Nelson, and K. E. Knudsen.** 2010. The retinoblastoma tumor suppressor controls androgen signaling and human prostate cancer progression. The Journal of clinical investigation **120:**4478-92.
110. **Sharma, A., W. S. Yeow, A. Ertel, I. Coleman, N. Clegg, C. Thangavel, C. Morrissey, X. Zhang, C. E. Comstock, A. K. Witkiewicz, L. Gomella, E. S. Knudsen, P. S. Nelson, and K. E. Knudsen.** 2010. The retinoblastoma tumor suppressor controls androgen signaling and human prostate cancer progression. J Clin Invest **120:**4478-92.
111. **Shen, M. M., and C. Abate-Shen.** 2010. Molecular genetics of prostate cancer: new prospects for old challenges. Genes & development **24:**1967-2000.
112. **Shi, Z., Z. Cai, A. Sanchez, T. Zhang, S. Wen, J. Wang, J. Yang, S. Fu, and D. Zhang.** 2011. A novel Toll-like receptor that recognizes vesicular stomatitis virus. The Journal of biological chemistry **286:**4517-24.
113. **Shi, Z., Z. Cai, A. Sanchez, T. Zhang, S. Wen, J. Wang, J. Yang, S. Fu, and D. Zhang.** 2011. A novel Toll-like receptor that recognizes vesicular stomatitis virus. J Biol Chem **286:**4517-24.
114. **Sircar, K., M. Yoshimoto, F. A. Monzon, I. H. Koumakpayi, R. L. Katz, A. Khanna, K. Alvarez, G. Chen, A. D. Darnel, A. G. Aprikian, F. Saad, T. A. Bismar, and J. A. Squire.** 2009. PTEN genomic deletion is associated with p-Akt and AR signalling in poorer outcome, hormone refractory prostate cancer. J Pathol **218:**505-13.
115. **Small, E. J., M. A. Carducci, J. M. Burke, R. Rodriguez, L. Fong, L. van Ummersen, D. C. Yu, J. Aimi, D. Ando, P. Working, D. Kirn, and G. Wilding.** 2006. A phase I trial of intravenous CG7870, a replication-selective, prostate-specific antigen-targeted oncolytic adenovirus, for the treatment of hormone-refractory, metastatic prostate cancer. Mol Ther **14:**107-17.
116. **Steck, P. A., M. A. Pershouse, S. A. Jasser, W. K. Yung, H. Lin, A. H. Ligon, L. A. Langford, M. L. Baumgard, T. Hattier, T. Davis, C. Frye, R. Hu, B. Swedlund, D. H. Teng, and S. V. Tavtigian.** 1997. Identification of a candidate

tumour suppressor gene, MMAC1, at chromosome 10q23.3 that is mutated in multiple advanced cancers. Nat Genet **15:**356-62.

117. **Stojdl, D. F., N. Abraham, S. Knowles, R. Marius, A. Brasey, B. D. Lichty, E. G. Brown, N. Sonenberg, and J. C. Bell.** 2000. The murine double-stranded RNA-dependent protein kinase PKR is required for resistance to vesicular stomatitis virus. J Virol **74:**9580-5.
118. **Stojdl, D. F., B. Lichty, S. Knowles, R. Marius, H. Atkins, N. Sonenberg, and J. C. Bell.** 2000. Exploiting tumor-specific defects in the interferon pathway with a previously unknown oncolytic virus. Nat Med **6:**821-5.
119. **Stojdl, D. F., B. D. Lichty, B. R. tenOever, J. M. Paterson, A. T. Power, S. Knowles, R. Marius, J. Reynard, L. Poliquin, H. Atkins, E. G. Brown, R. K. Durbin, J. E. Durbin, J. Hiscott, and J. C. Bell.** 2003. VSV strains with defects in their ability to shutdown innate immunity are potent systemic anti-cancer agents. Cancer Cell **4:**263-75.
120. **Strong, J. E., M. C. Coffey, D. Tang, P. Sabinin, and P. W. Lee.** 1998. The molecular basis of viral oncolysis: usurpation of the Ras signaling pathway by reovirus. EMBO J **17:**3351-62.
121. **Sun, X., V. K. Yau, B. J. Briggs, and G. R. Whittaker.** 2005. Role of clathrin-mediated endocytosis during vesicular stomatitis virus entry into host cells. Virology **338:**53-60.
122. **Taura, M., M. A. Suico, K. Koyama, K. Komatsu, R. Miyakita, C. Matsumoto, E. Kudo, R. Kariya, H. Goto, S. Kitajima, C. Takahashi, T. Shuto, M. Nakao, S. Okada, and H. Kai.** 2012. Rb/E2F1 regulates the innate immune receptor Toll-like receptor 3 in epithelial cells. Molecular and cellular biology **32:**1581-90.
123. **Taylor, B. S., N. Schultz, H. Hieronymus, A. Gopalan, Y. Xiao, B. S. Carver, V. K. Arora, P. Kaushik, E. Cerami, B. Reva, Y. Antipin, N. Mitsiades, T. Landers, I. Dolgalev, J. E. Major, M. Wilson, N. D. Socci, A. E. Lash, A. Heguy, J. A. Eastham, H. I. Scher, V. E. Reuter, P. T. Scardino, C. Sander, C. L. Sawyers, and W. L. Gerald.** 2010. Integrative genomic profiling of human prostate cancer. Cancer Cell **18:**11-22.
124. **Tsai, C. C., J. I. Kai, W. C. Huang, C. Y. Wang, Y. Wang, C. L. Chen, Y. T. Fang, Y. S. Lin, R. Anderson, S. H. Chen, C. W. Tsao, and C. F. Lin.** 2009. Glycogen synthase kinase-3beta facilitates IFN-gamma-induced STAT1 activation by regulating Src homology-2 domain-containing phosphatase 2. Journal of immunology **183:**856-64.
125. **Tseng, P. C., W. C. Huang, C. L. Chen, B. S. Sheu, Y. S. Shan, C. C. Tsai, C. Y. Wang, S. O. Chen, C. Y. Hsieh, and C. F. Lin.** 2012. Regulation of SHP2 by PTEN/AKT/GSK-3beta signaling facilitates IFN-gamma resistance in hyperproliferating gastric cancer. Immunobiology **217:**926-34.
126. **Vidal, L., H. S. Pandha, T. A. Yap, C. L. White, K. Twigger, R. G. Vile, A. Melcher, M. Coffey, K. J. Harrington, and J. S. DeBono.** 2008. A phase I study of intravenous oncolytic reovirus type 3 Dearing in patients with advanced cancer. Clinical cancer research : an official journal of the American Association for Cancer Research **14:**7127-37.
127. **Vivanco, I., N. Palaskas, C. Tran, S. P. Finn, G. Getz, N. J. Kennedy, J. Jiao, J. Rose, W. Xie, M. Loda, T. Golub, I. K. Mellinghoff, R. J. Davis, H. Wu, and C. L. Sawyers.** 2007. Identification of the JNK signaling pathway as a functional target of the tumor suppressor PTEN. Cancer Cell **11:**555-69.
128. **Wang, S., J. Gao, Q. Lei, N. Rozengurt, C. Pritchard, J. Jiao, G. V. Thomas, G. Li, P. Roy-Burman, P. S. Nelson, X. Liu, and H. Wu.** 2003. Prostate-specific

deletion of the murine Pten tumor suppressor gene leads to metastatic prostate cancer. Cancer Cell **4:**209-21.

129. **Wang, S. I., R. Parsons, and M. Ittmann.** 1998. Homozygous deletion of the PTEN tumor suppressor gene in a subset of prostate adenocarcinomas. Clin Cancer Res **4:**811-5.
130. **Wang, Y., S. W. Hayward, A. A. Donjacour, P. Young, T. Jacks, J. Sage, R. Dahiya, R. D. Cardiff, M. L. Day, and G. R. Cunha.** 2000. Sex hormone-induced carcinogenesis in Rb-deficient prostate tissue. Cancer Res **60:**6008-17.
131. **Whang, Y. E., X. Wu, H. Suzuki, R. E. Reiter, C. Tran, R. L. Vessella, J. W. Said, W. B. Isaacs, and C. L. Sawyers.** 1998. Inactivation of the tumor suppressor PTEN/MMAC1 in advanced human prostate cancer through loss of expression. Proc Natl Acad Sci U S A **95:**5246-50.
132. **Wollmann, G., M. D. Robek, and A. N. van den Pol.** 2007. Variable deficiencies in the interferon response enhance susceptibility to vesicular stomatitis virus oncolytic actions in glioblastoma cells but not in normal human glial cells. J Virol **81:**1479-91.
133. **Wollmann, G., P. Tattersall, and A. N. van den Pol.** 2005. Targeting human glioblastoma cells: comparison of nine viruses with oncolytic potential. Journal of virology **79:**6005-22.
134. **Wong, L. H., K. G. Krauer, I. Hatzinisiriou, M. J. Estcourt, P. Hersey, N. D. Tam, S. Edmondson, R. J. Devenish, and S. J. Ralph.** 1997. Interferon-resistant human melanoma cells are deficient in ISGF3 components, STAT1, STAT2, and p48-ISGF3gamma. J Biol Chem **272:**28779-85.
135. **Wu, M., L. Shi, A. Cimic, L. Romero, G. Sui, C. J. Lees, J. M. Cline, D. F. Seals, J. S. Sirintrapun, T. P. McCoy, W. Liu, J. W. Kim, G. A. Hawkins, D. M. Peehl, J. Xu, and S. D. Cramer.** 2012. Suppression of Tak1 promotes prostate tumorigenesis. Cancer research **72:**2833-43.
136. **Wu, M., L. Shi, A. Cimic, L. Romero, G. Sui, C. J. Lees, J. M. Cline, D. F. Seals, J. S. Sirintrapun, T. P. McCoy, W. Liu, J. W. Kim, G. A. Hawkins, D. M. Peehl, J. Xu, and S. D. Cramer.** 2012. Suppression of Tak1 promotes prostate tumorigenesis. Cancer Res **72:**2833-43.
137. **Wu, X., K. Senechal, M. S. Neshat, Y. E. Whang, and C. L. Sawyers.** 1998. The PTEN/MMAC1 tumor suppressor phosphatase functions as a negative regulator of the phosphoinositide 3-kinase/Akt pathway. Proceedings of the National Academy of Sciences of the United States of America **95:**15587-91.
138. **Wu, X., J. Wu, J. Huang, W. C. Powell, J. Zhang, R. J. Matusik, F. O. Sangiorgi, R. E. Maxson, H. M. Sucov, and P. Roy-Burman.** 2001. Generation of a prostate epithelial cell-specific Cre transgenic mouse model for tissue-specific gene ablation. Mechanisms of development **101:**61-9.
139. **Yang, C. H., A. Murti, and L. M. Pfeffer.** 1998. STAT3 complements defects in an interferon-resistant cell line: evidence for an essential role for STAT3 in interferon signaling and biological activities. Proceedings of the National Academy of Sciences of the United States of America **95:**5568-72.
140. **Yoneyama, M., M. Kikuchi, T. Natsukawa, N. Shinobu, T. Imaizumi, M. Miyagishi, K. Taira, S. Akira, and T. Fujita.** 2004. The RNA helicase RIG-I has an essential function in double-stranded RNA-induced innate antiviral responses. Nat Immunol **5:**730-7.
141. **Yu, H., D. Pardoll, and R. Jove.** 2009. STATs in cancer inflammation and immunity: a leading role for STAT3. Nat Rev Cancer **9:**798-809.
142. **Zelefsky, M. J., Y. Yamada, Z. Fuks, Z. Zhang, M. Hunt, O. Cahlon, J. Park, and A. Shippy.** 2008. Long-term results of conformal radiotherapy for prostate

cancer: impact of dose escalation on biochemical tumor control and distant metastases-free survival outcomes. Int J Radiat Oncol Biol Phys **71:**1028-33.

143. **Zhang, Q., Y. A. Yu, E. Wang, N. Chen, R. L. Danner, P. J. Munson, F. M. Marincola, and A. A. Szalay.** 2007. Eradication of solid human breast tumors in nude mice with an intravenously injected light-emitting oncolytic vaccinia virus. Cancer Res **67:**10038-46.

144. **Zhao, K. W., D. Li, Q. Zhao, Y. Huang, R. H. Silverman, P. J. Sims, and G. Q. Chen.** 2005. Interferon-alpha-induced expression of phospholipid scramblase 1 through STAT1 requires the sequential activation of protein kinase Cdelta and JNK. The Journal of biological chemistry **280:**42707-14.

CURRICULUM VITAE

Nanmeng Yu

Department of Biochemistry
Wake Forest School of Medicine
Medical Center Blvd
Winston Salem, NC 27157
336-716-2270

125 Crowne Chase Dr, Apt 16
Winston Salem, NC 27104
336-608-9457

EDUCATION

M.D., expected May 2015
Wake Forest School of Medicine, Winston Salem, NC

Ph.D. candidate
Ph.D. in Biochemistry, expected December 2013
Wake Forest School of Medicine, Winston Salem, NC

B. A. in Biochemistry and Molecular Biology, *Magna Cum Laude*
Agnes Scott College, Decatur, GA, 2004 - 2008

AWARDS and HONORS

M.D./ Ph.D. Fellowship, 2008 – present
McLennan Medical Fellowship, 2008 – present
American Society of Virology Travel Award, 2012 and 2013
Wake Forest Graduate School of Arts and Sciences Alumni Travel Award, 2012 and 2013
Phi Beta Kappa, 2008
Charles A. Dana Scholar, 2004 - 2008
Dean's Honor List, 2004 - 2008
International Vision Scholar, 2005 - 2008
Summer Frierson Clarke Scholar, 2005

PROFESSIONAL AFFILIATIONS

American Society of Virology
American Chemical Society, 2006-2008

PUBLICATIONS

Yu, N., Cramer S.D., Puckett, S., Douglas S. Lyles. Changes in susceptibility to vesicular stomatitis virus during progression of prostate cancer. (manuscript in preparation)

ABSTRACTS

Yu, N. and Douglas S. Lyles. 2013. Changes in susceptibility to vesicular stomatitis virus during progression of prostate cancer. American Society of Virology Conference.

Yu, N. and Douglas S. Lyles. 2012. Changes in susceptibility to vesicular stomatitis virus during progression of prostate cancer. American Society of Virology Conference.

Yu, N. and Douglas S. Lyles. 2012. Changes in susceptibility to vesicular stomatitis virus during progression of prostate cancer. Southeastern Regional Virological Conference.

Yu, N. and Douglas S. Lyles. 2009. The role of TAK1 in the susceptibility of tumor cells to vesicular stomatitis virus infection. Medical student research day. Wake Forest School of Medicine.

Yu, N. and Suzy Torti. 2008. The role of MON1a, in modifying ferroportin in breast cancer cells. Medical student research day. Wake Forest School of Medicine.